TRIBHUVAN UNIVERSITY

INSTITUTE OF ENGINEERING

PULCHOWK CAMPUS, LALITPUR

NEPAL

THESIS NO: 078/MSPSE/003

Shunt Active Power Filter for Harmonics Compensation Based on Three Phase Voltage Source Inverters

by

Arjun Maharjan

A THESIS

SUBMITTED TO THE DEPARTMENT OF ELECTRICAL ENGINEERING IN PARTIAL FULFILLMENT OF THE REQUIREMENTS FOR THE DEGREE OF MASTER OF SCIENCE IN POWER SYSTEM ENGINEERING

MASTER OF SCIENCE IN

POWER SYSTEM ENGINEERING

December, 2023

Shunt Active Power Filter for Harmonics Compensation Based on Three Phase Voltage Source Inverters

by

Arjun Maharjan

Roll No.:078/MSPSE/003

Thesis Supervisors

Asso. Prof. Basanta Kumar Gautam (Ph.D.)
Program coordinator, Master of Science in Power System Engineering
Department of Electrical Engineering Pulchowk Campus, Lalitpur

Asso. Prof. Sujan Adhikari (Ph.D.)
Hillside College of Engineering, Balkumari, Kathmandu

A THESIS

SUBMITTED TO THE DEPARTMENT OF ELECTRICAL ENGINEERING IN PARTIAL FULFILLMENT OF THE REQUIREMENTS FOR THE DEGREE OF MASTER OF SCIENCE IN POWER SYSTEM ENGINEERING

MASTER OF SCIENCE IN
POWER SYSTEM ENGINEERING

December, 2023

CERTIFICATE OF APPROVAL

The undersigned certify that they have read and recommended to the Institute of Engineering for acceptance, a thesis entitled "**Shunt Active Power Filter for Harmonics Compensation Based on Three Phase Voltage Source Inverters**" submitted by **Arjun Maharjan** in partial fulfillment of the requirements for the degree of **Master in Power System Engineering**.

_____

Asso. Prof. Basanta Kumar Gautam (Ph.D.)
Program coordinator, Master of Science in
Power System Engineering
Department of Electrical Engineering
Pulchowk Campus, Lalitpur
(Thesis Supervisor)

_____

Surendra Rajbhandari
Former DMD
Nepal Electricity Authority
(External Examiner)

_____

Asso. Prof. Sujan Adhikari (Ph.D.)
Hillside College of Engineering
Balkumari, Kathmandu
(Thesis Supervisor)

_____

Asst. Prof. Yuvraj Adhikari
Head of Department
Department of Electrical
Engineering, Pulchowk
Campus, Lalitpur

December 2023

Abstract

Power quality of the power distribution systems havedegraded because of the extensive use of power electronic devices. These nonlinear loads cause non-sinusoidal currents & voltageswith harmonic components. Some of the major power quality issues due to non-sinusoidal currents and voltage with harmonic component are impact on power capacitor, Transformer, motors, telecommunication, energy and demand metering etc. Shunt active power filters (SAPF) are used to acquire balanced and sinusoidal supply currents via way of means of injecting compensation current. There are two major control loop namely outer control loop and inner outer loop with one extra loop. The outer control loop measures source current and voltage & generates the reference reactive & active power that to be compensated by the SAPF. The inner control loop effectively tracks the reference compensating currents in d-q coordinate using PI controllers. While extra loop is associated with capacitor of voltage source inverter (VSI). The constant voltage across the capacitor is maintained. So, there is active power loss which is achieved by comparing reference voltage with the standard voltage and send the error to the PI controller. Simulation results are obtained from MATLAB/Simulink under various non-linear loadconditions.

The cases considered here are as follows:

i) 3 phase 3 wire full wave rectifier with varying load: The MATLAB/Simulink was developed and tested with load and result was compared with the traditional approach without harmonics compensation. The THD level is within limit as per IEEE 516 standard.

ii) Different loading conditions: Same process as of case i) was performed and results are within limit as per IEEE 516 standard.

iii) 3 phase 4 wire full wave rectifier with resistive and inductive load with different loading condition: Same process as of case i) was performed and results are within limit as per IEEE 516 standard.

iv) 3 phase 3 wire full wave rectifier with VFD load: The three-phase motor is developed in MATLAB/Simulink which was tested and investigated the impact of VFD load in SAPF.

v) The MATLAB/Simulink of SAPF was tested with non-linear load in industries at Balaju industrial area of Nepal. The THD level are within limit as per IEEE 516 standard for all load except VFD load.

In all cases the improved pf of the system is about unity was obtained with the compensated system except with the VFD load.

Index Terms— shunt active power filter (SAPF), total harmonic distortion (THD), voltage source inverter (VSI), , variable frequency drive (VFD), variable speed drive (VSD)

ACKNOWLEDGEMENT

I express my profound gratitude towards my thesis supervisors Associate Prof Dr. Basanta Kumar Gautam and Associate Prof Dr. Sujan Adhikari for the excellent supervision, invaluable guidance and constant encouragement, throughout the progress of this work. My sincere thanks go to both of my supervisors, for taking so much interest in my academic and personal aspects. Once again, I am heartily thankful to supervisors for their continuous moral support and inspiration.

I express my sincere appreciation to all teachers and staff of Electrical Engineering Department, IOE, Pulchowk for their help.

I am as well indebted to the Balaju Industrial District Management office and all industries under it for providing/helping in data collection.

Last but not the least; I would like to extend my profound gratitude to my family, especially my mother and dear wife, for unconditional love and support.

TABLE OF CONTENTS

LIST OF FIGURES

LIST OF TABLES

Annexes

Annex 1: MATLAB results for Table III : Performance comparison of SAPF under different loading condition for 3 phase 3 wire system.

Annex 2 : MATLAB results for Table IV : Performance comparison of SAPF under different loading condition for 3 phase 3 wire system.

Annex 3: Approval for getting load information in industries of Balaju Industrial Area

Annex 4: Non-Linear Load information of different industries in Balaju Industrial Area

Annex 5 : Paper Publication

List of Abbreviation

SAF- Shunt Active Filter

SAPF- Shunt Active Power Filter

VSI- Voltage Source Inverter

THD- Total Harmonics Distortion

LPF- Low Pass Filter

HPF- High Pass Filter

PI- Proportional Integral

IEEE- Institute Electrical and Electronic Engineers

Std- Standard

VFD- Variable Frequency Drive

VSD- Variable Speed Drive

MATLAB	-Matrix Laboratory
AC	-Alternating Current
DC	-Direct Current

CHAPTER 1. INTRODUCTION

1.1 Background

Electrical power is expected to account for approximately sixty percent of total global power usage by 2035. Data centers, industrial, and commercial applications with a non-linear nature are depicted in Fig. 1, which represents power electronics-based equipment. Hence, the power grid supplies harmonic current drawn by them, and power quality issues can arise. The main problems associated with current harmonics include generator failure, faulty energy and demand meter reading, which concerns the utility, and computer network failures, as well as vibrations in motors, which concern the consumers.

Hence, current harmonics are to be suppressed within the recommended limits to prevent the distortion of sinusoidal voltage and current. Shunt active filters (SAFs) are particularly popular as harmonic reduction solutions due to recent advances in power electronic switches and because they offer optimal results across a broad spectrum of versatile operating situations, as opposed to passive filters.

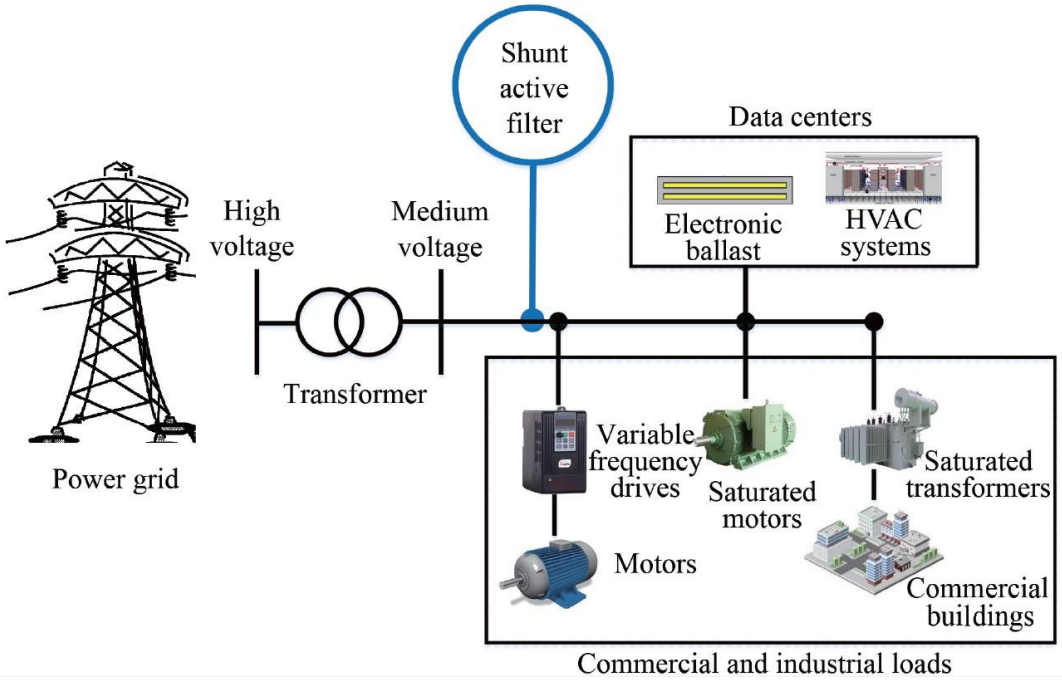

Fig. 1. Grid with nonlinear devices & SAF connected to reduce harmonics

For devices with non-linearity, the current is not proportional to the applied voltage. Nonlinear devices in power grids lead to non-sinusoidal voltages and currents with harmonic distortion. They draw currents with harmonically distorted waveforms from the power grid, and the current distortion increases with the applied voltage. Unlike passive filters, a shunt active power filter (SAPF) is a well-established solution for harmonic compensation due to the advancements in power electronic switches and its performance across a wide range of operating conditions.

In this thesis, an SAPF with a voltage source inverter (VSI) was proposed to achieve stable and sinusoidal supply current in a simple power system by injecting compensation currents. A simplified diagram of the SAPF arrangement is shown in Fig. 2. The three-phase AC source provides power to devices with non-linearity. The specific device with non-linearity considered here is the 3-phase diode full-bridge rectifier, followed by a varying device, RL. The SAPF is connected in parallel to the system to supply compensating current for this non-linear device.

Thus, the distorted current requirement of the device is addressed by the SAPF, and consequently, the source supplies only currents that are sinusoidal, maintaining about unity power factor. The summation of the supply current (Is) and the compensating current (Ic) results in the total current for the devices with non-linearity (I_nl), represented by the characteristic "rabbit ear" waveform. SAPF generates compensation currents, and coupling inductors are provided to mitigate peak-frequency currents that occur during inverter switching.

Two key control loops are connected to the SAPF: the outer loop for current control and the inner loop. The outer control loop measures the device current (i_L) & supply voltage (v_s) and uses instantaneous p-q theory to generate reference active and reactive powers which are remunerated by the SAPF. The inner control loop contains of a proportional-integral control (PI) & is intended to be followed competently the reference current in the dq-domain range. The system is simulated in Simulink/MATLAB under various nonlinear (3-phase rectifier) devising situations. The presentation of this method is associated to simulation results without a conventional inverter connected to a PI control. Additionally, the performance of the system is evaluated against inductive or capacitive devices. This ensures that SAPF also compensates for the system power factor.

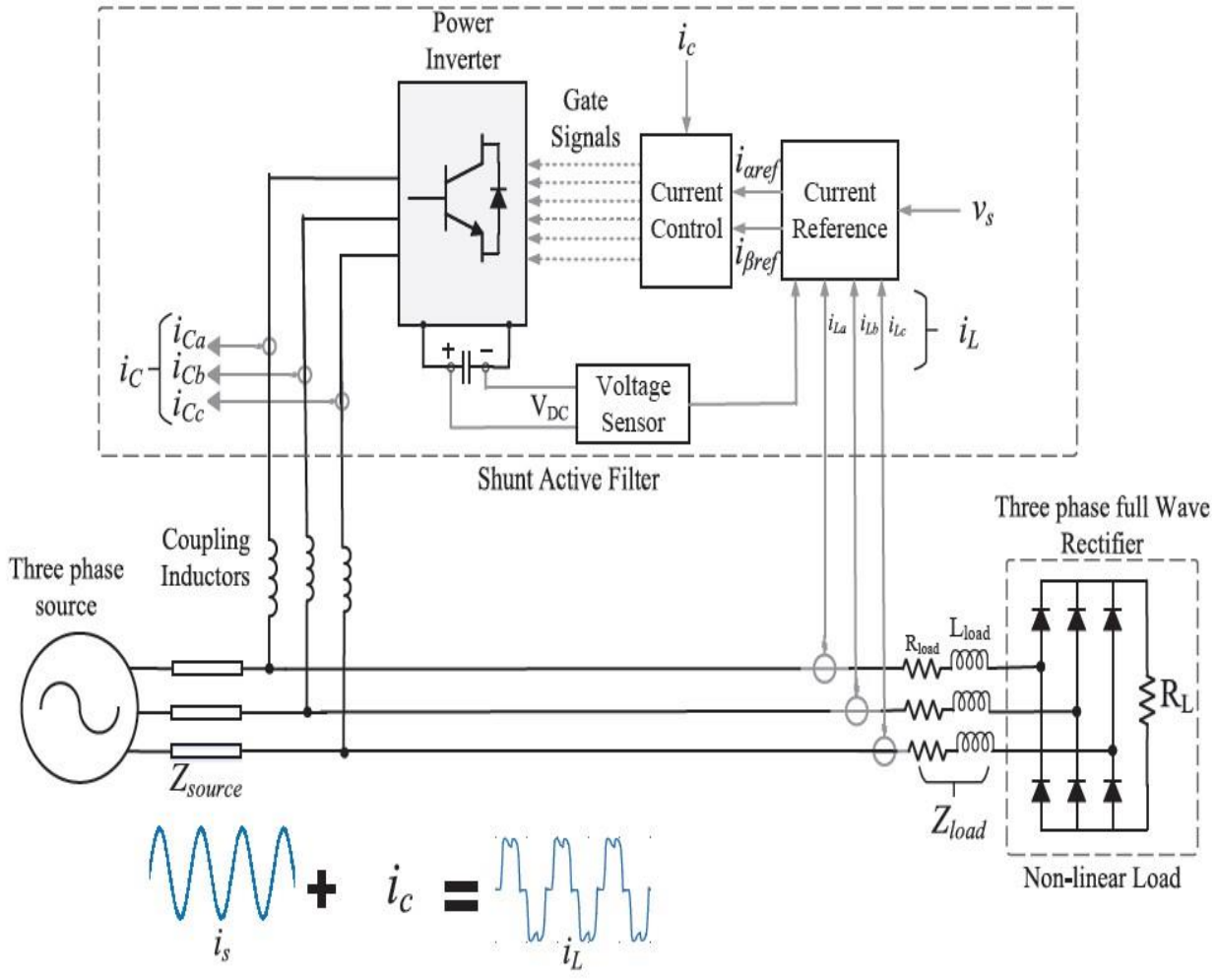

Fig. 2. Overall representation figure of a SAF with non-linear device connected to source for harmonics reduction

SAPF systems compensate for individual harmonic components and average overall harmonic distortion with acceptable transients. The Total Harmonic Distortion (THD) of a current signal is the summation of the current waveform, containing all harmonic elements associated with the fundamental element of the current waveform, and it measures the distorted harmonic content. IEEE Standard Recommendation No. 519 on power systems harmonic control states that the total harmonic distortion current of the power source should be within five percent. This standard is based on strict requirements for discrete harmonic elements.The basic idea of SAPF is to compensate for the required upper-order harmonic active power and current needs of the device using a power electronics-based Voltage Source Inverter (VSI). Hence, the fundamental element of the device current only needs to be provided by the source. Due to the limited bandwidth for control, the dynamics of the Proportional-Integral (PI) control are poor. As a consequence, SAPF might not be able to provide the required performance if the device is highly nonlinear. However, SAPF gives satisfactory performance under these conditions based on the simulation results.

Furthermore, a hysteresis band current control approach should be implemented to improve the dynamics of the inner current loop. Although there are complications to be dealt with, dynamic performance can be improved with the hysteresis-based approach. The higher switching frequency operation increases switching losses, electromagnetic interference issues, and creates difficulties in filter design compared to SAPF with PI control.

The outline of this thesis can be listed as follows.

Goals for implementing SAPF:

- Compensation of upper-order hormonal active power & currents requirements of the device with PI control-based VSI.
- Hence The supply just needs to provide the essential portion of the device current.

For the simulation, system configuration and benchmark used:

- Design of 3 phase power system consisting of a 3-phase source supplying a non-linear device.
- Design of 3 phase Power Inverter supplying compensating currents for the power system.
- Design of Outer & Inner current control loop for the power inverter.
- Design of VSD/VFD
- Design of 3 Φ 4W power scheme consisting of a 3-Φ source supplying a device with non-linearity.

Classification of Scenarios considered to appraise the presentation of SAPF:

- Comparison with the system without connecting the inverter.
- Presentation of the system under varying device conditions (varying RL).
- Power factor improvement with the SAPF system (for inductive or capacitive device).

1.2 Problem Statement

Shunt Active Power Filters (SAPFs) and Passive Power Filters are two different technologies used to mitigate power quality issues. Each has its advantages and disadvantages, and the choice between them depends on specific requirements and application characteristics. Here are some advantages of Shunt Active Power Filters over Passive Filters:

i) Dynamic Compensation:

SAPFs: Shunt Active Power Filters can provide dynamic compensation. They continuously monitor the device and inject compensating currents in active-time, adapting to changes in the device conditions.

Passive Filters: Passive filters have fixed parameters and are not capable of adjusting to changes in the system.

ii) Flexibility and Adaptability:

SAPFs: Active filters can be programmed to compensate for a extensive array of harmonic frequency and power factor variations. They offer more flexibility in addressing different power quality issues.

Passive Filters: Passive filters are designed for specific frequency and may not be as adaptable to changes in the power system or devices.

iii) Performance Under Variable Devices:

SAPFs: Active filters perform well under variable and dynamic devices, providing consistent compensation regardless of device changes.

Passive Filters: The performance of passive filters may degrade under variable devices or changes in the system.

Size and Weight:

SAPFs: Active filters are generally smaller and lighter compared to passive filters with equivalent compensation capabilities.

Passive Filters: Passive filters can be bulky and heavy, especially for higher power applications.

Wide Range of Applications:

SAPFs: Shunt Active Power Filters can address a variety of power quality issues, including active power reimbursement, pf improvement & harmonic moderation.

Passive Filters: Passive filters are typically designed for specific purposes, and a combination of different filters may be needed to address various power quality issues.

Efficiency:

SAPFs: Active filters can be more efficient as they generate compensating currents only when needed, reducing energy consumption compared to passive filters that continuously dissipate power.

Passive Filters: Passive filters can have inherent losses due to the resistive elements, which may reduce overall system efficiency.

Maintenance and Reliability:

SAPFs: Active filters may have fewer wear-and-tear components compared to some passive filter elements, leading to potentially lower maintenance requirements.

Passive Filters: Some passive filter components, such as capacitors and inductors, may have a limited lifespan and could require periodic maintenance or replacement.

1.3 Objectives

The main objectives of the study is to design 3 phase shunt active power filter (SAPF) with a voltage source inverter (VSI) which obtain balanced and sinusoidal source current in a simple power system by injecting compensation currents and it is applied in the industries of Nepal e.g. industries of Balaju Industrial Area.

1.4 Scope

- Improvement of the THD of the source current under conditions mentioned before.
- Improvement of the power factor under inductive or capacitive loading

conditions.

- Individual harmonic magnitude meets the IEEE Std. 519 requirement.
- Further investigation of VSD/VFD as a device.
- Stability of transfer function of SAPF.
- Application of SAPF in industries of Nepal.

CHAPTER 2. LITERATURE REVIEW

2.1 3 phase Control & modeling of VSIs

The 3-phase modeling voltage source inverters (VSIs) entails expressing the active inverter models through equation statistically or, more precisely, transfer functions. The transfer functions are valuable for designing controls tailored to 3-phase VSIs. Frequently, transform theories of dq (direct & quadrature domain) are applied in the inverter systems control design.

2.2 3 phase VSIs

3 phase VSI transform direct current (dc) voltages into alternating current (AC) voltages with required frequency & amplitude. Pulse width module (PMW) techniques control the voltage amplitude and frequency, earning these inverters the design of PWM inverters. PWM methods are employed to generate a waveform in alternating o/p from the inverter that closely resembles a sinusoidal type. Frequently, filters with low-pass are incorporated at the o/p of pulse PMW inverters to facilitate the attainment with minimal harmonic content of sinusoidal waveforms. Inverters serve various applies, like renewable sources grid integer, quality power improvement, standby/uninterruptible power supplies, electric drives in industries and electric vehicles, among others. The design of inverters involves the utilize of electronic switches such as MOSFETs, BJTs and IGBTs. Gener of PWM signals manipulate these switches through various module techniques. Inverters, also known as conversion of DC to AC in bidirectional nature, meaning they can function as rectifiers (converting AC signals to DC) or inverters (DC signals to AC conversion) according with providing of the converter switches to the switching signals.

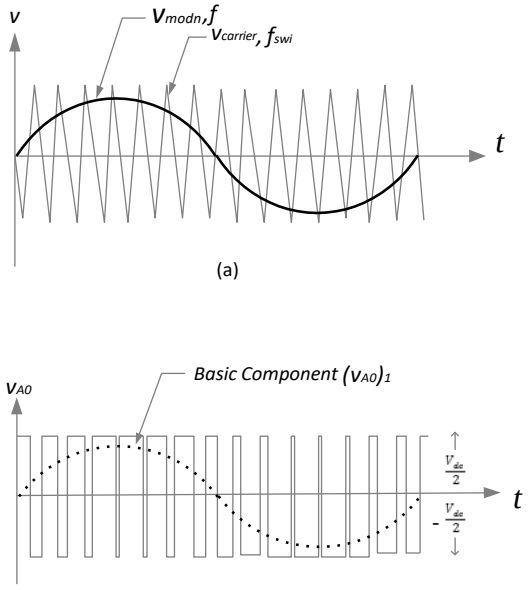

Fig. 3 (a). Modulated sine wave for single phase (b). single phase Op inverter voltage & its basic component.

For general of the switching signals, sinusoidal PWM is one among techniques of module for the inverter. With a frequency f , sinusoidal modulating signal ($V_{\mathrm{mod}n}$)is compared with a frequency (f_{swi}) with a triangular carrier wave (V_{carri}) as given by Fig. 3 (a)[22]. The f_{swi} of s/w signal is determined by frequency. of the V_{carri} wave & frequency. of $V_{\mathrm{mod}n}$ is determined by the frequency. of the basic (V_{A0}) comp. of the inverter o/p voltage. The ratio of amplitude module m_a defined as the r of magnitude of $V_{\mathrm{mod}n}$ and magnitude of V_{carri} , thus m_a is given by

$$m_a = \frac{|V_{\mathrm{modn}}|}{|V_{carri}|} \qquad (2.1)$$

Here, $|V_{\mathrm{modn}}|$ and $|V_{carri}|$ denote the magnitudes of the modulating and magnitude of carrier signals, respectively. Typically the magnitude. of the carrier wave is maintained at a constant

level, making the magnitude of the modulation signal the determinant of the m_a. Likewise, the frequency. module ratio is defined as the ratio of frequency between the modulating signal & carrier signal and the, m_f, as

$$m_f = f_{swi} / f \qquad (2.2)$$

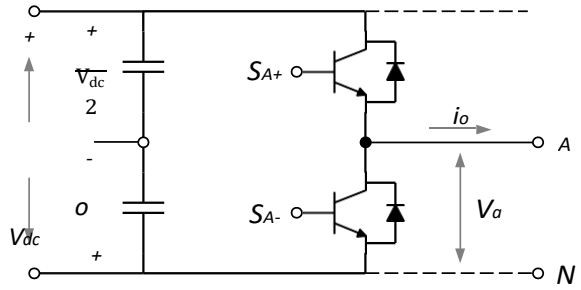

Fig.4. 1-phase PWM inverter.

The inverter with 1Φ depicted in Fig. 4, switching signals generated govern the switches S_A- & S_A+ through the comparison of the carrier signal & the modulating signal. The resulting o/p voltage V_{A0} is determined by the below equation,

$$\left.\begin{array}{l} If\ \ Vmod\ >\ Vcarrier; SA+ is\ ON\ ;\ VA0 = 1/2Vdc \\ If\ \ Vmod < Vcarrier; SA+ is\ ON\ ;\ VA0 = -1/2Vdc \end{array}\right\} \qquad (2.3)$$

Fig. 5 illustrates for m_a = 0.8 and m_f = 15, the basic component & its o/p voltage V_{A0} of the 1Φ inverter . The basic component amplitude of the o/p voltage, denoted as $|V_{A0}|1$, is given by: $|VA0|_{1=} m_a / (Vdc/2)$ (2.4)

where, m_a is the amplitude module ratio & Vdc is the DC voltage.

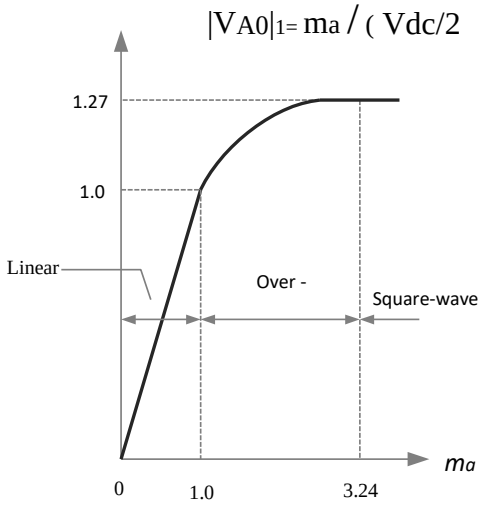

Fig. 5. Graph of normalized inverter output voltage with respect to input DC voltage as a function of amplitude module ratio

The existence of a linear relationship among the o/p ac voltage the & input dc voltage that is given by m_a represented by Fig. 5[22]. When m_a is higher than 1.0, over-module occurs & the amplitude of the basic frequency component does not vary linearly with the m_a. Moreover, the inverter o/p voltage results at very large module indexes in square wave o/p instead of multiple pulses.

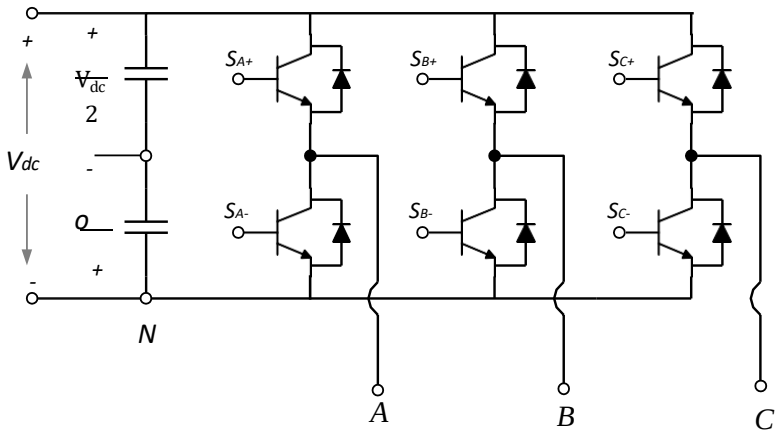

Fig. 6. 3 phase PWM inverter.

3Φ PWM comprise 3 leg switches, each corresponding to a phase, is shown in Fig. 6 [22]. The every phase is phased with the others by 120° generates the switching signals to ensure that the o/p voltage produced.

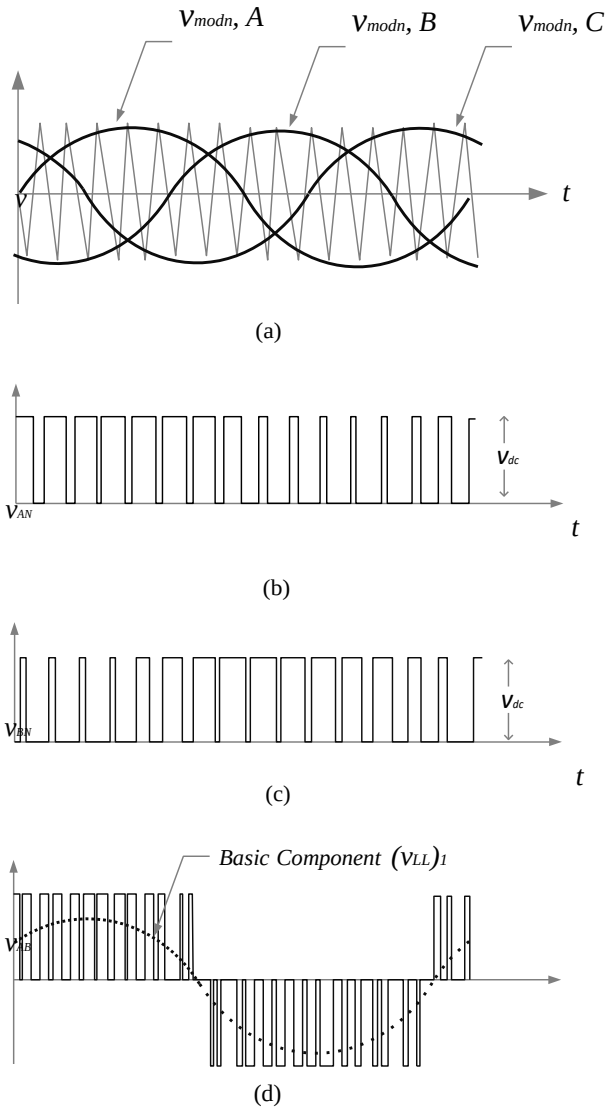

Fig.7. Three phase inverter waveforms.

Comparison of triangular wave with the out of phase signals with each other, are compared , as illustrated in Figure 7(a) [22]. The o/p voltage of each leg of the inverter is rely on m_a & the dc voltage (Vdc) . W.r.t the neutral point N, the waveforms of the o/p voltage for phases A, B & C are depicted in Fig. 7(b) [22] and (c) [22], respectively. Likewise, the L-L voltage V_{AB} and its Basic component are depicted in Fig. 7(d) [22]. The highest value of the basic component of the o/p voltage for phase A wrt the neutral, denoted as $|V_{AN}|1$, is given by:

$$|V_{AN}|1 = m_a / (\text{Vdc}/2) \qquad (2.5)$$

Thus, the amplitude module ratio plays a crucial role in control the o/p voltage of the 3Φ inverter.

2.3 3 Phase Represent Frames

The three phase represent frames are,

i. abc-reference frame
ii. $\alpha\beta$-reference frame
iii. Synchronous reference frame (dq)

The 3Φ current & voltage are represented along the three axes in the abc-reference frame, where the axes are spaced 120 degrees apart. Each phase current and voltage are sinusoidal, and the abc-reference frame is stary.

In the αβ-frame, the same balanced current and voltage are represented by two axes, α and β. The α-domain aligns with the a-domain of the abc-domain, and the β-domain is perpendicular to the α-domain. By reducing the number of axes from three to two, control in the αβ-frame requires fewer control loops. However, the voltage or current along the αβ-axes remains sinusoidal functions of time. For balanced devices, the α and β axes are also balanced, and the

0 domain of the αβ0 reference frame is zero. In the case of unbalanced devices with -ve & zero sequence elements, the αβ axes become unequal, and the 0 domain of the αβ0 reference frame is non-zero. Clarke transform can transfer quantities in the abc-frame into the αβ-frame.

Synchronous reference. domain control, also known as dq-control, involves converting grid current & voltage into a edge rotating synchronously with the grid voltage vector through Park Transform. This transform turns 3Φ period changing indicators into dc indicators.

Though the facility of dropping the quantity of obligatory control loops belongs to control in the αβ-frame, going from 3 to 2, the reference., response, and feedforward signals generally remain sinusoidal purposes of period. Achieving acceptable present & minor steady-state faults may require reimburse of up instructions, and closed-loop bandwidths must be adequately greater than the frequency. of the reference. instructions. Addressing this challenge, dq-frame-based control proposals explain.

The 3Φ voltage reference. signal obtained is transformed to the dq-frame using Clarke's transform and then transformed back to the abc-reference frame by inverse Clarke's transform as shown in below

,

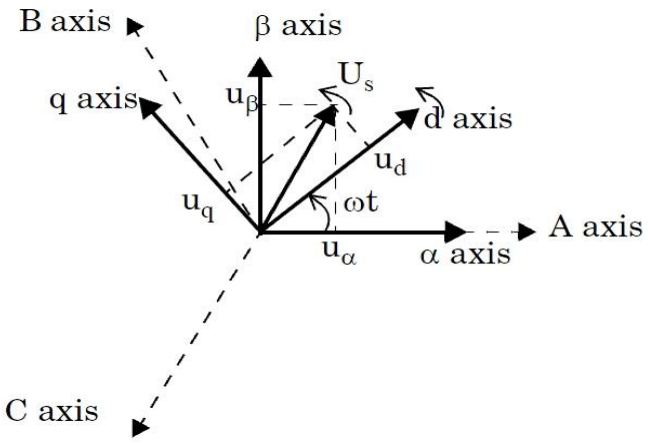

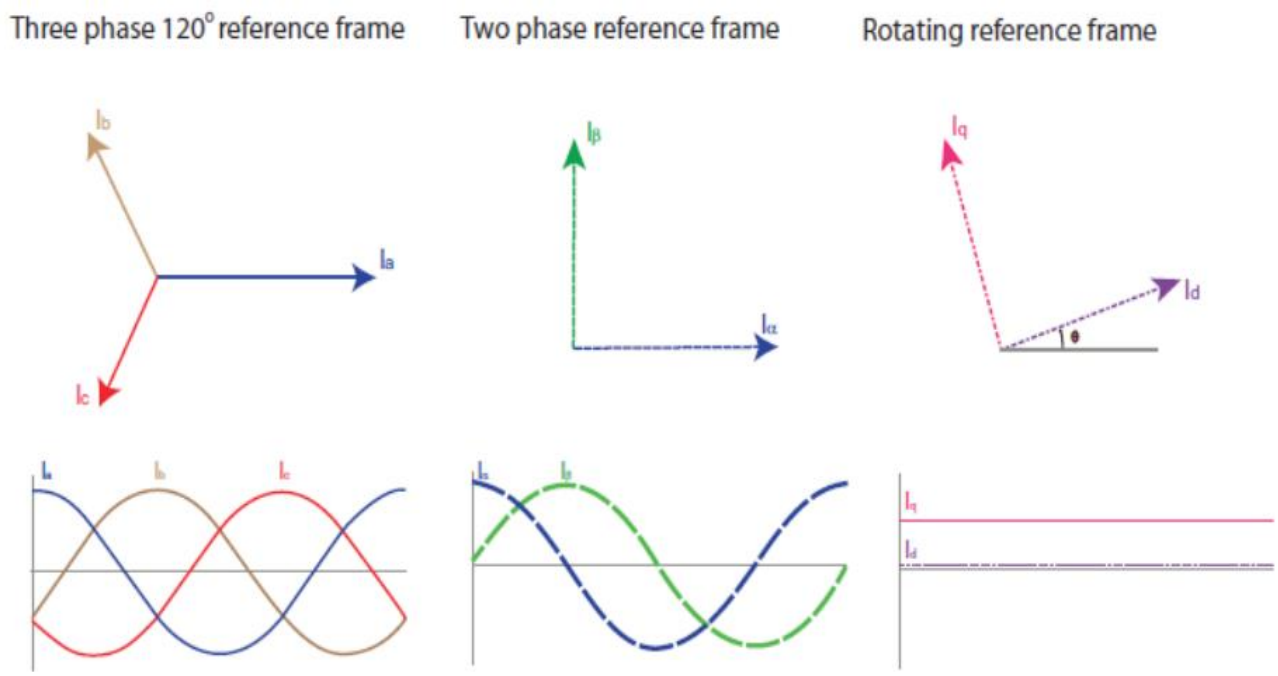

Fig. 8. Different reference frames

$$\begin{bmatrix} v_0 \\ v_\alpha \\ v_\beta \end{bmatrix} = \sqrt{\frac{2}{3}} \begin{pmatrix} \frac{1}{\sqrt{2}} & \frac{1}{\sqrt{2}} & \frac{1}{\sqrt{2}} \\ 1 & \frac{-1}{2} & \frac{-1}{2} \\ 0 & \frac{\sqrt{3}}{2} & \frac{-\sqrt{3}}{2} \end{pmatrix} \begin{bmatrix} v_a \\ v_b \\ v_c \end{bmatrix} \tag{2.6}$$

$$\begin{bmatrix} i_0 \\ i_\alpha \\ i_\beta \end{bmatrix} = \sqrt{\frac{2}{3}} \begin{pmatrix} \frac{1}{\sqrt{2}} & \frac{1}{\sqrt{2}} & \frac{1}{\sqrt{2}} \\ 1 & \frac{-1}{2} & \frac{-1}{2} \\ 0 & \frac{\sqrt{3}}{2} & \frac{-\sqrt{3}}{2} \end{pmatrix} \begin{bmatrix} i_a \\ i_b \\ i_c \end{bmatrix} \tag{2.7}$$

The axes of αβ0-frame are orthogonal. The α-domain is parallel to a-domain of abc-frame and the direction of β-domain is determined according to the rot sequence of abc.

2.4 dq modeling of 3 phase VSI

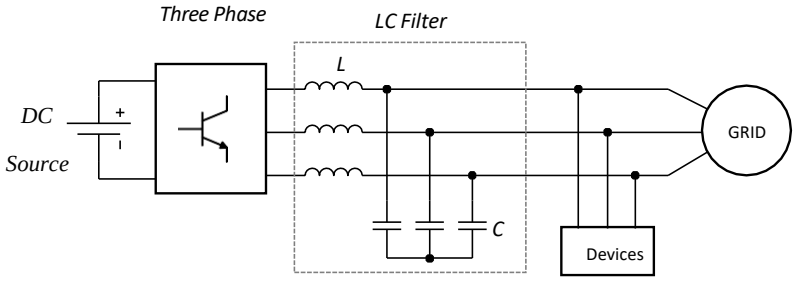

Fig. 9. 3 phase PWM inverter connected to the grid with LC filter and devices.

Fig. 9 [22] illustrates a grid-connected 3-phase PWM inverter, along with local devices & LC filter. The LC filter functions as a 2nd order low pass filter, mitigating the unnecessary harmonics generated by the electronic system within the 3Φ inverter. 3Φ inverter with grid connected develops a model, the system depicted in Fig. 9 [22] can be simplified by representing it with ideal 3Φ maintained voltage sources, while neglecting the effects of switching, as depicted in Fig.9 [22]. In this simplified represent, the grid is symbolized by a 3Φ voltage source with its eq. impedance values, and current sources represents the local devices.

.

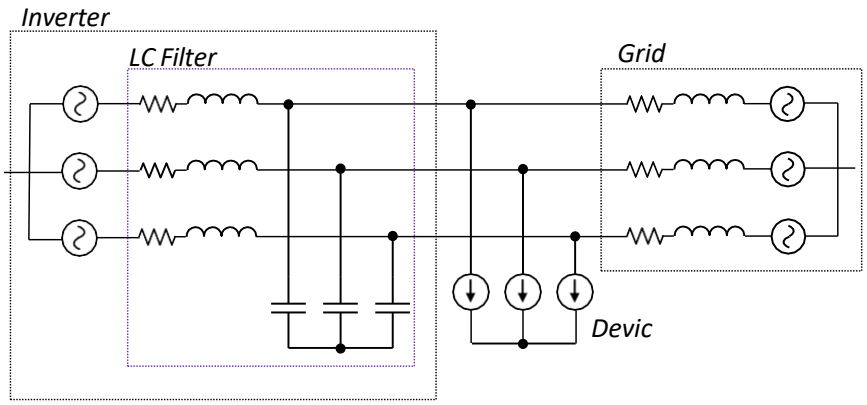

Fig. 10. the grid Connection & 3Φ ideal sources inverter replace.

To enhance the simplicity of the model, the 3Φ inverter system present in Fig. 10 [22] can be condensed into a per-phase model, as depicted in Fig. 11 [22]. The impact of source & the grid

can be encapsulated in a single source current equivalent to the net current. However, this model operates in the abc frame, where the variables are time-variant, making it challenging to use linear control design principles for the inverter system's controls. Therefore, the design of suitable controls for the system necessitates a d-q eq. system

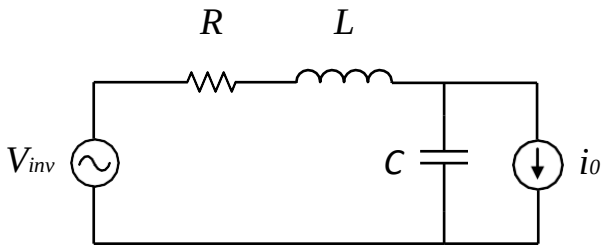

Fig. 11. 3 phase inverter per phase equivalent model .

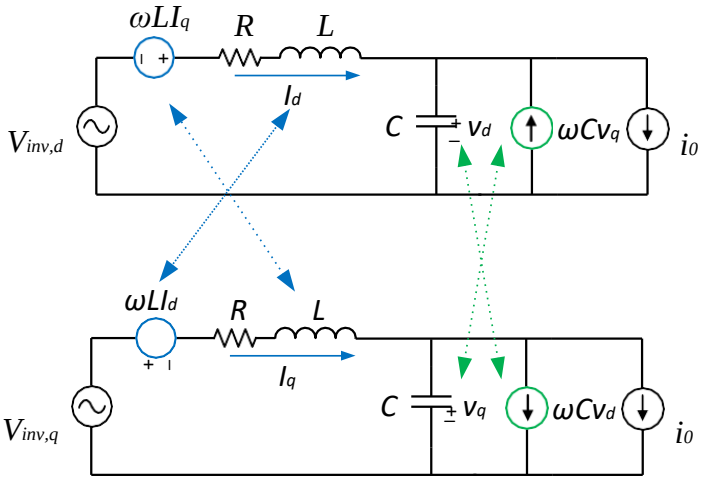

Fig. 12. 3 phase inverter dq equivalent model .

Fig. 12 [22] illustrates the eq. dq system of the grid-connected 3Φ inverter. This dq similar system comprises 2 circuits for the dq-system . The model resembles the 3Φ model depicted in Fig. 11 [22], with the addition of cross-coupling terms. The cross coupling terms IqωL helps the inverter voltage $V_{d,ind}$, & a feed forward term VqωC is introduced. Notably, these additional terms in the d-system circuit are influenced by the q-system voltage & current parts

in place of the d-system parts, resulting in them being referred to as cross-coupling components due to this cross-coupling effect. Likewise, in the q-system circuit, cross coupling term IdωL rejects the inverter voltage & 2 extra source current , $V_{d,ind}$ and VdωC, are defined.

2.5 3 phase voltage source inverters dq-based control

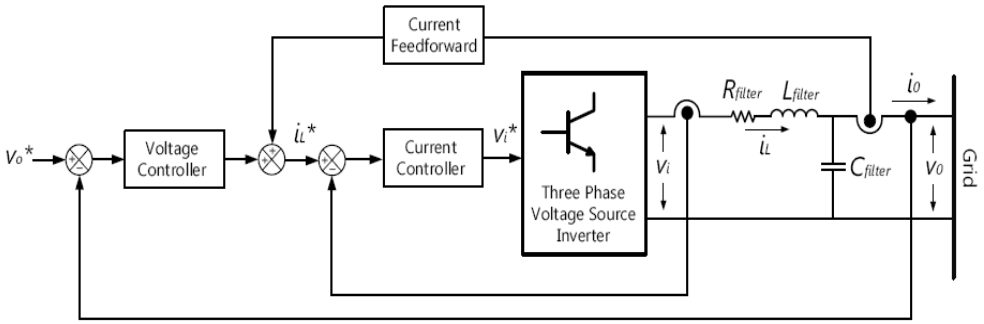

Fig. 13. Characteristic control System of inverter.

Fig. 13 [22] depicts a standard control system for a 3-Φ PWM inverter, including its current & voltage loops. The closed-loop control employs a 2-loop structure. The inward loop of control manages the current, encircling the inductor of filter & the VSI, thereby creating a CCS. Likewise, the outside loop oversees the control of the inverter's o/p voltage. The voltage loop is designed to monitor gradual conversion in the reference. voltage V_0^*& decrease errors resulting from varis in the output current i0A current feedforward mechanism is employed to enhance disturbance rejection from other sources.

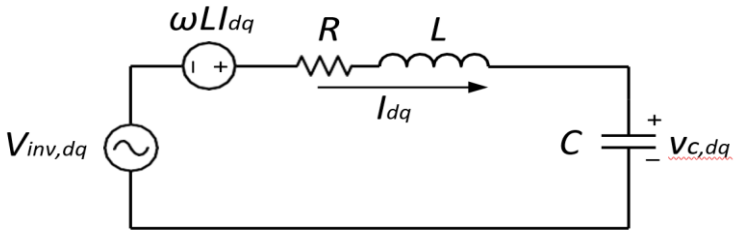

Fig. 14. Current controller design with simplified dq equivalent model .

If the current vary across the inductor remains consistently proportional to the applied voltage, the dq equation. system presented in Fig. 12[22] can undergo further simplify, as illustrated in Fig. 14 [22]. In this streamlined system, the inductor current is influenced by the voltage disparity among voltage capacity & the voltage inserted by the VSI & the capacitor voltage. The cross-coupling terms & the voltage over the capacitor are regarded as disturbances to the control model. Now, by utilizing the Kirchhoff's voltage law (KVL) equation, the plant transfer function , denoted as G(s), is given by

$$G(s) = \frac{I_{dq}}{V_{inv,dq}} = \frac{\frac{1}{L}}{s + \frac{R}{L}} \tag{2.8}$$

Here, s represents the Laplace transform variable, & internal resistance R of the inductor filter. This configuration results in a current commander environment, as depicted in Fig. 15[22]:

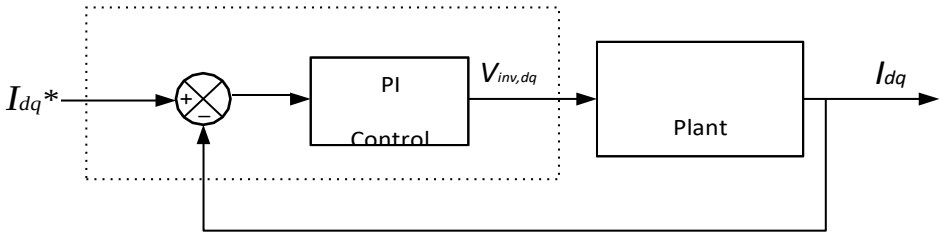

Fig.15. Design of current controller with eq. dq-domain for simplicity .

In case of previously omitted voltage over the capacitor & cross-coupling participates, the result is a current commander structure, as illustrated in Fig.16[22],

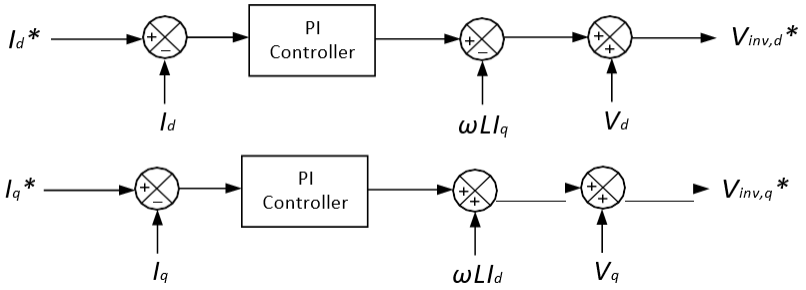

Fig.16. Current control structure incorporating feedforward of the cross-coupling parts & voltage over capacitor

2.6 LC filter design

A simple circuit, illustrated in Fig. 17 [22], shows the LC filter for the 3-phase VSI. In this represent, Vinv denotes the without filter inverter o/p voltage, while C & L represent CL filter capacitor & inductor values. Additionally, R signifies the eq resistor at the inverter o/p of full power during when operation.

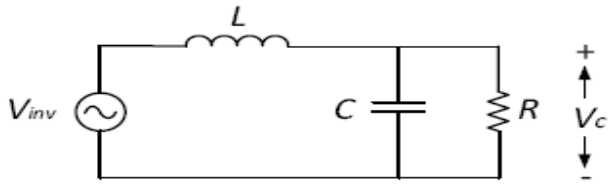

Fig. 17. Typical filter circuit of LC .

The eq resistance, R_{eq}, was determined by

$$R_{eq} = \frac{V^2}{\frac{P}{3}} \tag{2.9}$$

Here, P is the power rating of the same & V represents the rating of unit phase inverter voltage . By formulating the Kirchhoff's voltage law (KVL) equations illustrated in Fig. 17 [22], the LC filter was characterized through transfer function of 2nd order, denoted as Gfilter(s), employing

$$G_{Filter}(s) = \frac{Vc(s)}{Vinv(s)} = \frac{\frac{1}{LC}}{s^2 + \frac{1}{CR}s + \frac{1}{LC}} \tag{2.10}$$

By using Eq. (2.10) the standard form of a 2nd order transfer function is given by,

$$G_{\text{sec}ond\_order}(s) = \frac{\omega^2{}_n}{s^2 + 2\zeta\omega_n + \omega^2{}_n} \tag{2.11}$$

Here, ζ represents the 2nd order damping ratio & ω_n is the natural frequationency of the same system.

.

2.7 Outline of transfer function for control in current system

For the Outline of transfer function for control in current system of the plant, $G_{plant}(s)$, was formulated by considering Equation (2.8) as

$$G(s) = \frac{I_L(s)}{V_{inv}(s)} = \frac{\frac{1}{L}}{s + \frac{R}{L}} \qquad (2.14)$$

A nominal resistance of 0.1 Ω was assumed for the inductor. Subsequently, the frequency reply of the plant was derived. The 3Φ inverter was maintained with a switching frequency ω_{sw} of 10 kHz. The current control cross over frequency ω_x was set to 1 kHz (or 6283 rad/s) value a ten times below the s/w frequency. This choice ensures a sufficiently fast response speed for the maintained current commander. likewise, the loop transfer phase margin function (combined current & plant commander) was chosen to be forty five degree at ω_x, providing an non rejectable overshoot system . Subsequently, the mag $| G_{plant}(\omega_x) |$) and phase ∠G plant(ω_x) for the plant were extracted from the frequency response plot at the desired crossover frequency. To minimize error on steady state & enhance amplitude at peak frequency, achieving a high gain at low frequency was desirable to decrease inverter s/w noises. Considering these factors, a updated PI type 2 control deemed suitable for current model. The specific transfer function PI type 2 used for the control was C_{PI2}(s)

$$C_{PI2}(s) = K_{PI} \frac{1 + s\tau}{s\tau} \frac{1}{1 + sT_p} \qquad (2.15)$$

Here, Kp represents the gain on proportional, τ is the constant of time for the system, & Tp is also the time constant but for the extra pole at peak frequency, employed to amplitude

high-frequency disturbances. These arbitrates are identified in the literature frequency response of a PI type 2 control, as depicted in Fig. 18

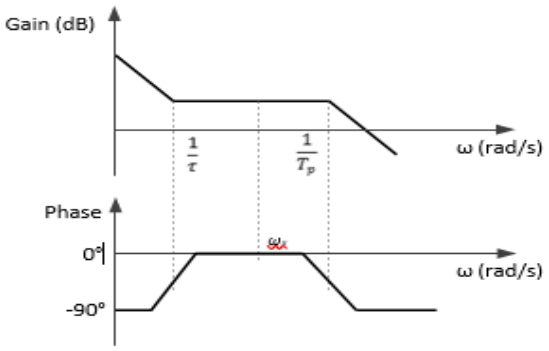

Fig. 18. PI type 2 controller asymptotic frequency response .

To determine the constants τ & Tp in Fig. 18 [22], the angle of boost θboost & the K factor were computed to ensure that the system achieves the required phase angle at the specified crossover frequency—45° at a cross over frequency of 1 kHz in this instance. The angle of boost angle (θboost) was determined

$$\theta_{boost} = \emptyset + 90° \tag{2.16}$$

where,

$$\emptyset = -(180° + \angle G_{plant}(\omega_x) - \text{Phase Margin}) \tag{2.17}$$

Calcul the K factor was done with the use of the boost angle by using

$$K = \tan\left(\frac{\theta_{boost}}{2} + 45°\right) \tag{2.18}$$

Calculation of fix values τ & Tp were done with

$$r = k / \omega_x \tag{2.19}$$

Finally, calcul of the gain on proportional, K_{PI} , was done as

$$K_{PI} = 1/ |G_{plant}(\omega_x)|$$

(2.20)

2.8 Effect of Harmonics Distortion

Harmonic distortion effects arise when nonlinear devices generate harmonic currents that are then came out into the power sources. Power eq. can be adversely reacted by these current , particularly power transformer, automobiles & power capacitors, leading to extra losses, over devising & rise of temperature. The presence of currents distortion can also lead noises on communication system & introduce power measuring faulty.

2.8.1) Effect on Power Capacitors

Issues related to distortion usually manifest initially on power bank of capacitor. A power bank of capacitor may experience resonance during peak voltage harmonics , along flow of the current through the power bank of capacitor being precisely huge & enough in monotonic harmonics. During resonance on power bank of capacitor has major impact of eleventh harmonics which is superimposed on the basic frequency. Thus power capacitor bank is implicated. In such resonance conditions, the root mean square (rms) current is often higher than the rated rms current for the capacitor. The IEEE Standard for Shunt Power Capacitors (IEEE Standard 18-1992) specifies the following continuous capacitor ratings

■ one hundred thirty five percentage of nameplate kvar

■ a hundred and ten percentage of rated rms voltage (which includes harmonics however with the exception of transients)

■ a hundred and eighty percentage of rated rms modern-day (which includes essential and harmonic modern-day)

■ one hundred twenty percentage of height voltage (which includes harmonics)

The capacitor is predominantly exposed to 2 harmonics: the fifth and the seventh. The distorted voltage comprises four percentage fifth and three percentage seventh. This leads to a 20% 5th harmonic current and a 21% 7th harmonic current. All resulting values remain well below standard limits in this scenario.

.

2.8.2) Effect on Transformers

The necessary power to concerned devices engineer Transformers to supply with minimal losses at the basic frequency. In both voltage & current harmonics distortion significantly contributes to additional heating. To neutralize upper frequency, transformer manufacturers make specific makes choices, like implementing transposed continuously cables in place of solid conductors & incorporating additional chilling tubes. With simplified guideline, a transformer where distorted current overs five percentage is considered a system for not rating due to harmonics. There are 3 impacts leading to rise transformer temperature when the current device contains harmonic comp:

a) RMS Current: The increase in current harmonics distortion in the transformer increases the rms peak value which leads the rise of heating inside the transformers.

b) Eddy Current Losses: They are brought in transformer of currents due to flux induced by magnetically. They brought on current glide withinside the winding, withinside center & in different engaging in our parts according with magnetic subject wrt transformer & purpose extra hot. The aspect of it losses will increase on rectangular of frequency for

inflicting eddy current. Hence , it will become completely essential aspect for rise of temperature in it.

c) Core Losses: The growth in core losses in the presence of harmonics can depend on the impact of harmonics on the applied voltage and the design of the transformer core. Increased distorted voltage may raise the eddy current within the core coating. The net effect depends on the thickness of core coatings and the quality of the core alloy of iron. The increase in these losses due to harmonics is typically not as significant as the previous ones.

2.8.3) Influence on Automobiles: Harmonic voltage distortion can significantly impact motors, manifesting as harmonic fluxes within the motor at the automobile ends. Although these harmonic fluxes don't notably contribute to automobile drive, they operate at a frequency dissimilar from the rotating part sync frequency, creating peak-frequency currents in the rotating part. This effect is similar to the consequences of negative sequence current at the basic frequency, causing additional losses.

Signs of harmonic voltage distortion in automobiles include reduced efficiency, accompanied by issues such as high-pitched noises, heating, and vibration. When representing motors at harmonic frequencies, the control rotating part reactance linked across the line is generally employed. Below-order harmonic voltage components, with larger magnitude and decreased apparent impedance motor, are typically more critical for automobiles.

As long as the voltage distortion adheres to the limits outlined in IEEE Standard 519-1992 (5% THD and 3% for any individual harmonic), there is usually no need to derate automobiles. However, problems like excessive heating arise when voltage distortion surpasses 8 to 10%. Correcting such distortion is crucial for the prolonged life of motors. Motors, in their interaction with the power system impedance concerning harmonic issues,

current flow, tend to elevate the system resonance by decreasing the net inductance. The impact on the model relies on the initial loc of the model harmonic before motor energize. Motors may also contribute to damping some harmonics comp based on the $\frac{X}{R}$ ratio of the fixed rotating part circuit. While this may aid in attenuating harmonic resonance in systems with numerous motors which is not large sized one and a low $\frac{X}{R}$ ratio, it cannot be relied upon for larger motors.

2.8.4) Effect on tele-transmissions

Consonant currents present in the distribution business system or in utility facilities can interfere with tele-transmission circuits that share a similar path. The produced voltage along similar lines with these harmonic currents typically falls within the bandwidth of typical audio transmissions. Harmonics between five hundred forty (9th) and twelve hundred hertz are especially distorted. The produced voltage per unit amp of current rises along the frequency, and triple harmonics (third, ninth, fifteenth) pose challenges in 4-wire models due to their phase alignment lines in a 3-phase circuit.

This direct conduction results in the straight produced pairing being equational for all the same lines, leading to a zero-equivalent voltage in the circle made with lines. In the past, pairing through the grounding point of an over-the-consumer conductor via produced posed a significant issue, especially along not closed tele-transmission circuits. However, with the widespread use of covered, circled-couple lines for tele-transmission circuits, such pairing has become less prominent.

Produced pairing may pose an issue when high currents induce an IR drop along the covered surroundings of the tele-transmission lines. The flow of current within the covered leads to this drop (refer to Fig. 20[15]), resulting in a voltage similar to the neutral point references at

the terminals of the tele-transmission conductor. Covered currents can also result from straight lines.As shown in Fig. 20[15], the covered runs in same neutral path with power lines. If existing neutral ground situs allow a substantial quantity of current to flow through covered, the resulting peak cover current & resistant fall will once more create a in similar volt-age through neutral references in the terminals of tele-transmission line.

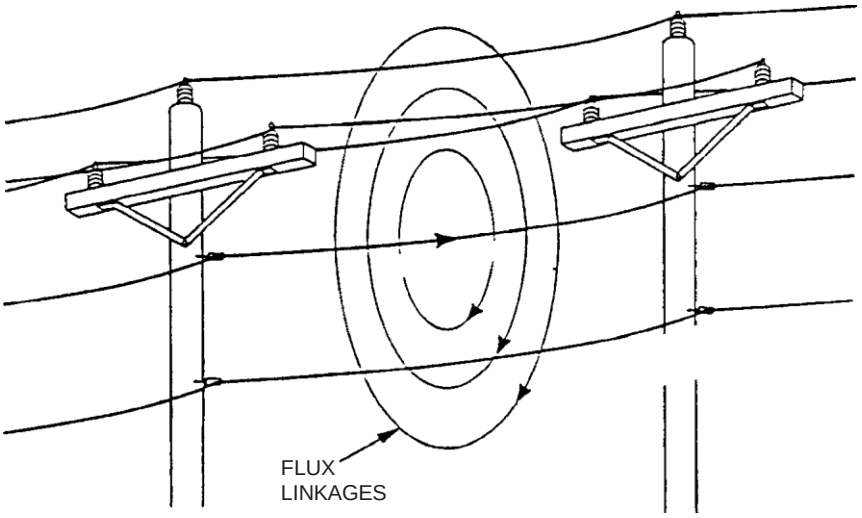

Fig.19. Power system remaining within inductive pairing current to tele-transmission circuit

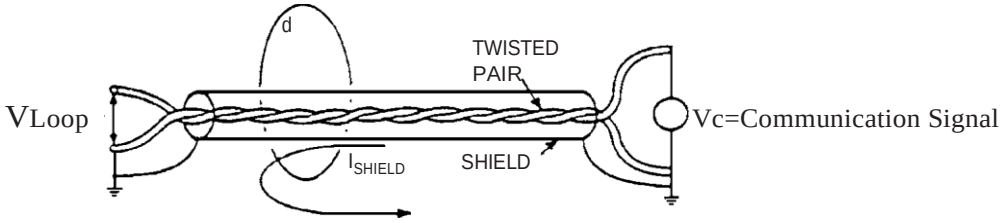

Fig.20 Voltage differences in ground references at cable ends due to an IR drop in the cable shield

.

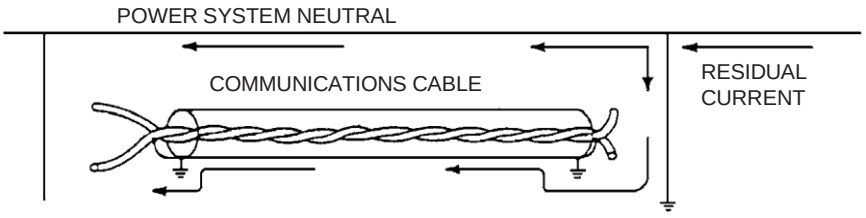

Fig.21. Similar ground way for flowing pair.

2.8.5) Effect on Electrical Metering & Demand Measurement

Utilities in the distribution system typically measure power usage in two main aspects: the sum of all power used and the maximum energy used during a specific time. Consequently, billing for larger commercial customers involves both energy charges and demand charges. Residential customers, on the other hand, are usually billed solely for their power usage.

The power price refers to the costs associated with the generation and delivery of power, calculated by the time used for kilowatt-hours (kWh). The calculation of the second component, the KVA rate, reflects the distributor's rates in maintaining sufficient capacity of energy to meet all users' power usage needs. KVA billing is often calculated through the peak fifteen or thirty-minute high KVA requirement for a specific time, measured in kilowatts (kW).

Both KVA and power bills are quantified using devices known as KVA and watthour devices. The KVA device is typically combined with a watthour device and incorporates periodic mechanisms to confirm high energy usage, resetting the required information to 0 during each periodic cycle (usually fifteen or thirty minutes).

Harmonic currents generated by nonlinear devices can adversely affect the accuracy of KVA devices and watthour devices. Conventional watthour devices operate based on the induction motor theory, where the rotating disk or rotor element within the meter spins at a velocity related to energy transfer. However, traditional disc-type magnetic watthour devices tend to show negative errors in harmonic frequency. In other words, they may record lower energy values in harmonic frequencies compared to the basic frequency, with less decrease at higher frequencies.

Generally, nonlinear devices reject harmonic energy back into the source model, while rectilinear devices contain harmonic energy due to distorted voltage. This relationship is illustrated in Fig. 22[15] by depicting the ways of the currents.

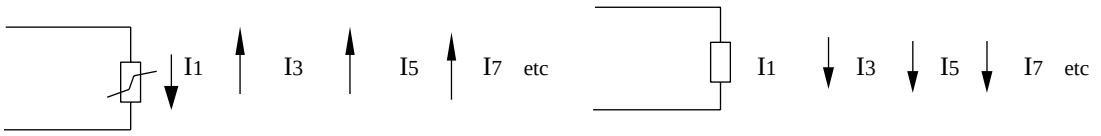

Fig.22. Primary way distorted current in (a) device with non-linearity & (b) device with linearity (with distorted voltage).

Hence in case of device with non-linearity in Fig. 22[15], reading of the device could be

$$P_{\text{measured}} = P_1 - a_{31}P_3 - a_{51}P_5 - a_{71}P_7 - \cdots \quad (2.26)$$

As represented by equation 2.26 for device with non-linearity, the measured power is less than that of actually dissipated the power. Here a_{31}, a_{51} & a_{71} are constant factors for multiplication with less than one value

Similarly, as represented by equation 2.27 for linear device the measure power will be as per the actual.

$$P_{\text{measured}} = P_1 + a_3P_3 + a_5P_5 + a_7P_7 + \cdots \quad (2.27)$$

Hence with the presence of harmonic the demand meter measure faulty power. This is the sever effect of it on measuring meter for demand and power meter.

2.9 Stability analysis of transfer function using bode plots

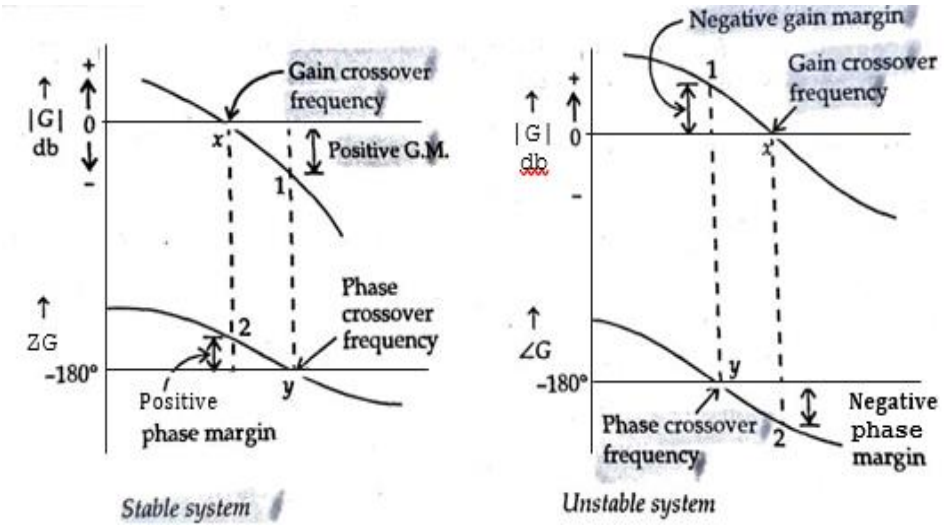

Fig. 23. Phase margin and gain margin

A positive gain margin indicates system stability, while a negative gain margin suggests instability. For a minimum-phase system to be stable, both the phase margin and gain margin must be positive, as illustrated in Fig. 23 [20].

The gain crossover frequency is where the magnitude curve intersects the 0 dB line, while the phase crossover frequency is the point at which the phase curve intersects the 180° line.

Gain Margin: Gain margin represents the permissible increase in gain before the system approaches the brink of instability. Mathematically, gain margin is expressed as the reciprocal of the magnitude of the system's gain G(jw) H(jw) at phase cross-over frequency.

$$G.M = 1/ G(jw)\, H(jw)|_{w=w_{C2}} \qquad (2.28)$$

w_{C2}= phase cross-over frequency.

Generally, G.M is expressed in decibels

Therefere, In decibels $G.M.=20\log x1/ G(jw) H(jw)|w=w_{C2}$ (2.29)

Or, $G.M.=20\log x G(jw) H(jw)|w=w_{C2}$ (2.30)

Phase Margin: In terms of gain, extra phase lag can be introduced without impacting the magnitude plot. Consequently, the phase margin is defined as the quantity of additional phase lag that can be introduced into the system before it approaches the threshold of instability. Mathematically, the phase margin (P.M) can be expressed as:

$$P.M= [<G(jw) H(jw)|w=w_{C2}] –(-180) \quad (2.31)$$

$$P.M.=180+<G(jw) H(jw)|w=w_{C2} \quad (2.32)$$

CHAPTER 3. METHODOLOGY

Fig. 2 depicts a clear illustration of the SAPF arrangement. The nonlinear device is connected to the 3Φ AC system, with the specific nonlinear device considered in this thesis being a 3Φ full-wave diode bridge rectifier connected to a varying device, RL. The SAPF is connected in parallel to the system to provide the harmonic and reactive power consumed by the nonlinear device. Subsequently, the SAPF caters to the harmonic current order of the device, ensuring that only current having a sinusoidal waveform through nearly unity power factor is drawn from the source.

The SAPF generates the reimbursed compensated current, ic. The nonlinear device current, iL, is the summation of the supply current, is, and ic. A coupling inductor is employed to mitigate high-frequency currents stemming from the switching of the Voltage Source Inverter (VSI). As discussed earlier, the SAPF control algorithm involves two primary control loops: a control loop for the inner system and an outer loop. The inner loop utilizes a PI control to track the reference current in the dq-domain. Meanwhile, the outer loop computes the device voltage supply and current, generating the reference reactive and active power to be reimbursed by the SAPF using the principle of a pq-based immediate system, as illustrated in Fig.24[18].

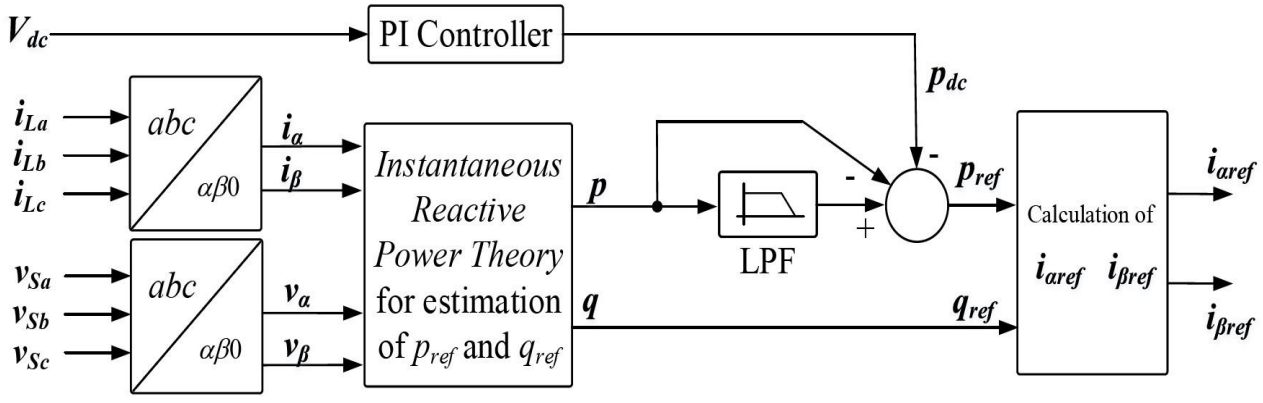

Fig. 24. Outer current control loop for the current reference generation ($i_{\alpha refer}$ and $i_{\beta ref}$)

3.1 Instantaneous p-q theory

Initially, 3-Φ supply instantaneous voltages (v_{sa}, v_{sb} & v_{sc}) & currents of the 3-phase device (i_{La}, i_{Lb} & i_{Lc}) & are observed and using the Clarke's transform transformed to α-β-0 coordinates (i_0, i_α, i_β, v_0, v_α and v_β as shown in eq. 3.1 & 3.2) as follows:

$$\begin{bmatrix} i_0 \\ i_\alpha \\ i_\beta \end{bmatrix} = \sqrt{\frac{2}{3}} \begin{pmatrix} \frac{1}{\sqrt{2}} & \frac{1}{\sqrt{2}} & \frac{1}{\sqrt{2}} \\ 1 & \frac{-1}{2} & \frac{-1}{2} \\ 0 & \frac{\sqrt{3}}{2} & \frac{-\sqrt{3}}{2} \end{pmatrix} \begin{bmatrix} i_a \\ i_b \\ i_c \end{bmatrix} \tag{3.1}$$

$$\begin{bmatrix} v_0 \\ v_\alpha \\ v_\beta \end{bmatrix} = \sqrt{\frac{2}{3}} \begin{pmatrix} \frac{1}{\sqrt{2}} & \frac{1}{\sqrt{2}} & \frac{1}{\sqrt{2}} \\ 1 & \frac{-1}{2} & \frac{-1}{2} \\ 0 & \frac{\sqrt{3}}{2} & \frac{-\sqrt{3}}{2} \end{pmatrix} \begin{bmatrix} v_a \\ v_b \\ v_c \end{bmatrix} \tag{3.2}$$

Next, the instantaneous active power (q) & active (p) consumed by the device are calculated using these currents andvoltages in α-β-0 coordinate as follows:

$$p = v_\alpha i_\alpha + v_\beta i_\beta = \bar{p} + \tilde{p} \tag{3.3}$$

$$q = v_\alpha i_\beta - v_\beta i_\alpha = \bar{q} + \tilde{q} \tag{3.4}$$

here, p˜ & $\bar{p}$ represent the low-frequency & high-frequency elements of immediate active power, while $\bar{q}$ and q˜ denote the low-frequency & high-frequency elements of immediate reactive power. The immediate active power received by the device (p˜+ $\bar{p}$) undergoes filter via a Butterworth-type LPF to eliminate the high-frequency harmonic element (p˜).

Afterward, the output of the LPF is subtracted from the primary instantaneous active power, isolating only the peak-frequency element (p˜). This combination necessarily forms a HPF, selectively extracting the peak-frequency elements of the device active power. In the context of SAPF, this represents the reference reimbursing active power (p_reference). All determined instantaneous reactive power contributes to the reference reimbursing reactive power (q_reference) owing to the SAPF, ensuring components for all reactive power required by the device and maintaining a power factor nearly one with the supply current.

An additional control loop, addressing the loss of active power across the capacitor, is implemented to uphold a fixed DC voltage over it. This involves comparing the standard voltage (700 V) to the capacitor DC voltage. The resulting error is then sent into a PI control, generating the reimbursing active power (p_loss). The inverter is treated as a fixed current supply for the DC part of the voltage control, guiding the PI control design for this supplementary control loop. As a result, for the DC part control, the transfer function of the plant is given by:

$$\frac{V_{DC}}{P_{loss}} = \frac{\frac{1}{CV_{co}}}{S + \frac{2}{RC}} \tag{3.5}$$

In this context, p_loss represents the loss across the capacitor, which is the compensating active power. V_dc signifies the DC bus voltage over the capacitor, the reference capacitor voltage is denoted by , esteemed capacitance is denoted by C, and resistance parallel with the capacitor is denoted by R. Following this, the reference active power computed earlier from the high-pass filter is combined for the DC voltage control with the reference active power loss. Consequently, the reference instantaneous active power and reactive power are

determined as follows:

$$\begin{bmatrix} i_{\alpha ref} \\ i_{\beta ref} \end{bmatrix} = \frac{1}{v_\alpha{}^2 + v_\beta{}^2} \begin{pmatrix} v_\alpha & -v_\beta \\ v_\beta & v_\alpha \end{pmatrix} \begin{bmatrix} \tilde{p} - p_{loss} \\ q \end{bmatrix} \tag{3.6}$$

Here, in the αβ-domain iαreference and iβreference represent the reference reimbursing currents. To enable tracking by the PI control, the reference current in the αβ-domain is transferred into dq-domain which is given by below equation:

$$\begin{bmatrix} i_{dref} \\ i_{qref} \end{bmatrix} = \begin{pmatrix} \cos(\omega t) & \mathrm{Sin}(\omega t) \\ -\mathrm{Sin}(\omega t) & \cos(\omega t) \end{pmatrix} \begin{bmatrix} i_{\alpha ref} \\ i_{\beta ref} \end{bmatrix} \tag{3.7}$$

In this expression, ωt represents the reference frame angle for synchronous, and Id reference & Iq reference denote the reference currents in the dq-domain model. Subsequently, the reference current in the dq-domain is input into a conventionally adjusted PI control, designed with a swapping frequency of twenty kilohertz, a cutoff frequency of four kilohertz, and a forty-five-degree margin angle. This control generates the control signal for the Pulse Width Modulated alternator for the inverter. In this scenario, the cutoff frequency is intentionally set comparatively high to enhance the bandwidth in the PI control. The proposed simulation model will be constructed and evaluated using MATLAB/Simulink, considering a 3Φ3W balanced system. The device with non-linearity consists of a 3Φ full-wave bridge diode rectifier with a DC device of 9000 W. The device simulation involves 6 diodes arranged in a 3Φ bridge arrangement, as depicted in Fig. 2[18]. The resistor RL's value will be determined using a straightforward equation.

$$P = \frac{V_r{}^2}{R_L} \tag{3.8}$$

In this equation, Vr represents the rectifier's output voltage, which, in our case, is 495 V. An energy storage capacitor with a 700 V DC rating is utilized. The PWM inverter operates at a s

frequency for switching of twenty kilo hertz. The total impedance of Grid part is specified as Zsource = $(\frac{1}{10} + j\ \frac{38}{10^5})$ Ω, & the impedance of the device part is considered as Zdevice = $(\frac{1}{10} + j\frac{38}{10})$ Ω. The simul elements of standard are provided in Table I, and those for the Variable Frequency Drive (VFD) device replication of the standard are detailed in Table II.

Table I		
S.N.	Parameter	Value
1	Inductance of coupler	10mH
2	Internal resistance of coupling inductor	$\frac{1}{10}\Omega$
3	Resistance of grid	$\frac{1}{100}\Omega$
4	Inductance of grid	10^{-6} H
5	Resistance of device part	$\frac{1}{100}\Omega$
6	Inductance of device part	$\frac{1}{100}$H
7	Capacitance of DC bus capacitor	2200 µF

Source of Table I parameter:[18]

Table II		
S.N.	Parameter	Value
1	DC filter capacitor	4200 µF
2	DC filter inductor	181 µH

Source of Table II parameter:[14]

In this thesis, The Total Harmonic Distortion (THD) is employed as the present metric to assess the effectiveness of the PI control approach. THD is calculated as follows:

$$THD = \frac{\sqrt{\left(I_2^{\,2} + I_3^{\,2} + I_4^{\,2} \ldots\ldots\ldots\ldots\ldots + I_n^{\,2}\right)}}{I_1^{\,2}} \qquad (3.9)$$

In this expression, I_2, I_3, I_4, ..., I_N represent the root-mean-square (RMS) values of harmonic 2, 3, 4, … up to N, correspondingly, and I1 is the RMS value of the basic supply current. The Nth harmonic order corresponds to the Nyquist frequency, which is 1/2 the modeling frequency of the chosen signal. In our scenario, the modeling frequency is one megahertz, and the substituting frequency is twenty megahertz. Consequently, the Nyquist condition is met.

3.2 Design of PI Control

The comprehensive illustration of the inner loop for current control in the Voltage Source Inverter (VSI) is presented in Fig. 25[18]. Faults in the dq-domain response currents (Iq & Id) are directed to PI controls, and the output from these controls generates the corresponding modifying indicator for the inverter of PWM type. The inverter's gate indicators are produced with this modifying indicator, considering cross-coupling parts IqωL & IdωL, and the addition of feed-forward parts. Following this, by using the inverse Park's transform, the indicator undergoes a transformation from dq to abc systems. The PI type-2 control includes an additional pole in the high-frequency range, aiding in attenuating the substituting rackets in the model.

The voltage source control by current comprises adjustments, the pairing inductor, and the PI control. The plant for the PI control's design is:

$$G_{plant(s)} = \frac{\frac{1}{L}}{s + \frac{r}{L}} \tag{3.40}$$

Considering the constraints outlined in Table I, the handover function for system is expressed as:

$$G_{plant(s)} = \frac{100}{s+10} \tag{3.41}$$

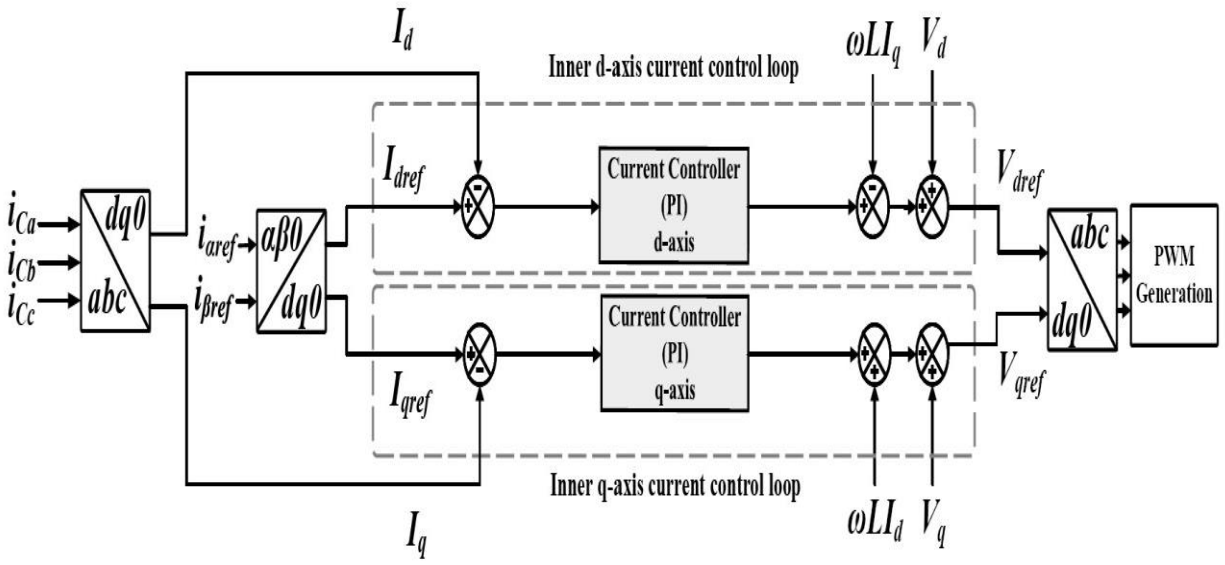

Fig. 25. overall diagram of the inner loop for current control in the VSI (fig.2.)

Reference Design of LC Filter 2.6, the PI type-2 control is:

$$H_{controller(s)} = \frac{251.54s + 2609023}{16.521e^{-6}s^2 + s} \tag{3.42}$$

Similarly, to maintain the voltage over the DC link capacitor, an additional PI control loop is essential, as explained in Section 3.1. To formulate this control loop, the allocation function provided in equation 3.5 is employed.

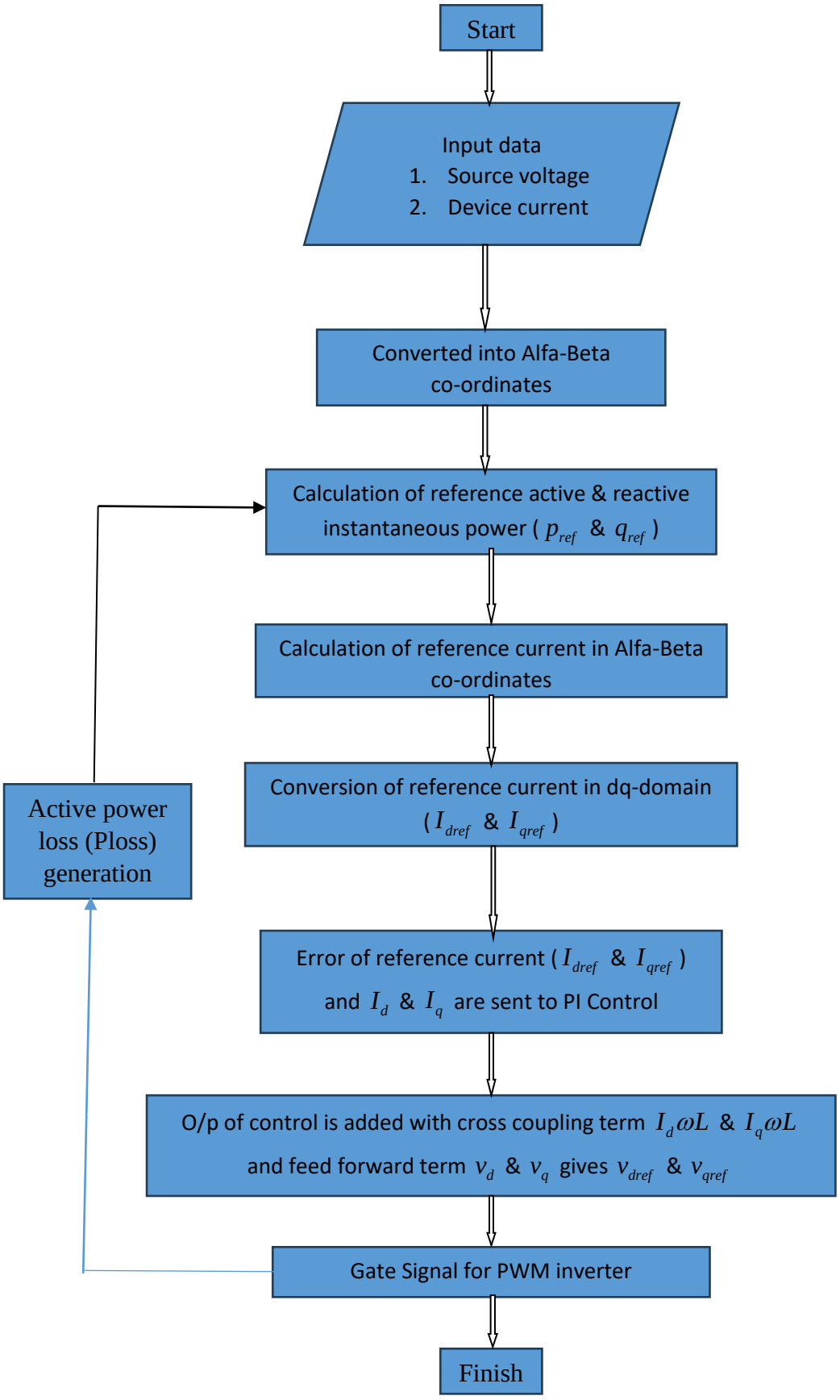

Fig. 26. Flow chart of the proposed method

CHAPTER 4. SYSTEM UNDER CONSIDER, TOOLS AND SOFTWARE

4.1 System Validation

MATPOWER's MATLAB Simulink system was chosen to assess the model's performance. After the system is tested, the model will be validated on distribution feeders in industries under the Balaju Industrial area.

4.2 Tools & Software

Technological advancements in computer architecture, software, and programming tools have made the modeling and analysis of power systems easier. In the past, modeling and analysis were difficult, time-consuming, and inaccurate. Many software tools use mathematical modeling to simulate the performance of a power system and its active components. MATLAB has been used in this thesis for simulation, along with the MATPOWER 7.1 environment.

4.3 MATLAB

MATLAB, short for Matrix Laboratory, is a user-friendly and highly interactive programming tool developed by MathWorks. It can be used to simulate a large number of engineering problems. In this thesis, the MATPOWER 7.1 package is integrated with MATLAB for the analysis of test bus systems.

4.4 MATLAB SIMULation AND MODELING

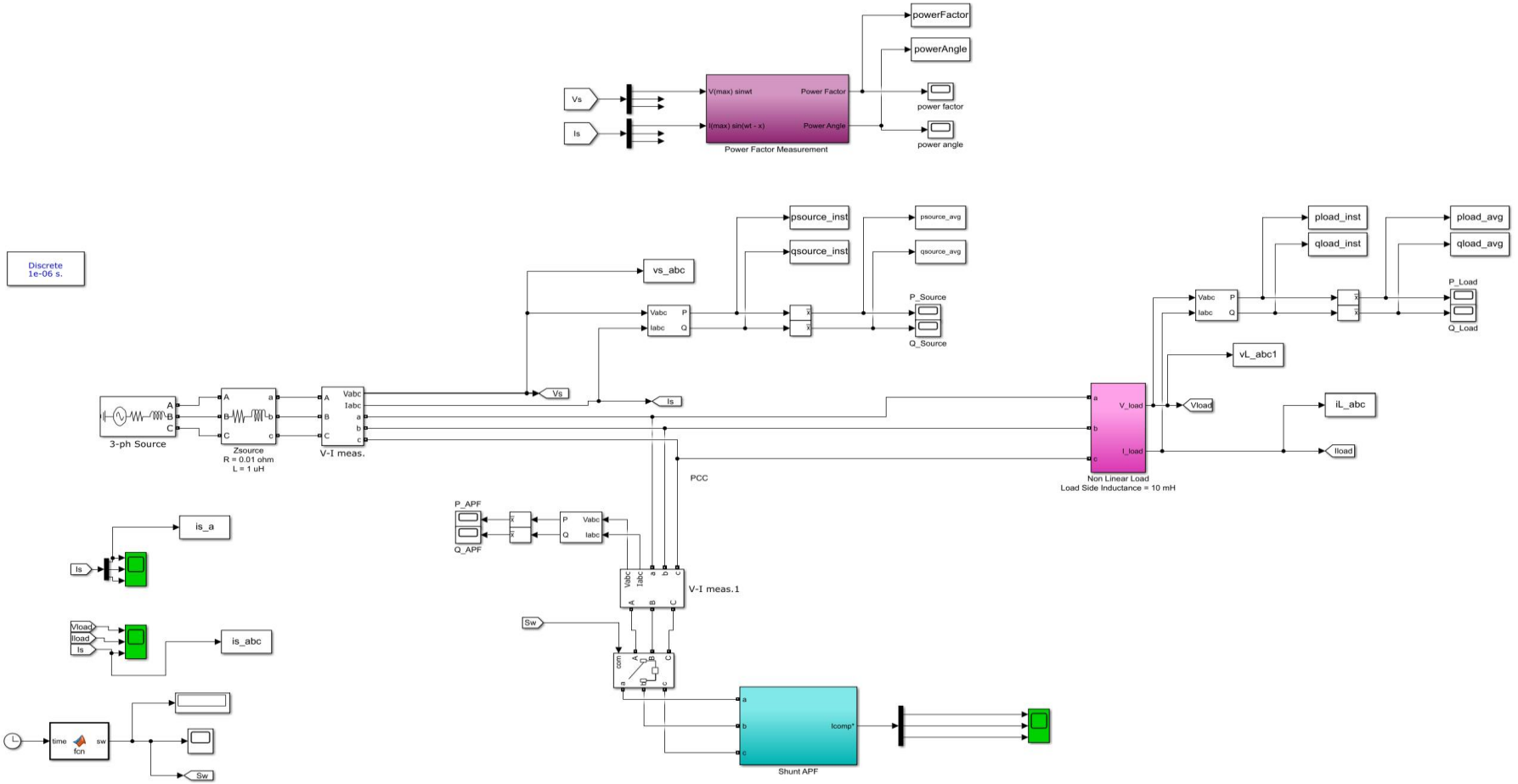

Fig.27. Overall, MATLAB Simulation of SAPF in 3phase 3wires System

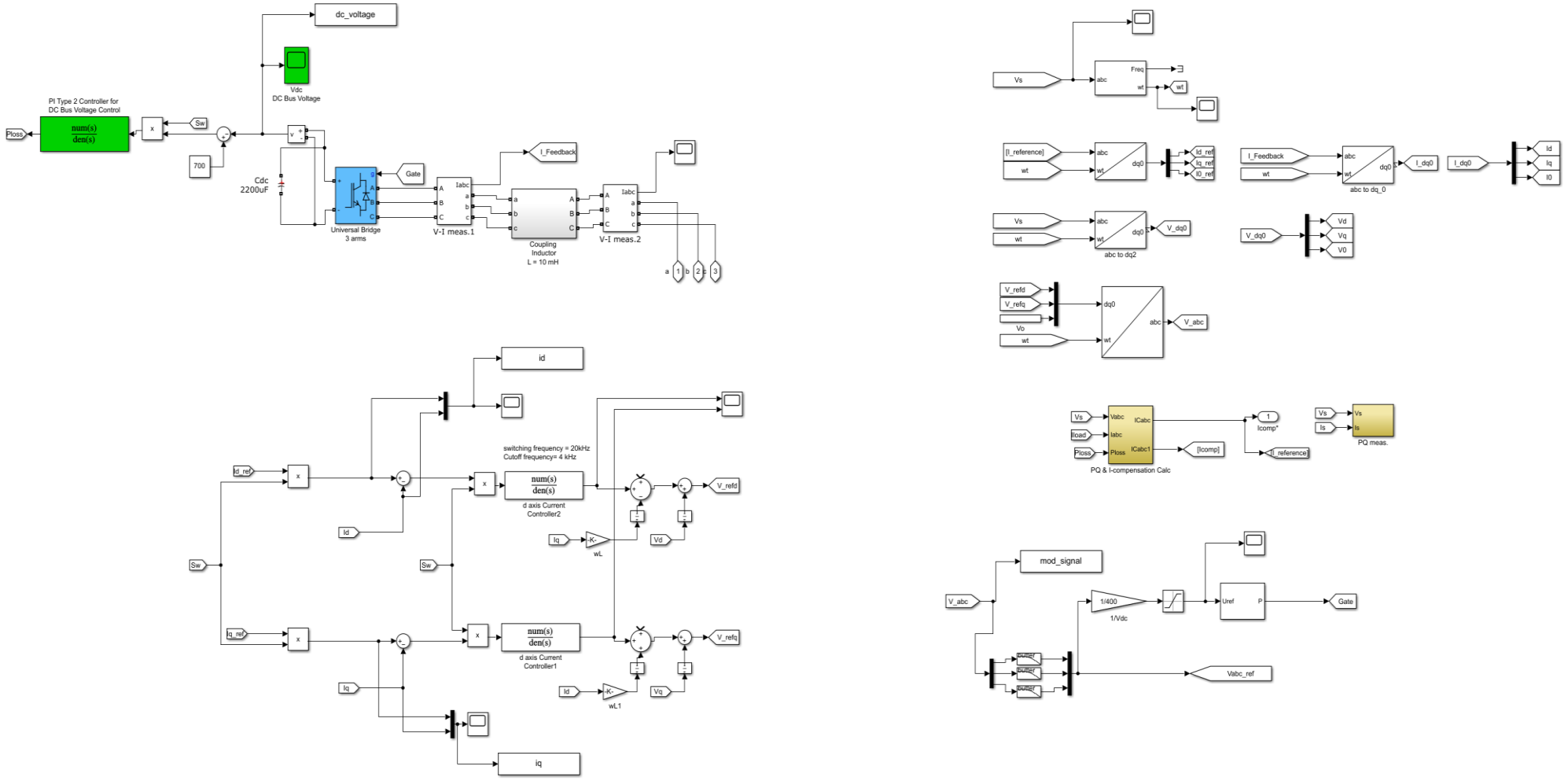

Fig.28.Overall, MATLAB Simulation inside SAPF Block

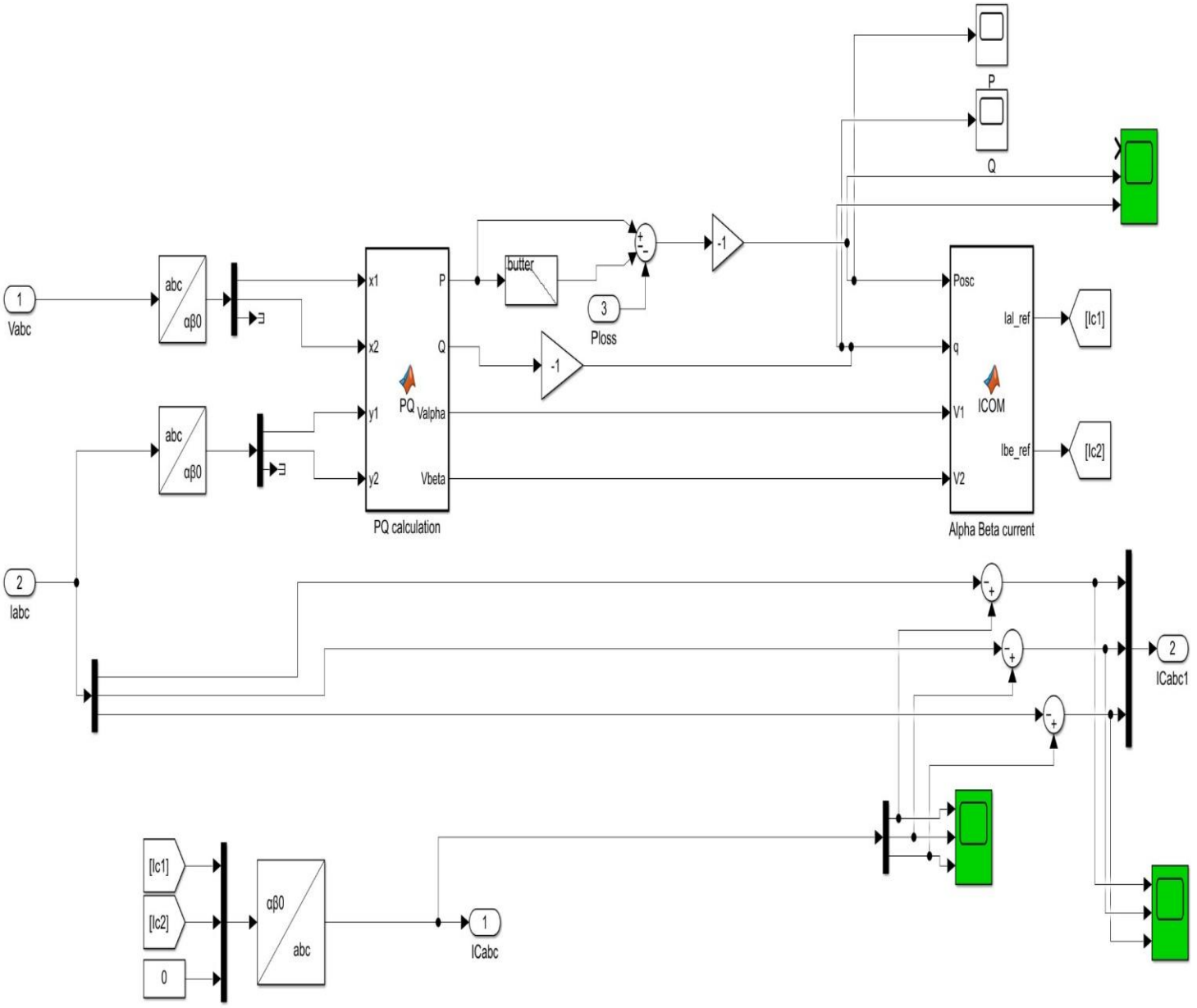

Fig.29. MATLAB simulation of outer loop inside Shunt APF block

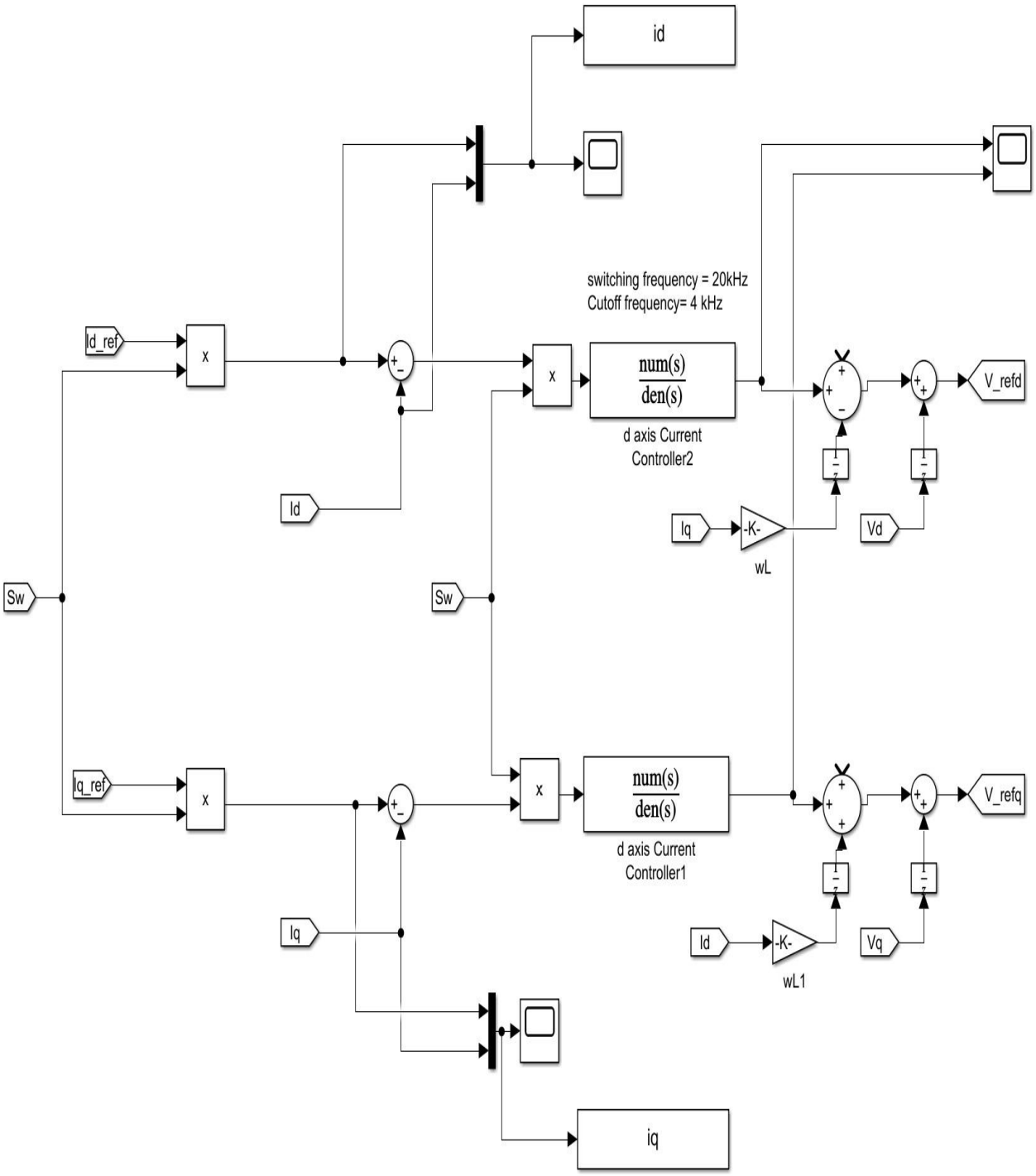

Fig.30. MATLAB simulation of inner loop inside Shunt APF block

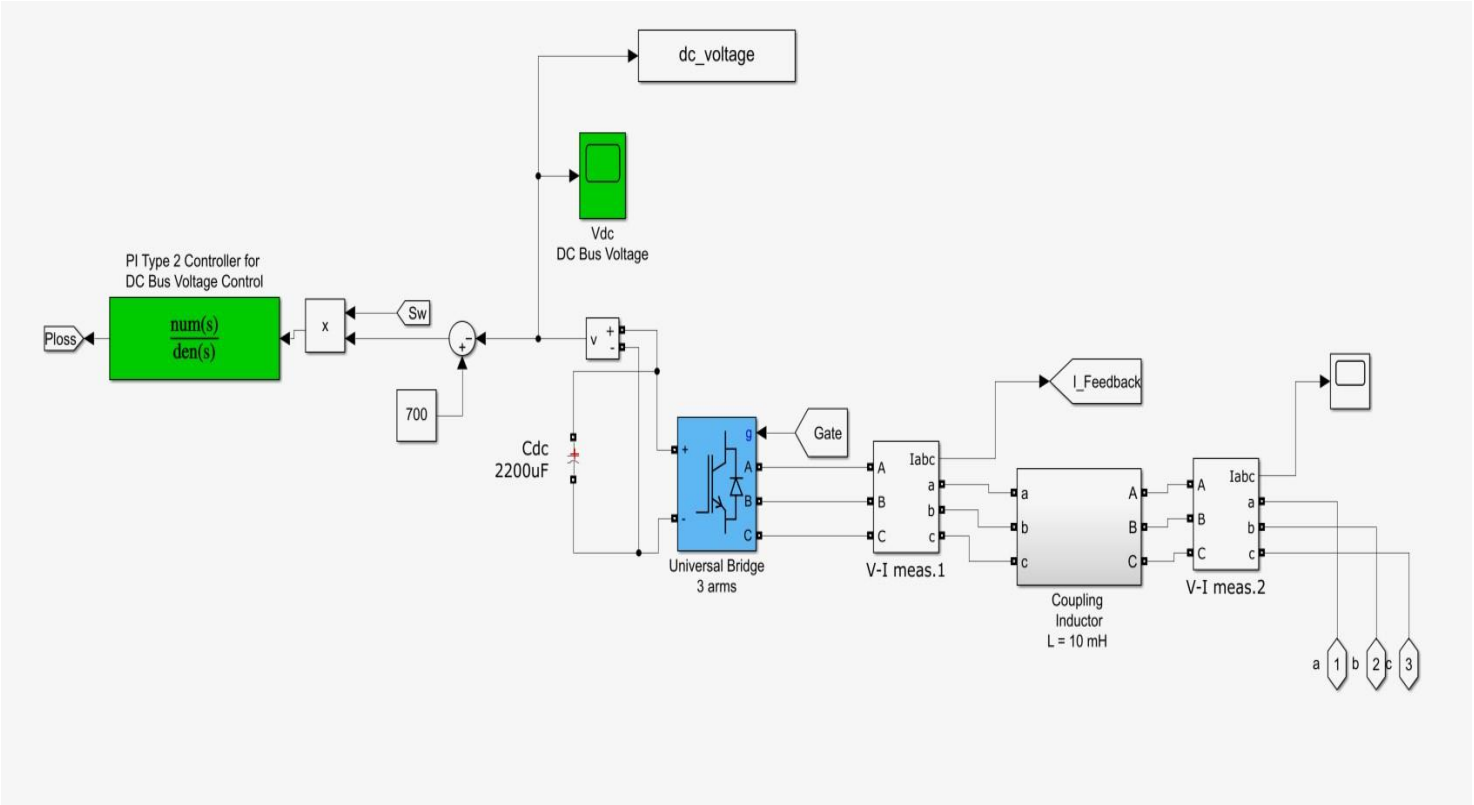

Fig.31. MATLAB simulation of extra loop inside Shunt APF block for 3 phase 3 wire system

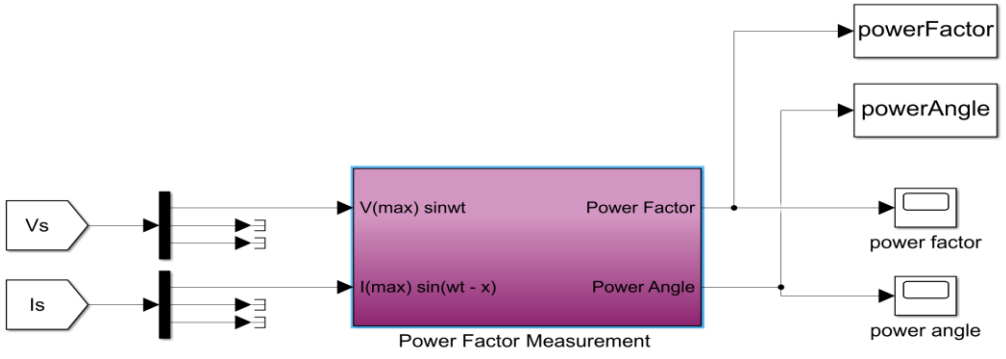

Fig.32.Power Factor Measurement in MATLAB Simul

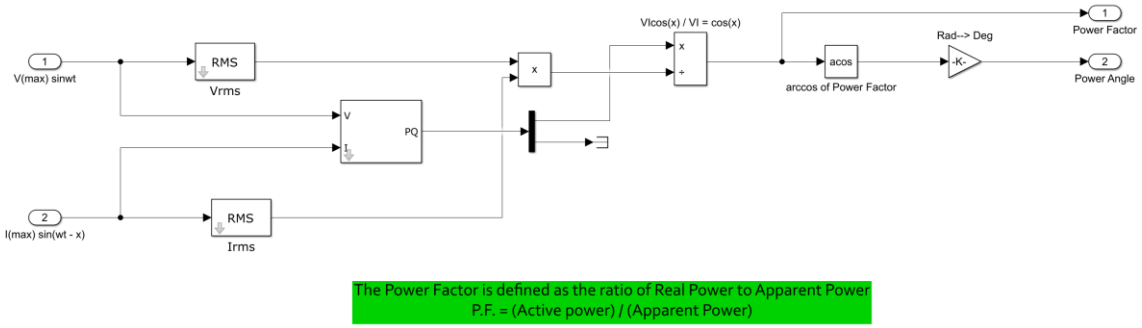

Fig.33.Components inside Power Factor Measurement block in MATLAB Simulation

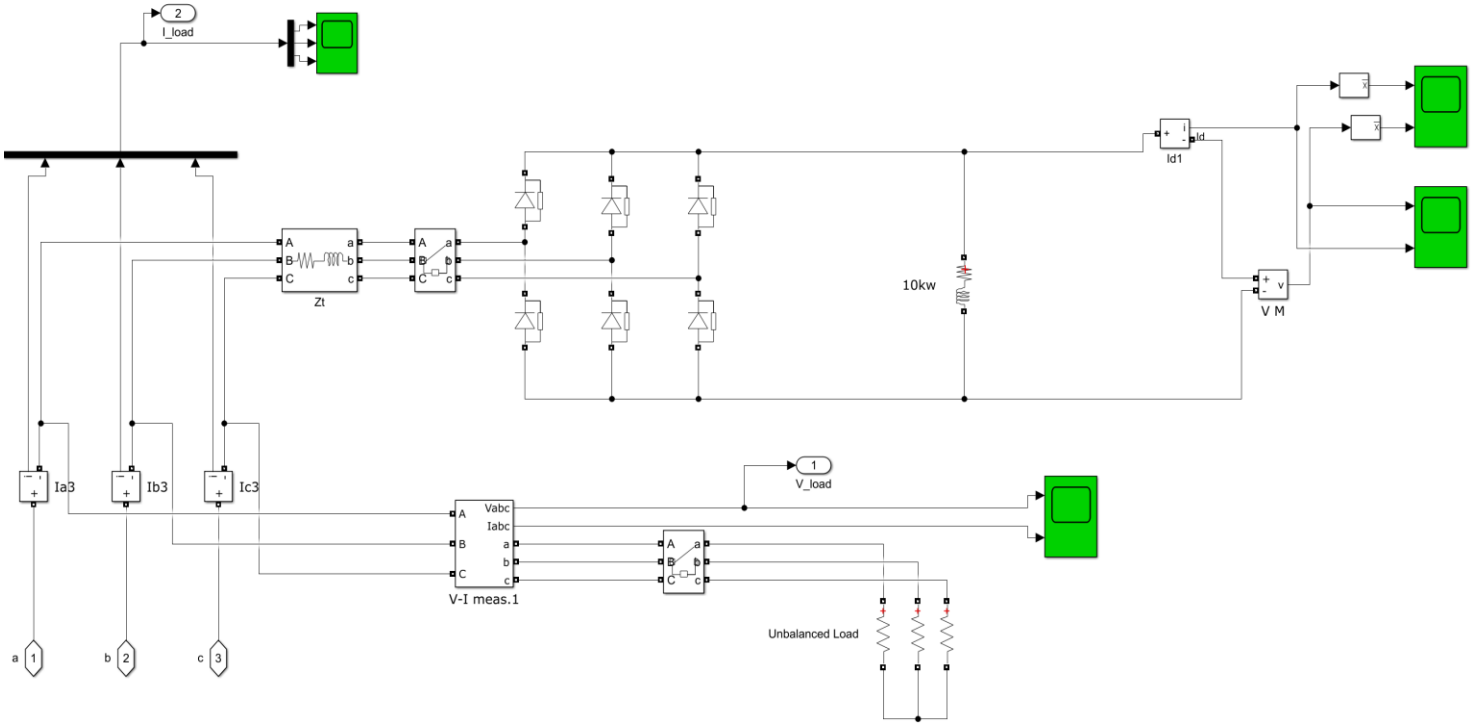

Fig.34.Non-Linear Three phase Device for 3phase 3wire System in MATLAB simulation

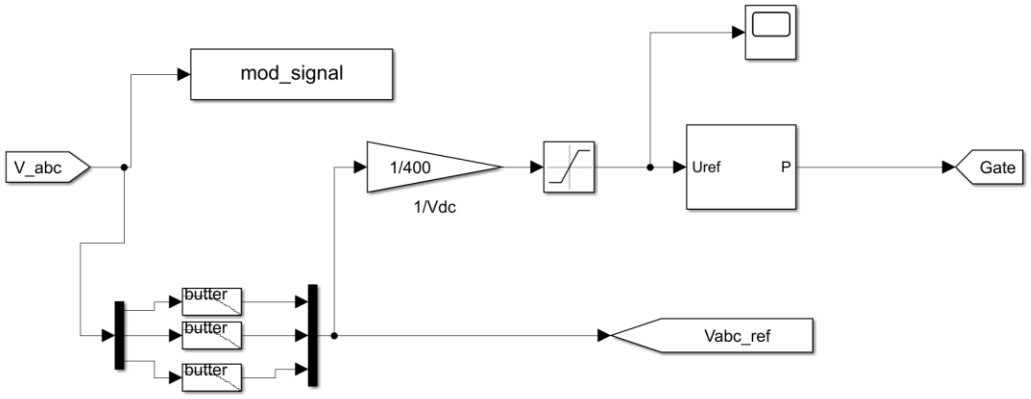

Fig. 35 MATLAB simulation of Gate signal for PWM inverter

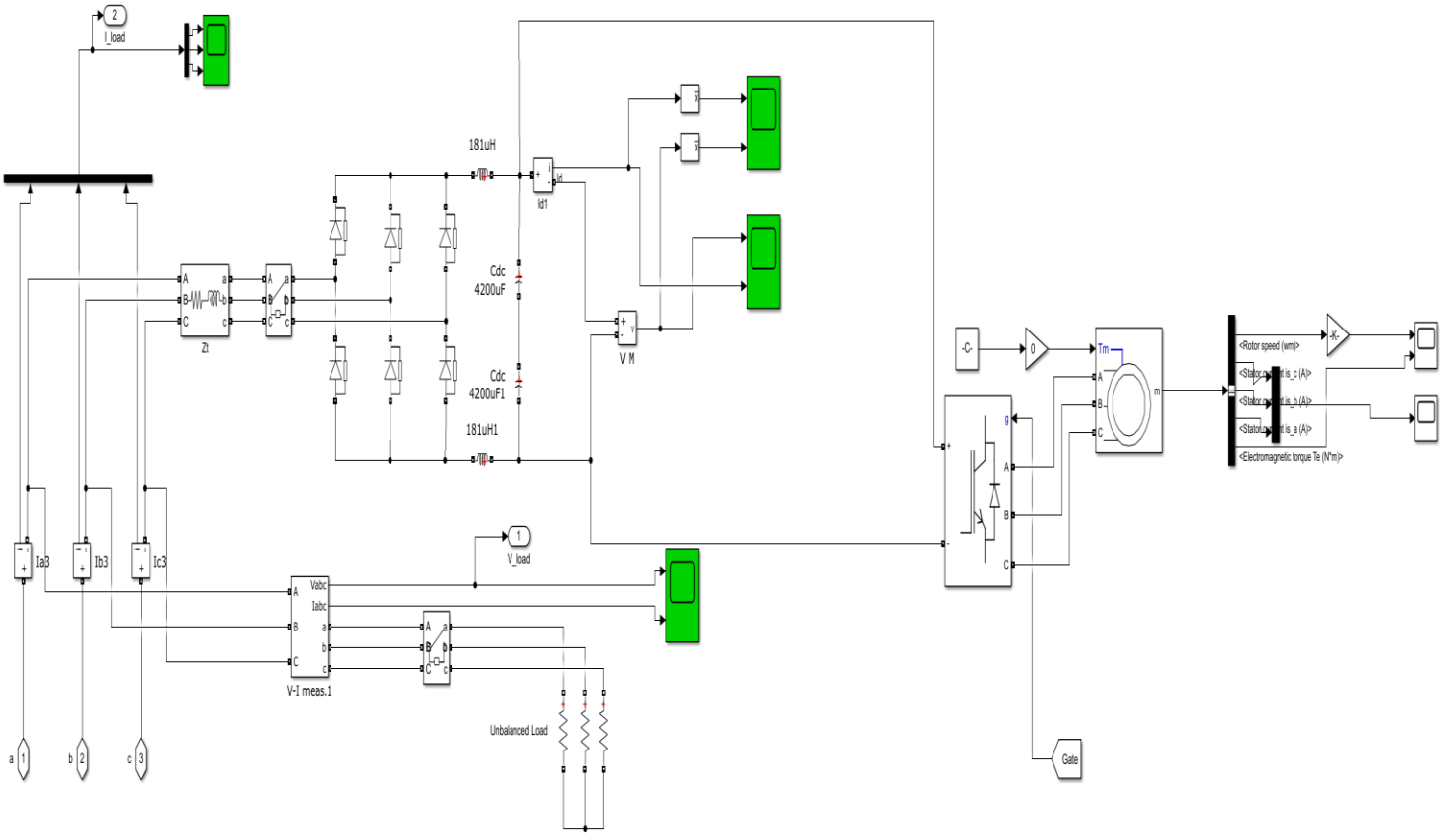

Fig.36. MATLAB simulation of VFD (variable frequency drive) as non-linear device

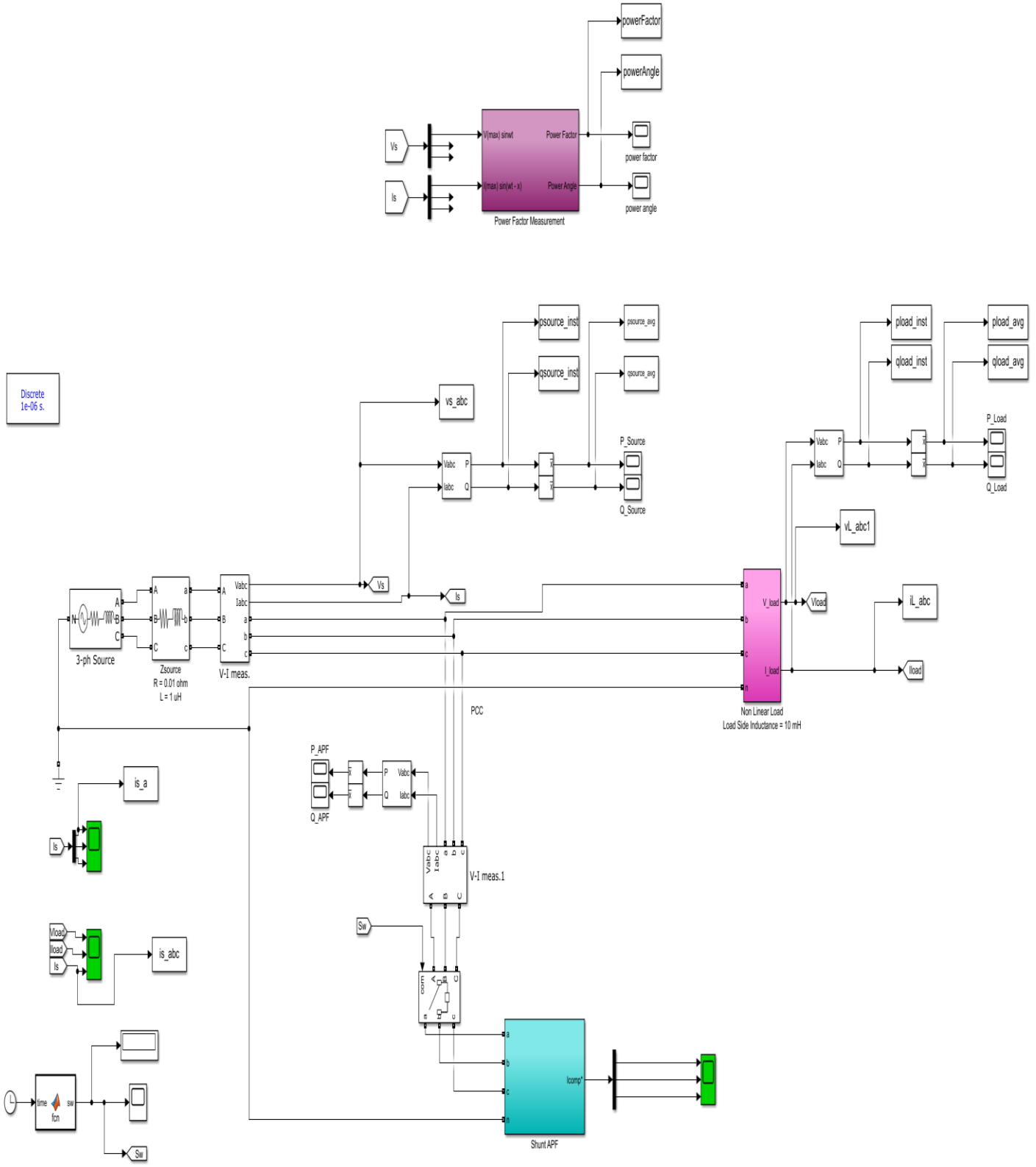

Fig.37. Over all MATLAB simulation & modeling of 3phase 4wire system

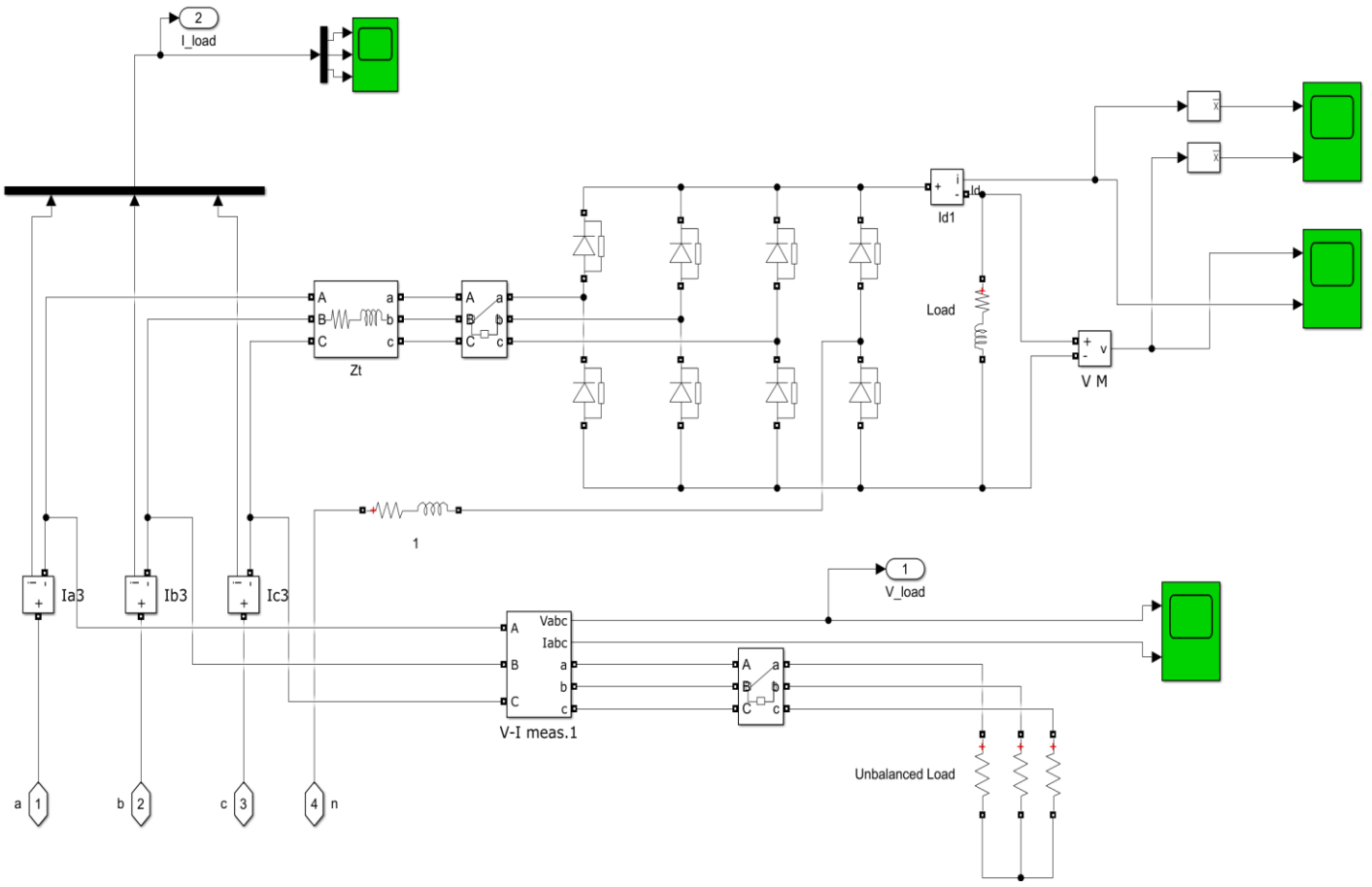

Fig.38. Non-Linear Three phase Device for 3phase 4wire System in MATLAB simulation

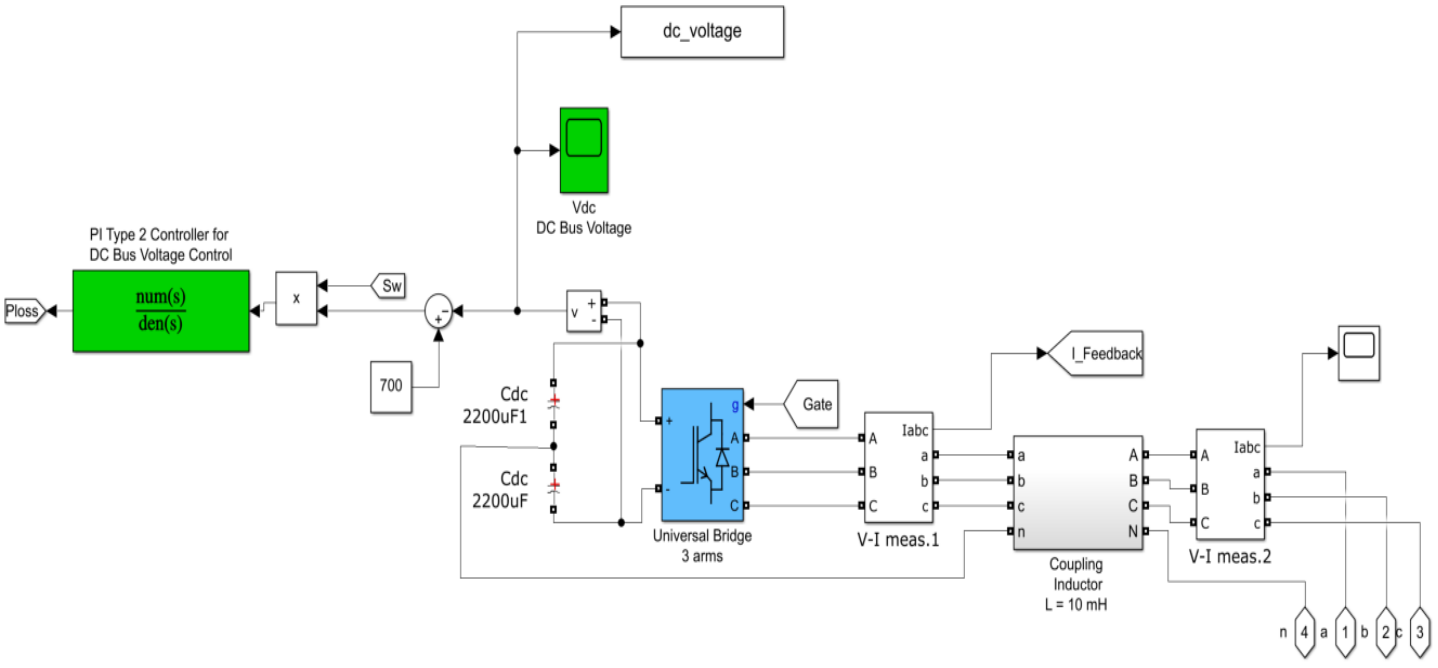

Fig.39. MATLAB simulation of extra loop inside Shunt APF block for 3phase 4wire System

CHAPTER 5. Results and Discussion

Five case studies were performed:

Case I: In the initial case study, the emphasis was on enhancing current harmonics by integrating a SAPF into a 3-phase 3-wire system with conventional PI control in the inner current loop.

Case II: The second case study involved evaluating the performance of the traditional PI control approach under varied device conditions for a 3-phase 3-wire system.

Case III: In the third case study, the focus was on improving current harmonics by incorporating a SAPF into a 3-phase 4-wire system with traditional PI control in the inner current loop, and this was evaluated under different device conditions.

Case IV: The fourth case was a performance investigation of SAPF where the three-phase device is a VFD.

Case V: The sixth case was an application of MATLAB simulation of SAPF in the industries of Nepal.

5.1 Case I:

For Case Study I, a 3-phase full diode bridge rectifier, as described in Chapter 1, was employed as the nonlinear device, as depicted in Fig. 1. A 27 Ω device resistance, determined from Eq. (39), was utilized to model the 9000 W device. The three-phase AC source, operating at a frequency of 50 Hz and a line-to-line root-mean-square (RMS) voltage of 400 V, was connected to this device. The Total Harmonic Distortion (THD) was then calculated using the fast Fourier transform (FFT) analysis tool in the powergui block within Simulink, considering 10 cycles of the source current waveform. For THD calculation, Eq. (40) with a sampling time of 1 μs was applied.

Before connecting the SAPF, the current (iS) supplied by the source exhibited distortion with a high THD of 18.19%, as illustrated in Fig. 40. In Fig. 41, a performance comparison

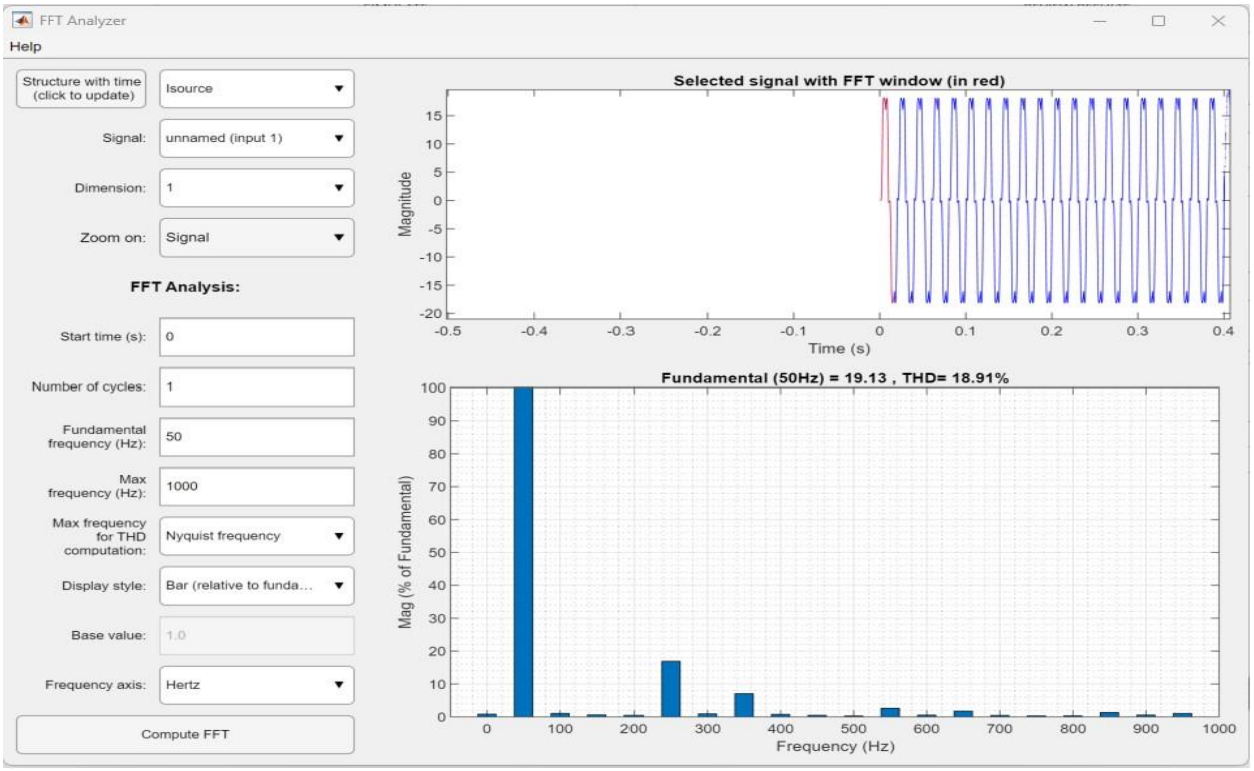

Fig.40. Fig: FFT analysis result for the source when no SAPF is connected

is presented between a traditional PI control and the PI control with a trailing bend for the quadrature current (Iq) and direct co-ordinate current (Id), denoted by "Id" in Fig. 16 and "Iq" in Fig. 42, respectively. "Idref" and "Iqref" represent the reference currents that need to be followed. Upon connecting the SAPF after 0.4s, the early capacitor charging instigated temporary performance with limited effects. After a few cycles, with the conventional PI control, the THD of the supply current reduced to 2.06%, as depicted in Fig. 43.

The 2.06% THD observed with the PI control alone resulted from inefficient tracking of the reference currents Idref and Iqref, as indicated in Figs. 41 and 42. However, the supply current transitioned to a sinusoidal waveform with fewer harmonic components. Consequently, as per Eq. (39), the THD was enhanced with the incorporation of SAPF. This improvement in total harmonics, reflected in terms of THD, was the rationale behind SAPF's inclusion. ability to deliver improved performance during step responses and variations in nonlinear devices.

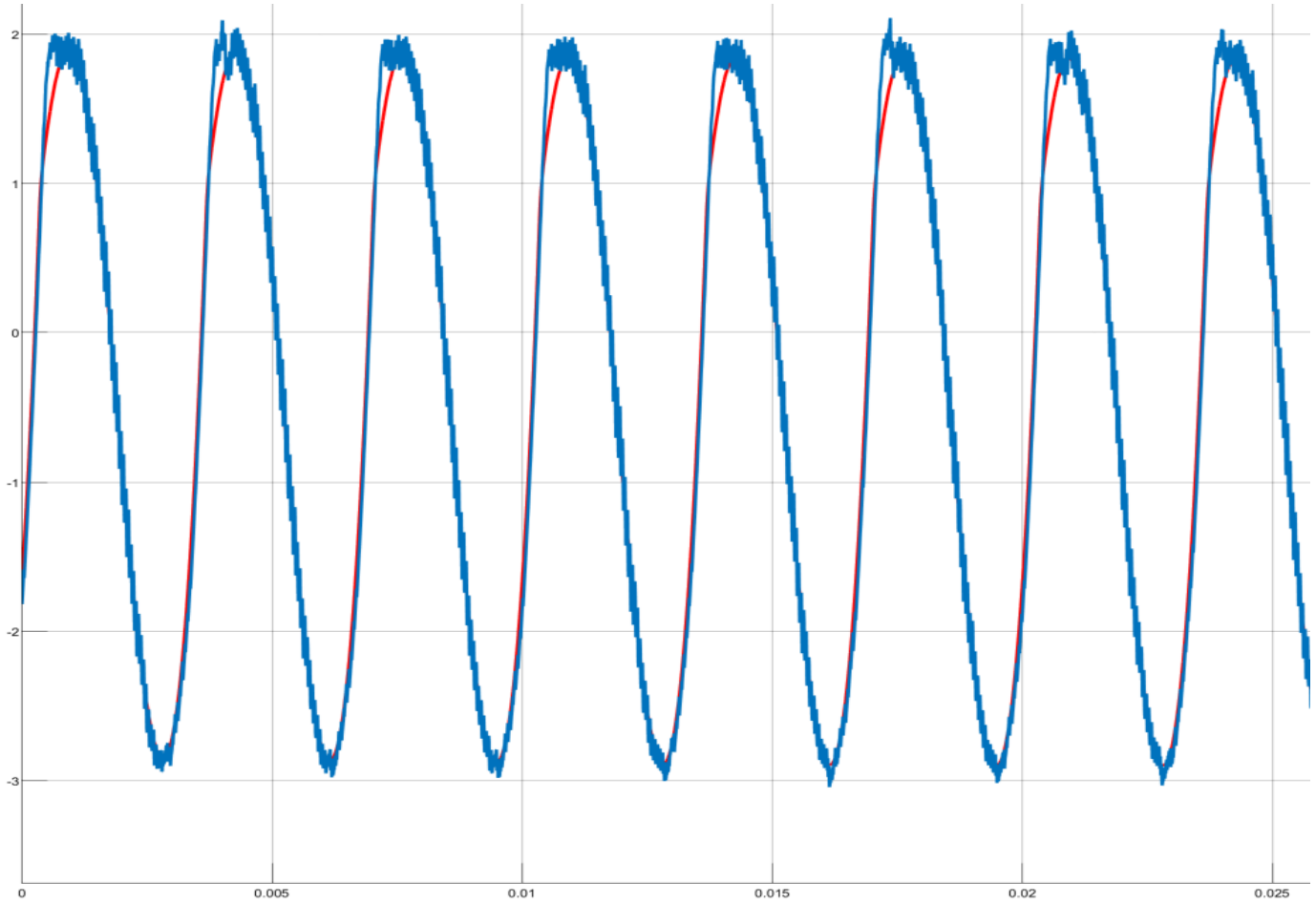

Fig 41: Performance of PI control technique with tracking curve in d-domain current I_d (Current Vs Time)

Figures 44, 45, and 46 depict the active response of the SAPF-connected system. In Fig. 44, the device current for the abc phase is shown. Fig. 45 displays the compensating current produced by the SAPF for the A phase. Fig. 46 illustrates the source current with the SAPF connected after 0.4 seconds, where the notches are attributed to tracking errors in Iq reference current, as shown in Fig. 18. Additionally, Fig. 17 presents the FFT analysis.

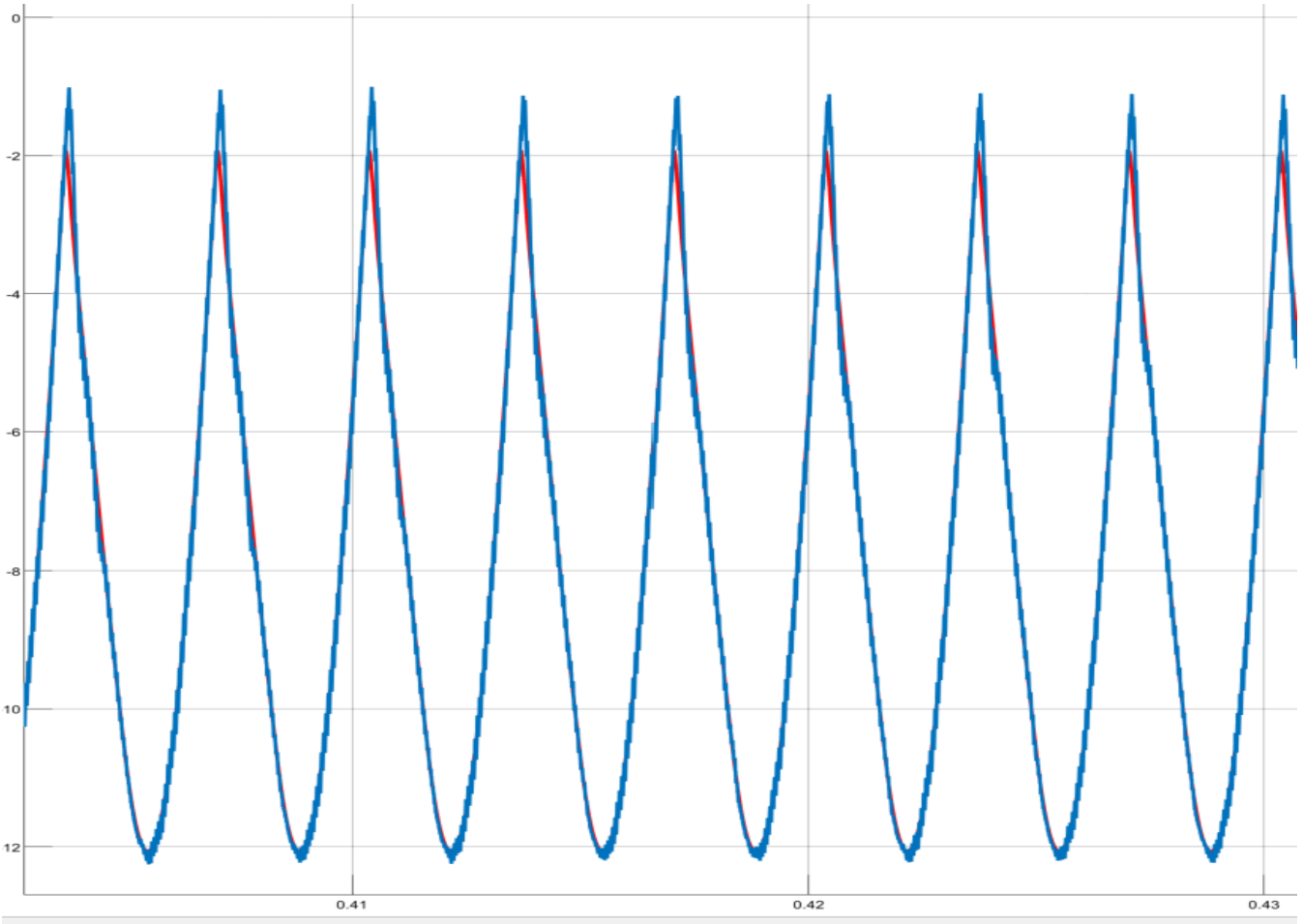

Fig 42: Performance of PI control technique for tracking curve in q- domain current Iq (Current Vs Time)

result from Simulink for the current supply when the SAPF is not connected. In Fig. 43, the FFT analysis result from Simulink is displayed for the source current when the SAPF is connected. The 5th, 7th, and 11th harmonics are dominant and challenging to remove by the LPF due to the nature of the 3-phase non-linear device being used. As depicted in Figure 47, the power factor of the system improves, approaching unity when the SAPF is connected for the 9 kW device.

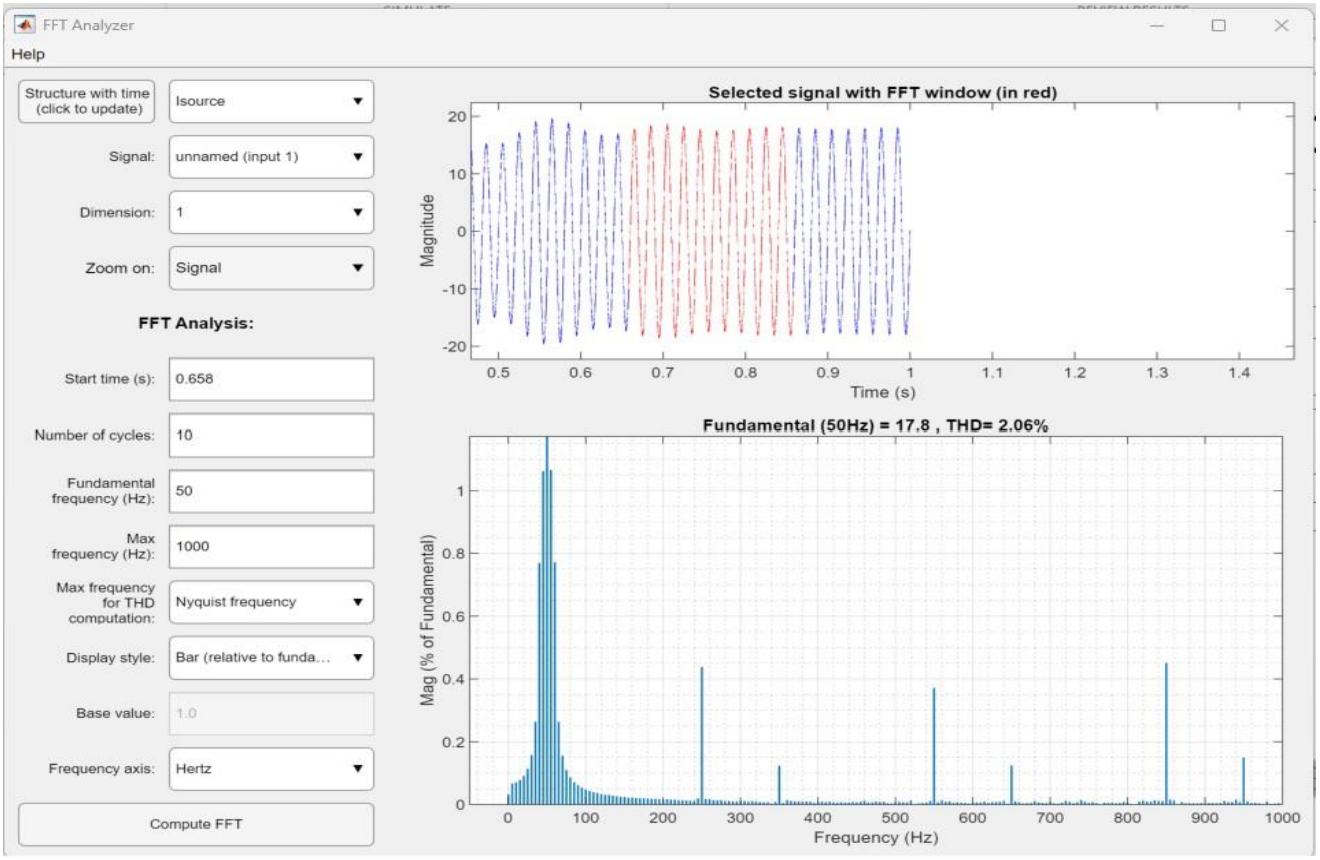

Fig.43. FFT analysis result for the source when SAPF is connected

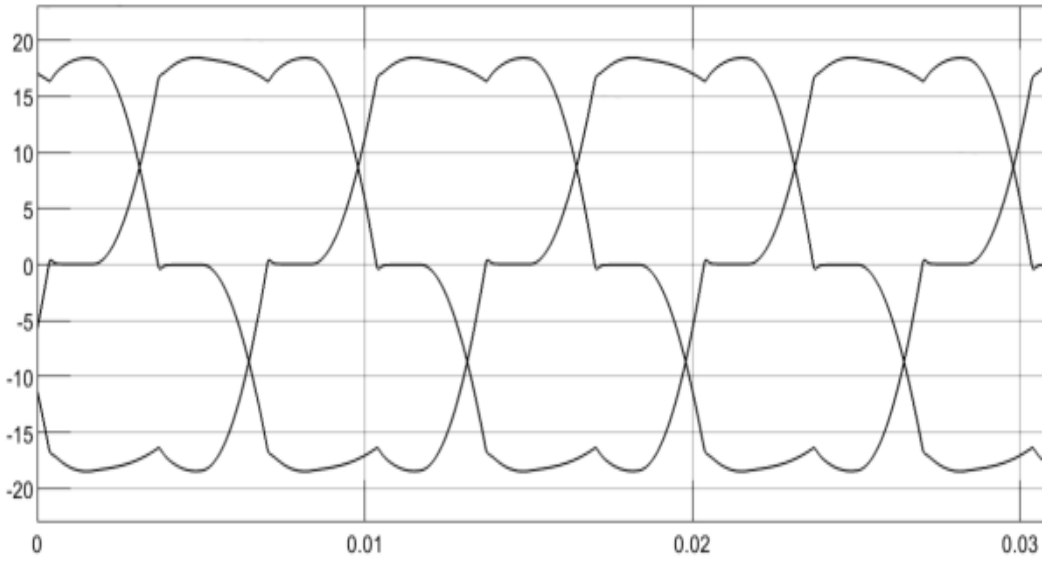

Fig 44: Dynamic response of the 3φ SAPF associated supply; displays the device current for abc phases (Device Current Vs Time)

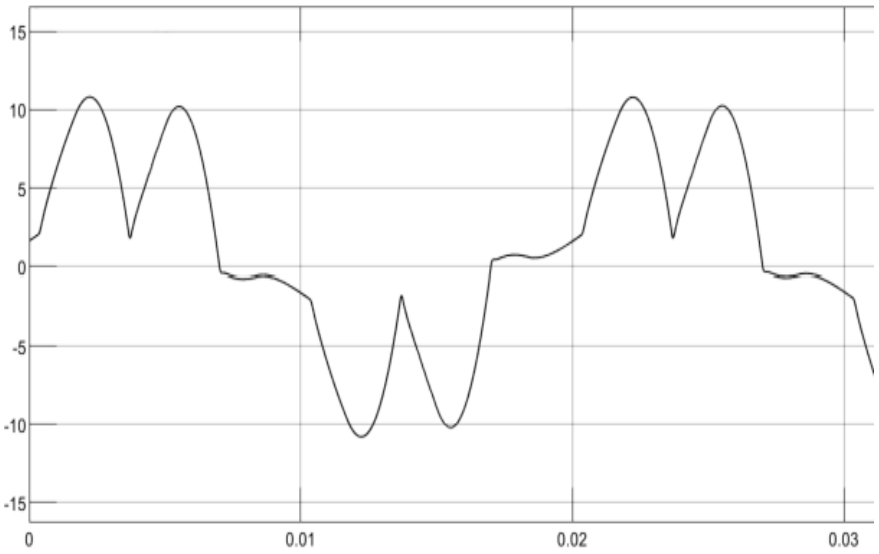

Fig 45: Dynamic response of the SAPF associated source; displays the compensating current produced by SAPF for phase a (Current Vs Time)

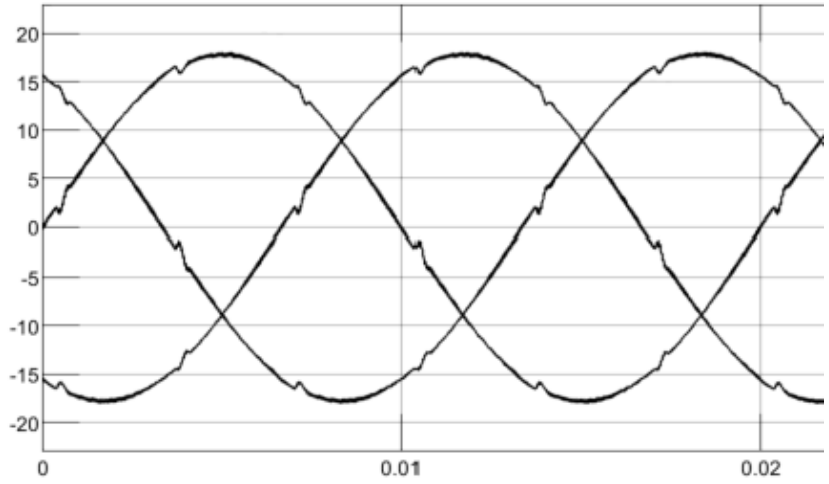

Fig 46: Dynamic response of the 3φ SAPF associated source after 0.4s; displays the source current where the notches are due to tracking errors in Iq reference current (Current Vs Time)

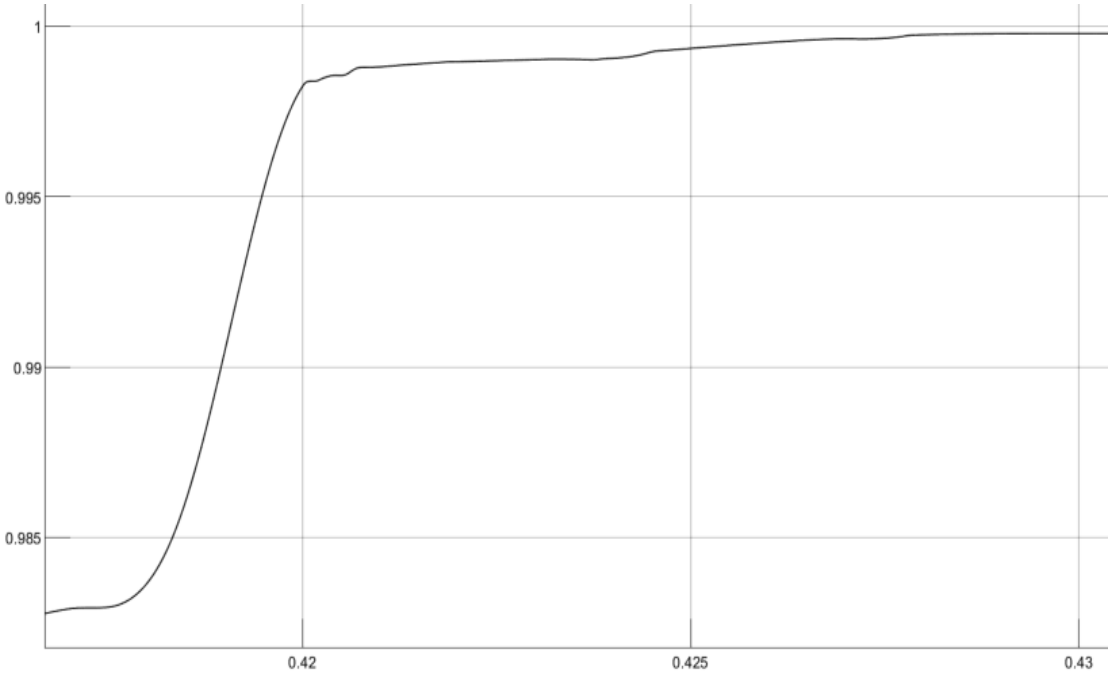

Fig 47: Development of the pf of the system when SAPF is connected (p.f. vs Time)

5.2 Case II

Various device conditions ranging from 1000 W to 20000 W were simulated by adjusting the RL value from 12 ohms to 245 ohms. Table III presents a THD comparison of the source current under these diverse loading circumstances. Without the SAPF in place, the THD performance was suboptimal across all device conditions. This can be attributed to the fact that THD increases as the device load decreases. Nevertheless, the control yielded the most favorable THD outcomes for the supply current.

Table III

Performance comparison of SAPF under different device conditions for 3phase 3wire

Device	THD Without SAPF	THD With SAPF
1000W (245ohm)	27.53%	5.8%
2000W (122ohm)	25.91%	4.96%
3000W (81.66ohm)	24.60%	4.17%
4000W (61.26ohm)	23.41%	4.01%
5000W (49ohm)	22.22%	3.91%
6000W (40.8ohm)	21.20%	3.69%
7000W (35ohm)	20.23%	2.69%
8000W (30.6ohm)	19.51%	3.63%
9000W (27.2ohm)	18.9%	2.06%

10KW (24.5ohm)	18.40%	2.98%
12KW (20.4ohm)	17.59%	1.94%
14KW (17.5ohm)	16.18%	2.75%
16KW (15.31ohm)	16.53%	2.83%
18KW (13.61ohm)	16.22%	4.03%
20KW (12.25ohm)	15.98%	4.85%

5.3 Case III

This is similar with the case I. only difference is case I for 3phase 3wire system while case III for 3phase 4wire system. Here also we took device 9KW device. The THD level before connection of SAPF was 18.82% while without SAPF was 3.47%.

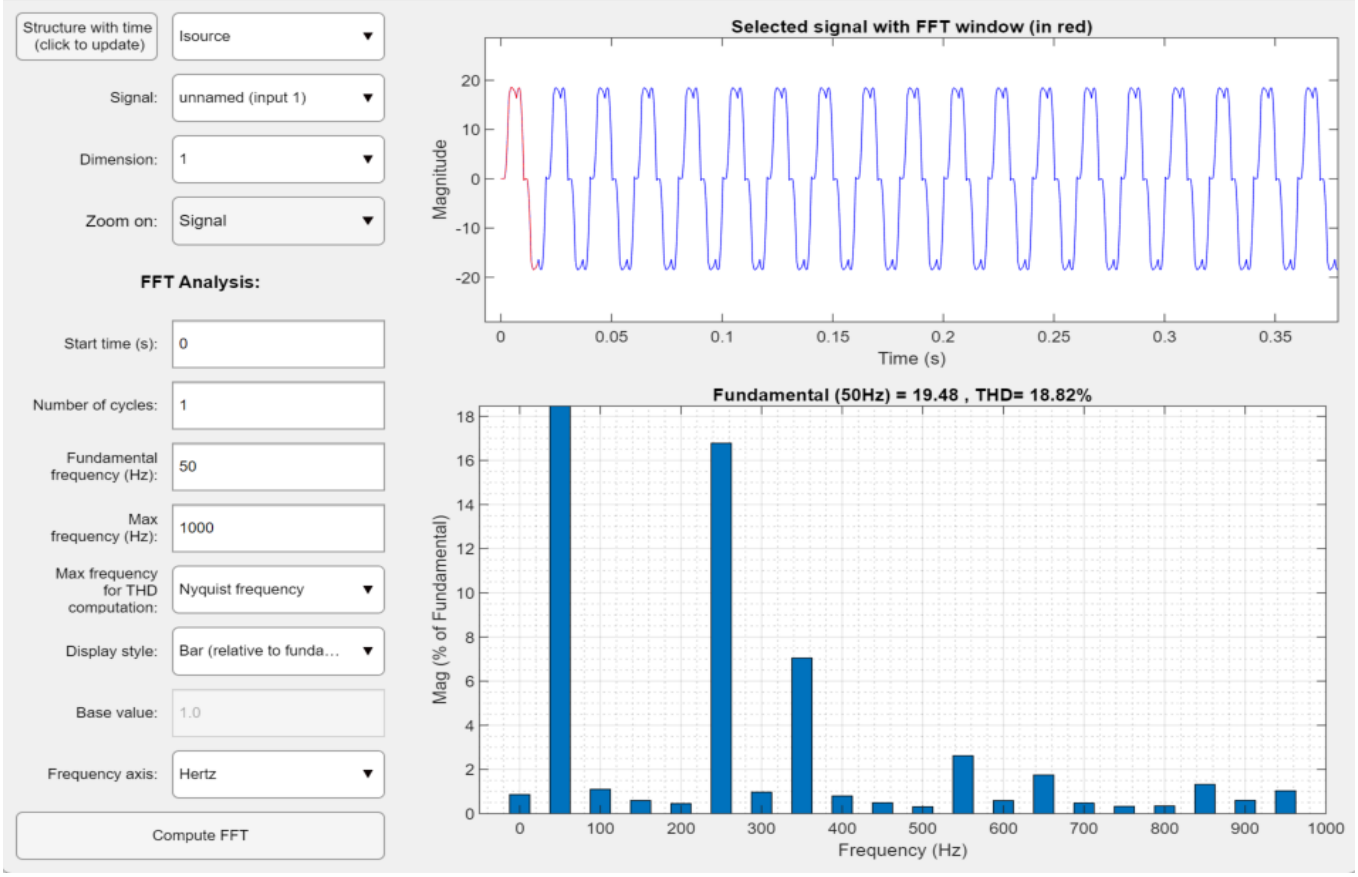

Fig.48. Fig: FFT analysis result for the source when no SAPF is connected

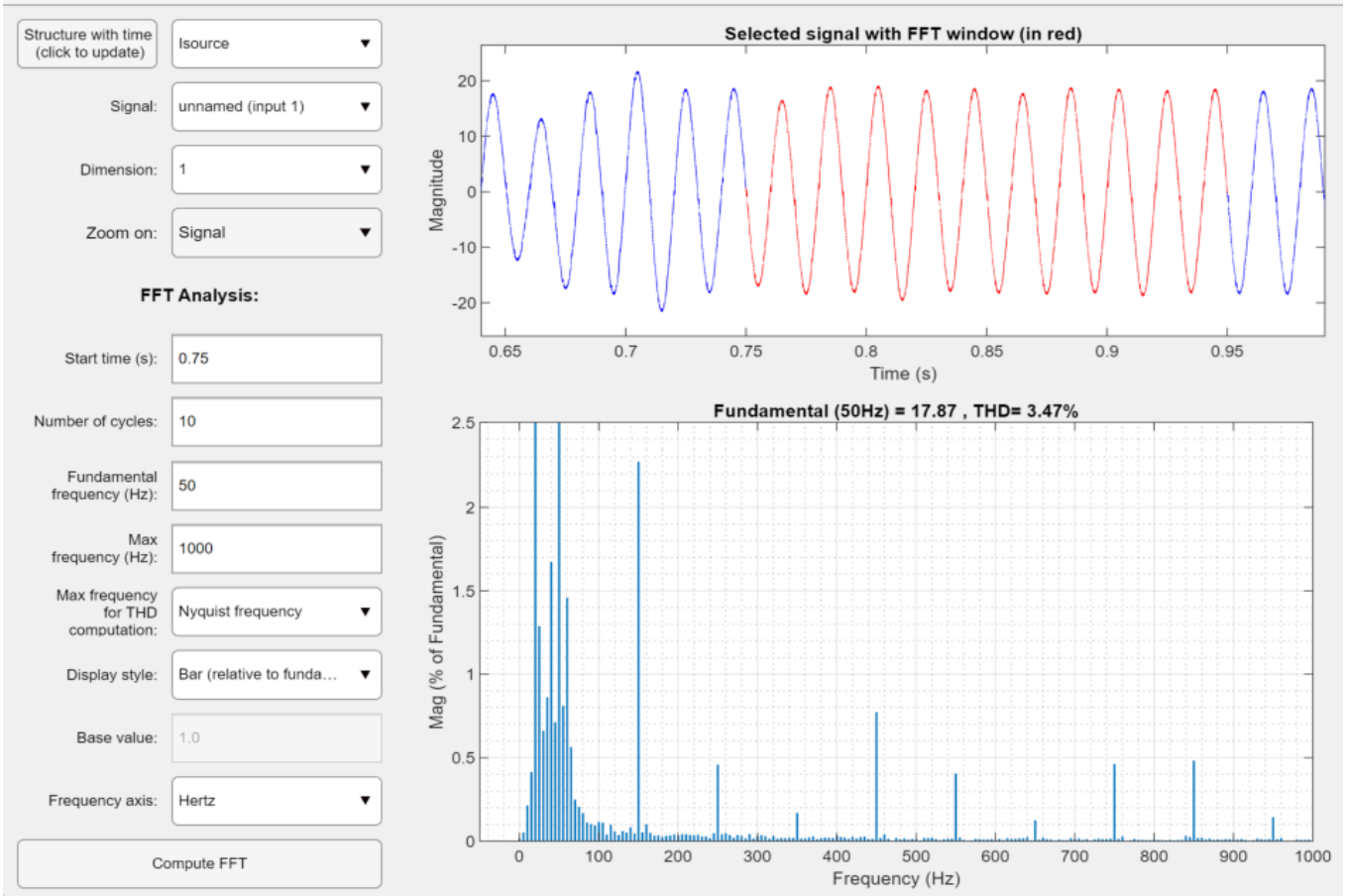

Fig.49. Fig: FFT analysis result for the source when SAPF is connected

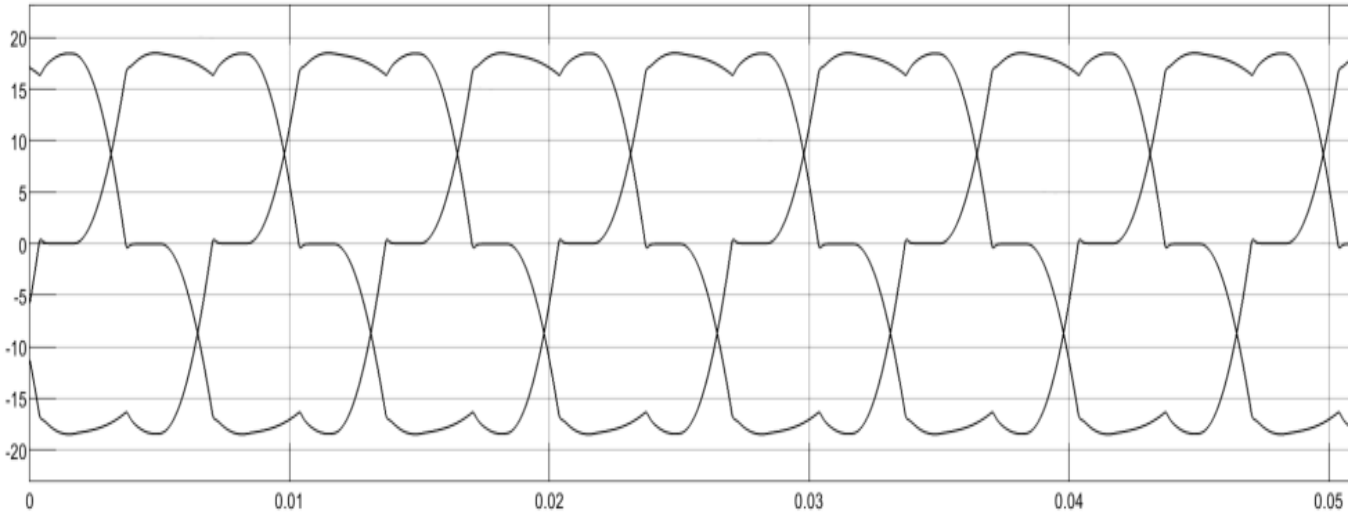

Fig 50: Dynamic response of the 3φ SAPF associated source; displays the device current for abc phases (Current Vs Time)

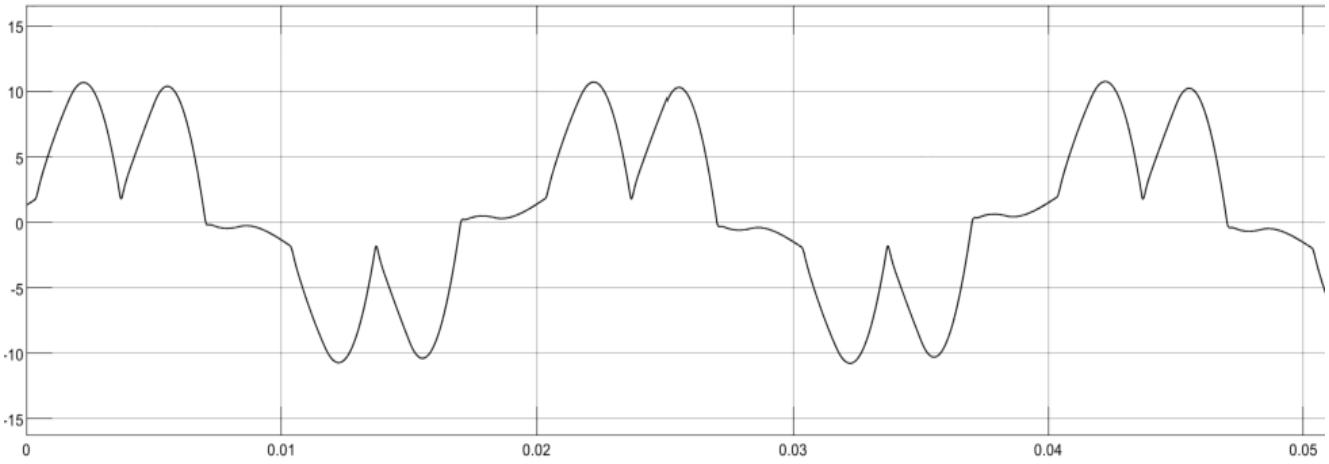

Fig 51: Dynamic response of the SAPF associated source; displays the compensating current produced by SAPF for phase a (Current Vs Time)

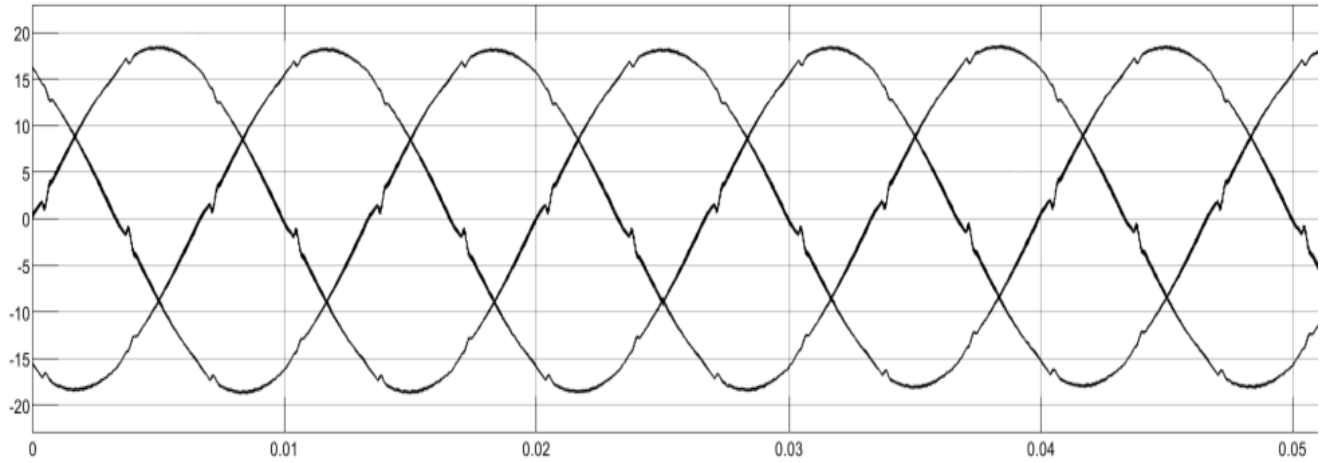

Fig 52: Dynamic response of the 3φ SAPF connected system after 0.4s; shows the source current where the notches are due to tracking errors in Iq reference current (Current Vs Time)

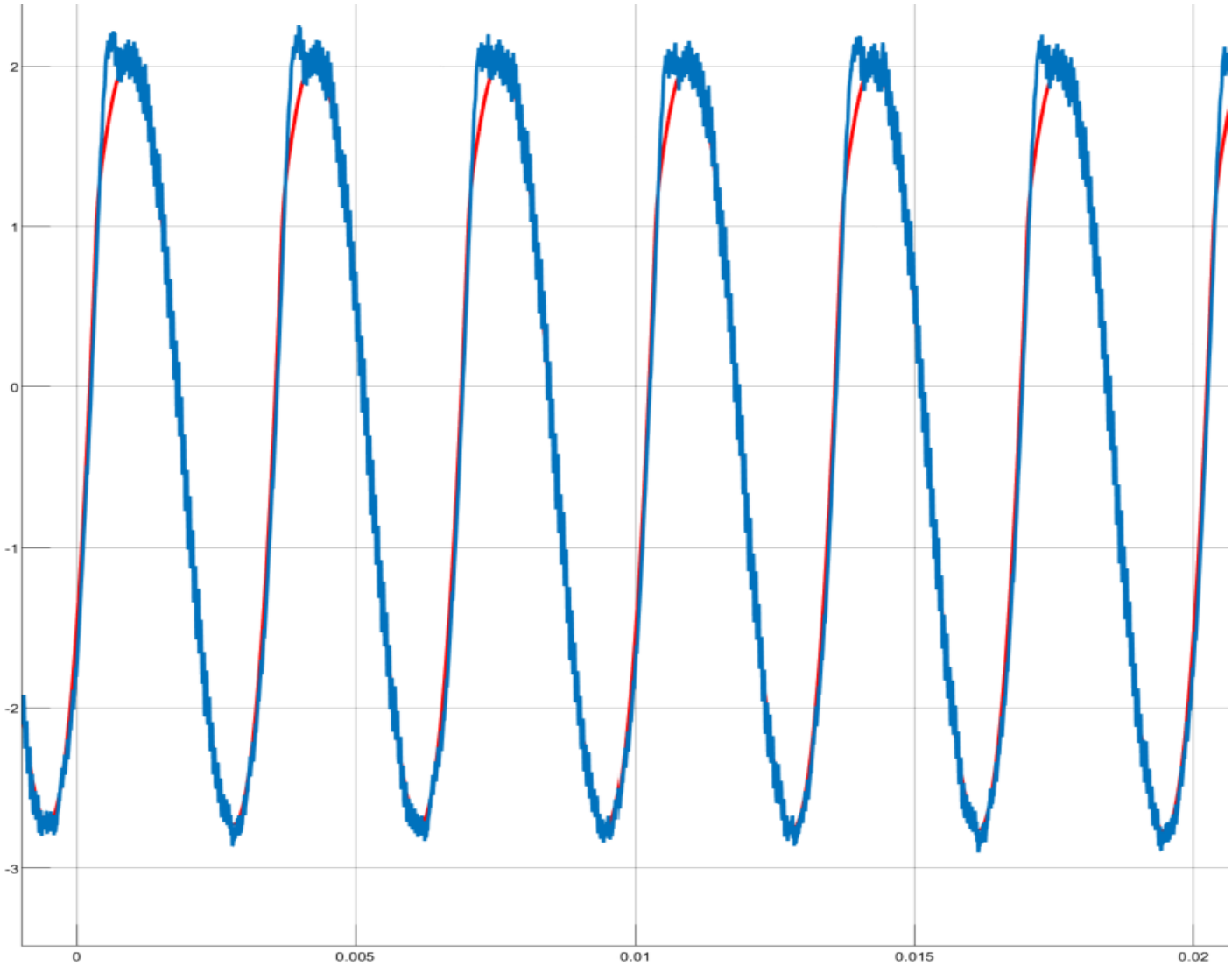

Fig 53: Performance of PI control technique with following arc for d-domain current Id (Current Vs Time)

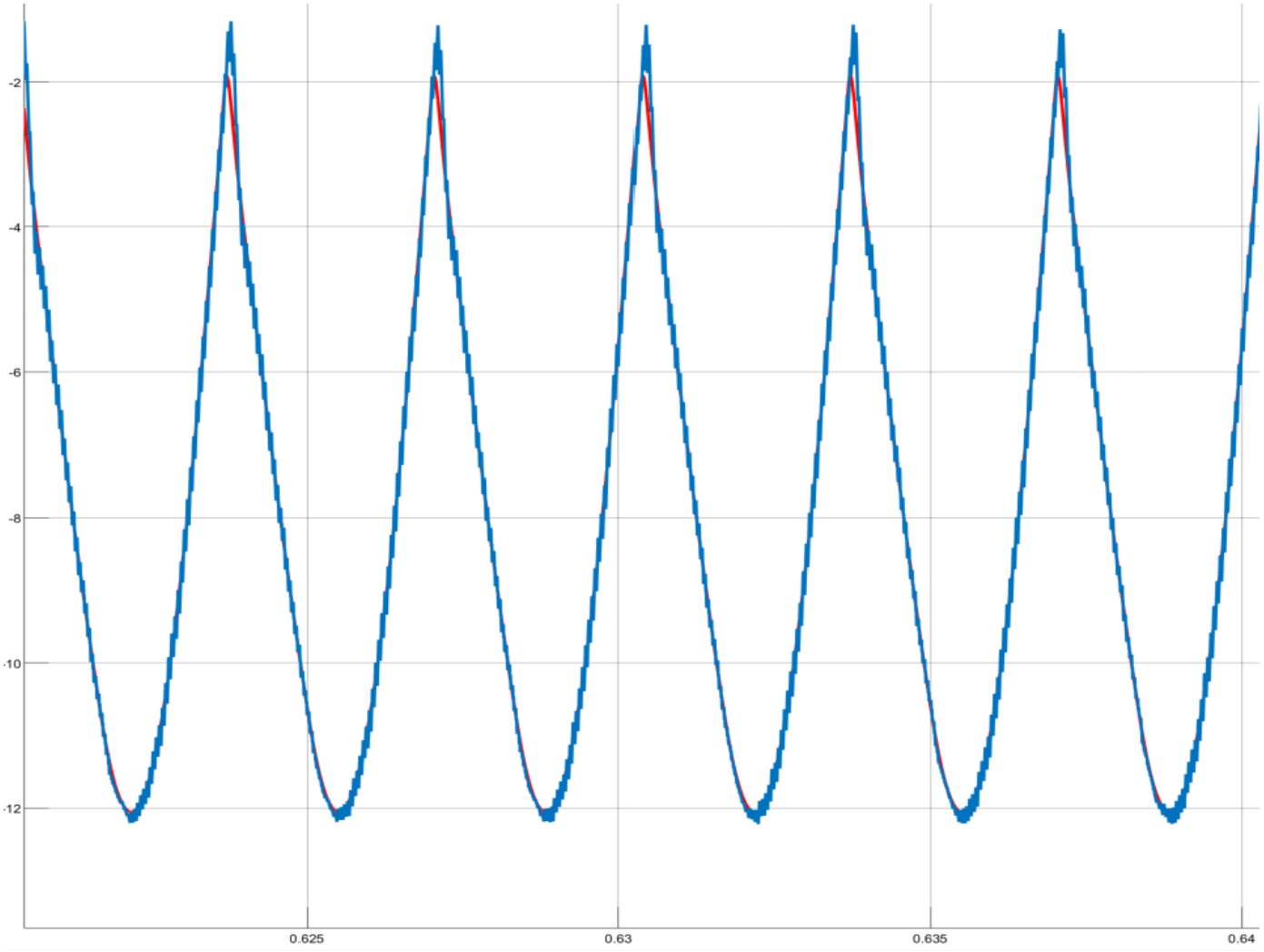

Fig 54: Performance of PI control technique with tracking curve for q-domain current Iq (Current Vs Time)

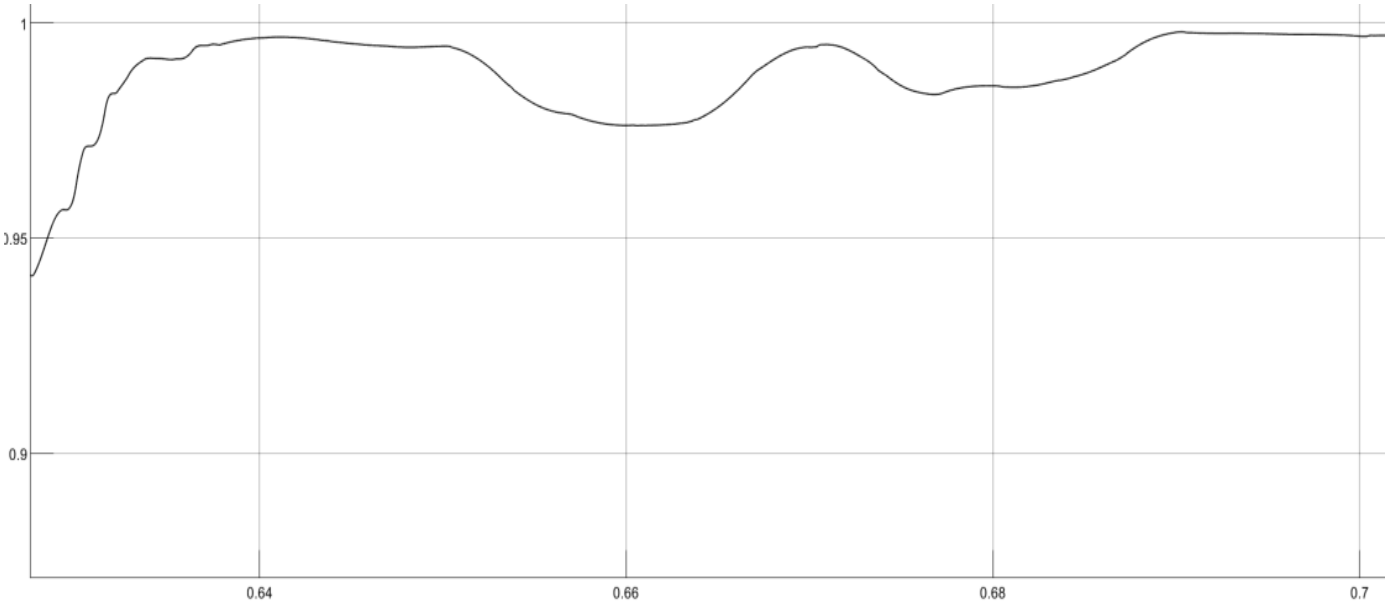

Fig 55: Development of the p to system when SAPF is connected (p.f. Vs Time)

Table IV

Performance comparison of SAPF under different loading conditions for 3phase 4wire

Device	THD Without SAPF	THD With SAPF
2000W (122ohm)	23.62%	4.52%
3000W (81.66ohm)	24.73%	4.38%
4000W (61.26ohm)	23.42%	3.43%
5000W (49ohm)	22.5%	4.37%
6000W (40.8ohm)	25.68%	4.33%
8000W (30.6ohm)	19.42%	4.87%
10KW (24.5ohm)	17.7%	3.40%
12KW (20.4ohm)	16.39%	4.63%
14KW (17.5ohm)	26.94%	6.47%

5.4 Case IV

The three-phase device, a Variable Frequency Drive (VFD), was integrated into the SAPF, and the Total Harmonic Distortion (THD) was studied. The same system was employed, as mentioned in case I. The only change is that the Varying RL device was replaced by a three-phase motor with a rating of 160 kW, as depicted in Fig. 36. The equivalent DC filter inductor and capacitor terms are 4200 microfarads and 181 microhenries (2 units), respectively

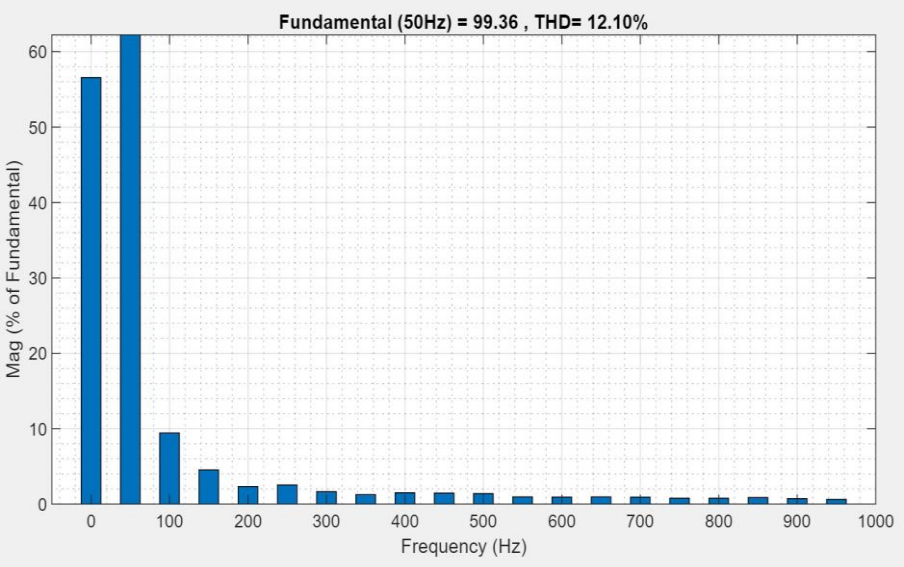

Fig 56: THD of VFD as a device without SAPF

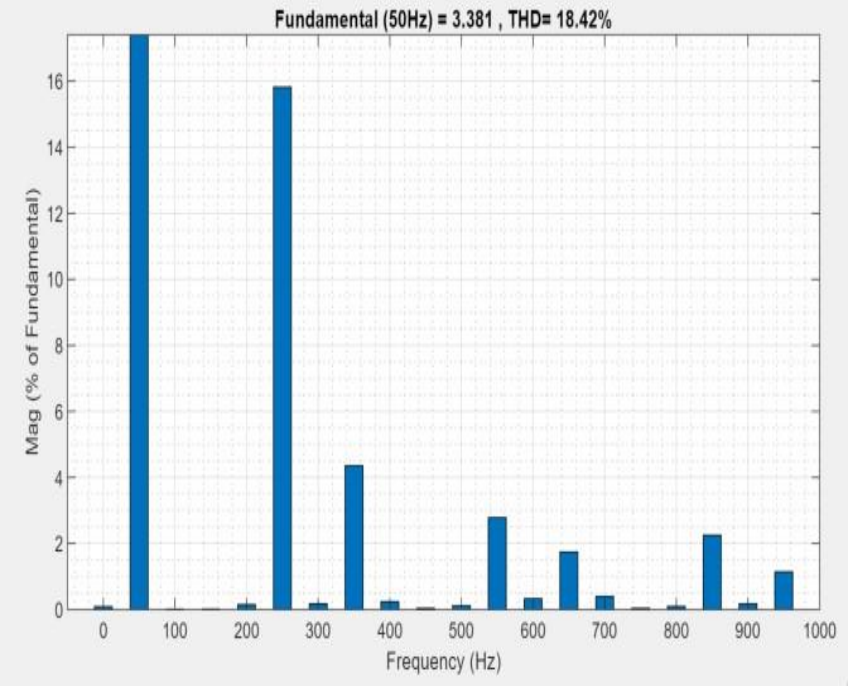

Fig 57: THD of VFD as a device with SAPF respectively

When the Variable Frequency Drive (VFD) was introduced as a device in conjunction with the SAPF, there was an increase in the THD level. This phenomenon can be attributed to the dynamic filter linked with the grid, resulting in a reduction of the short-circuit impedance observed by the rectifier. Consequently, this reduction amplifies harmonic current distortion in the input of the rectifier.

5.5 Case V

The simulated and tested SAPF was utilized to assess device data obtained from the industries of Balaju Industrial Area, and it was validated accordingly. The device data is attached in the annex. The blue bar represents the THD level when SAPF is not connected, and the red bar represents the THD level when SAPF is connected after 0.4 seconds

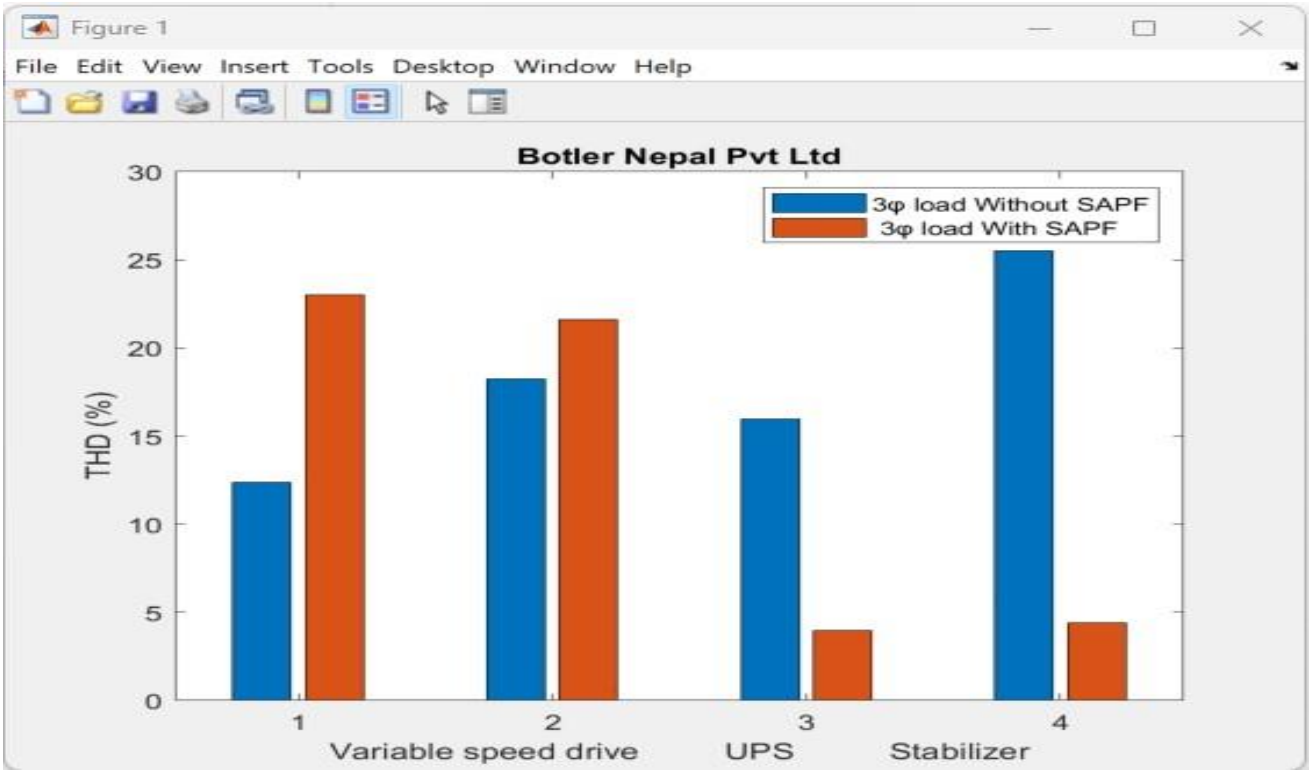

Fig 58: THD level of Bolter Nepal for 3φ device

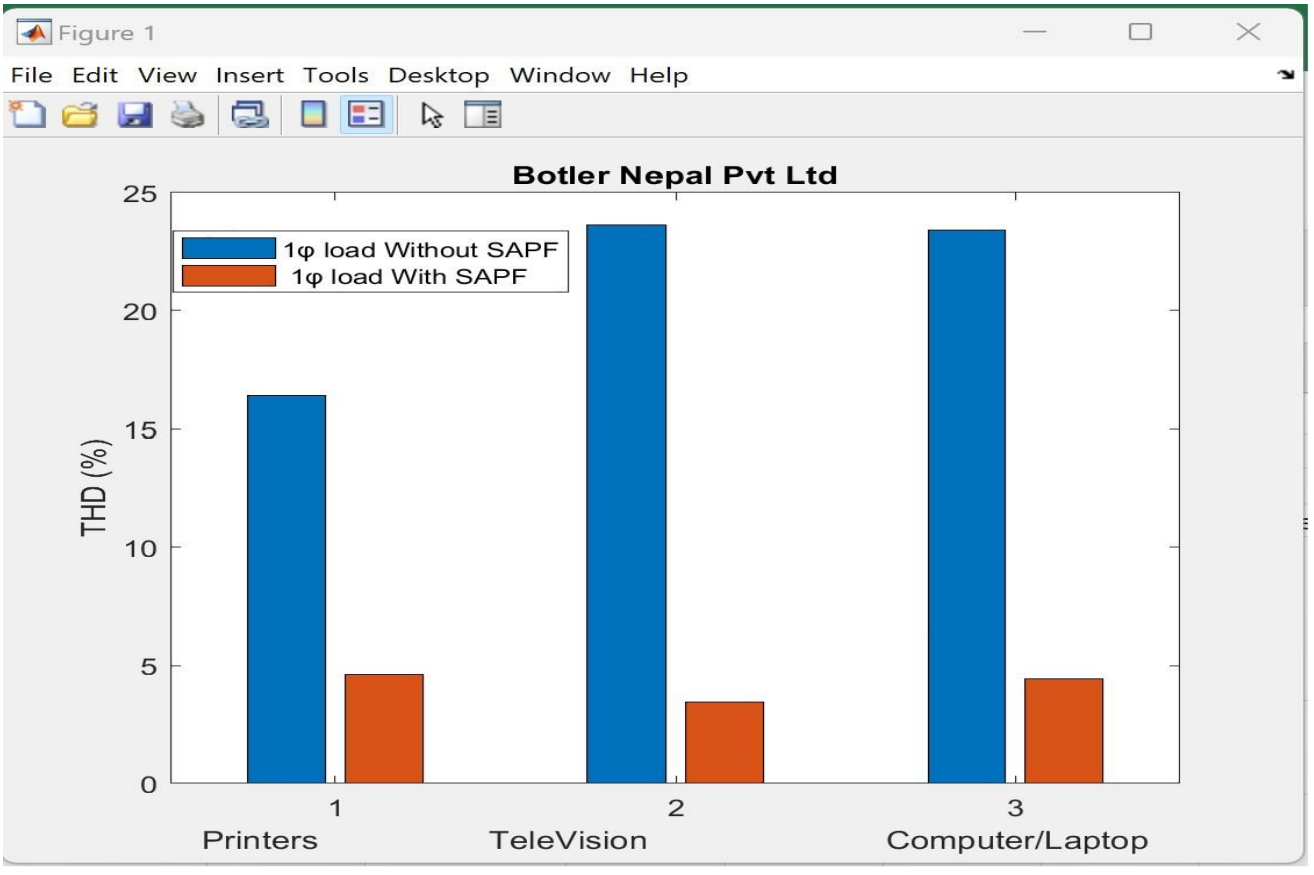

Fig 59: THD level of Bolter Nepal for 1φ device

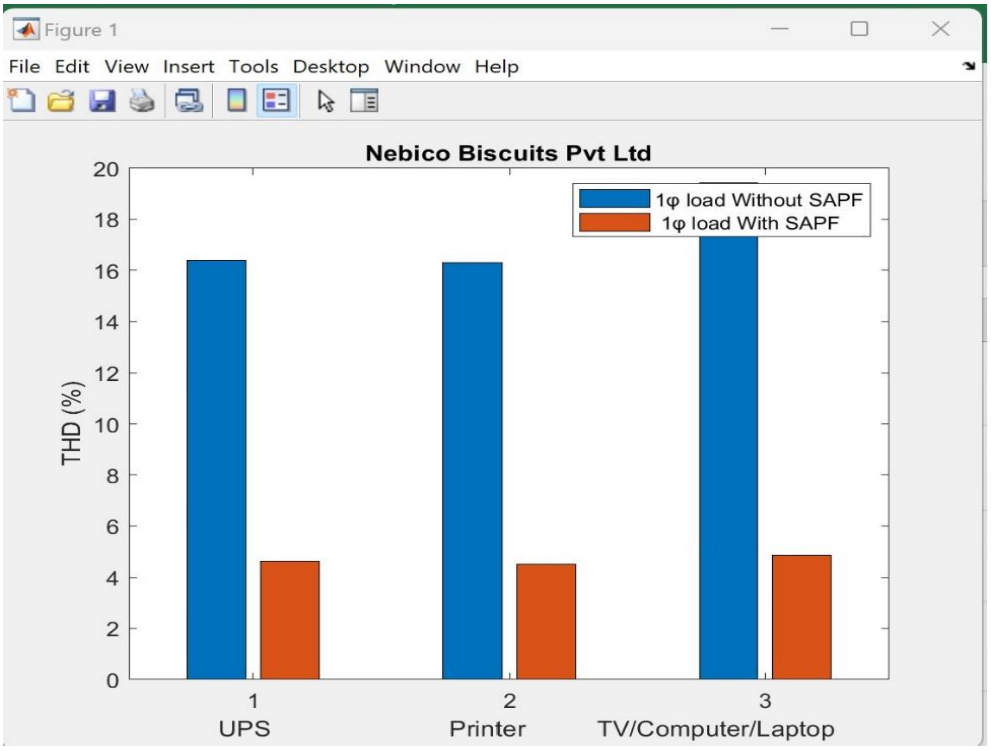

Fig 60: THD level of Nebico Biscuits for 1φ device

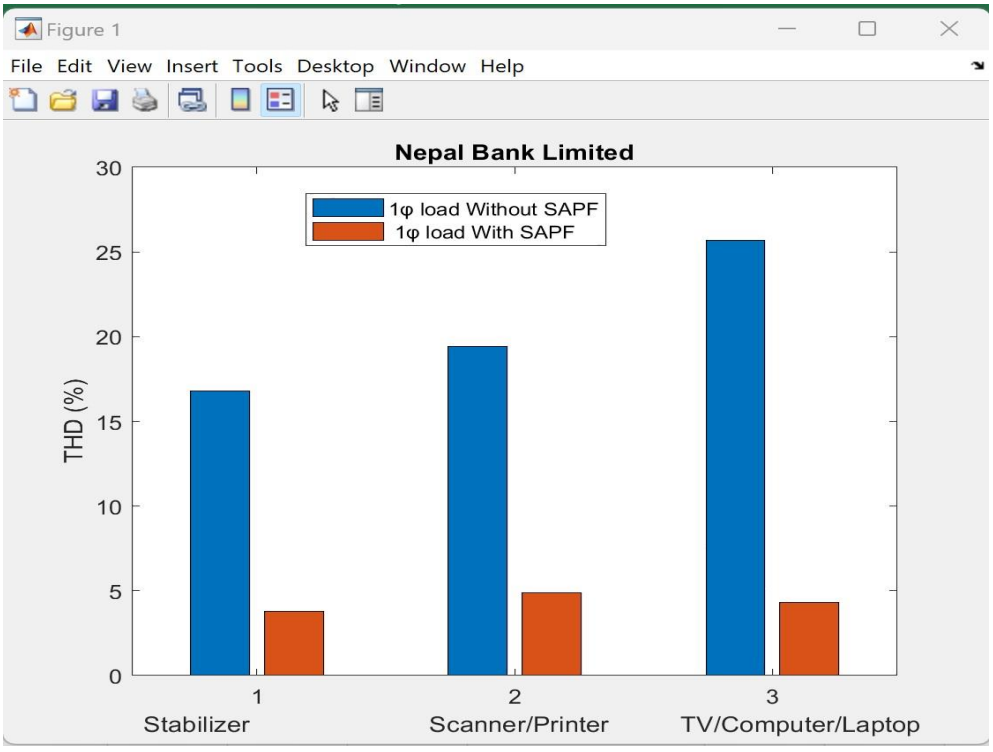

Fig 61: THD level of Nepal Bank Limited for 1φ device

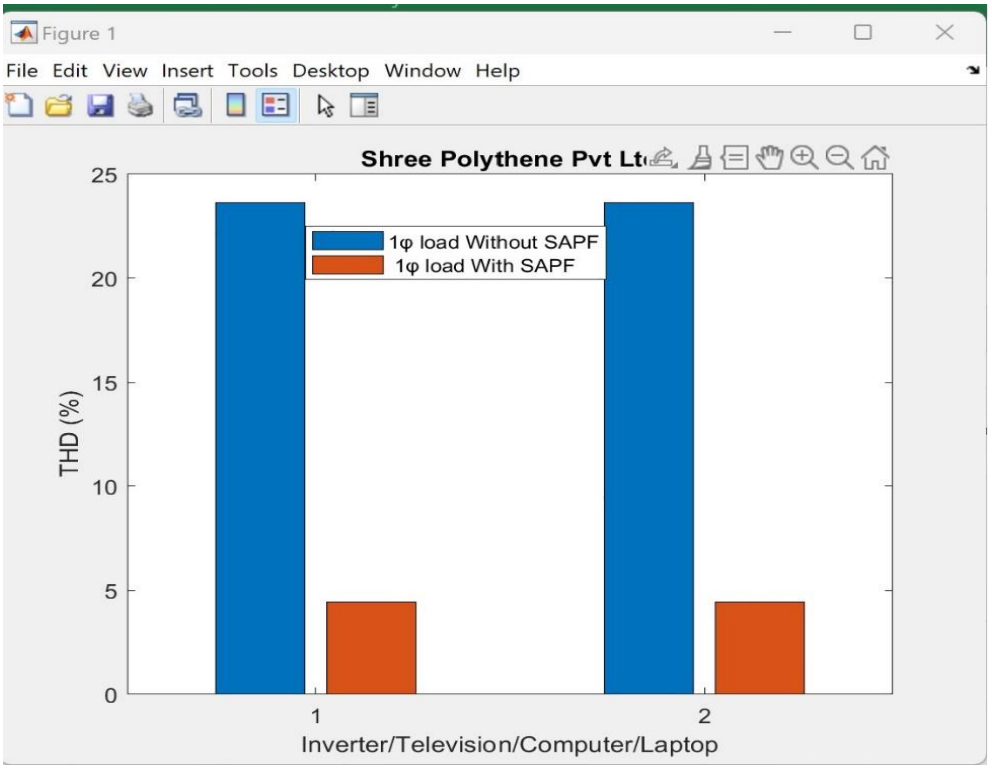

Fig 62: THD level of Shree polythene for 1φ device

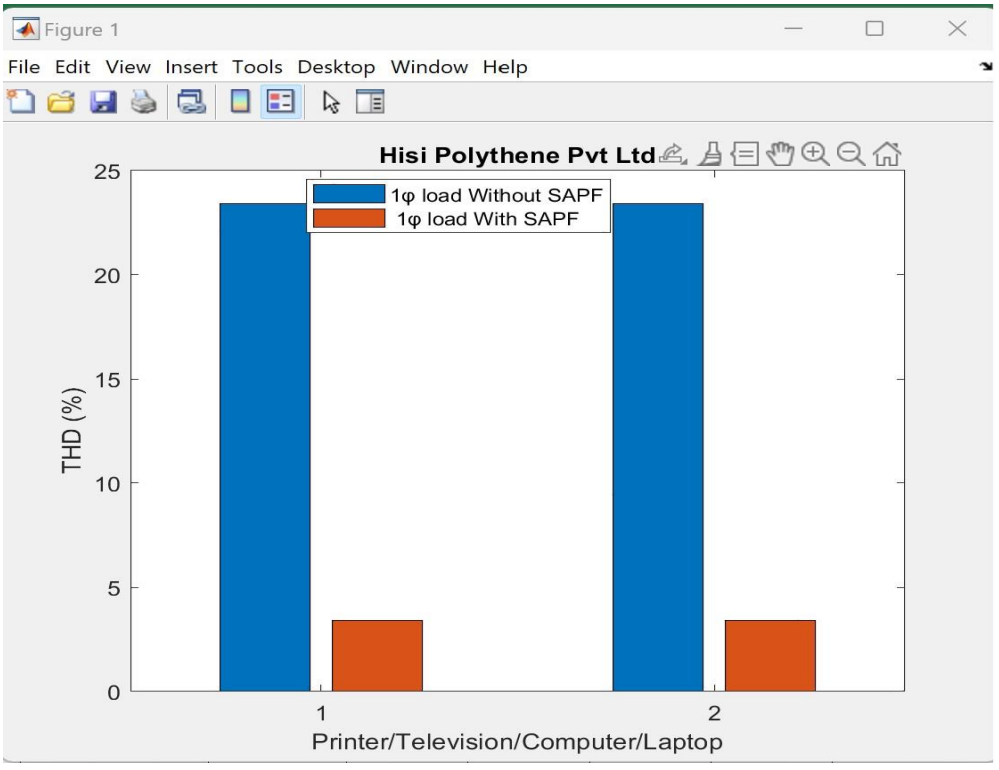

Fig 63: THD level of Hisi Polythene for 1φ device

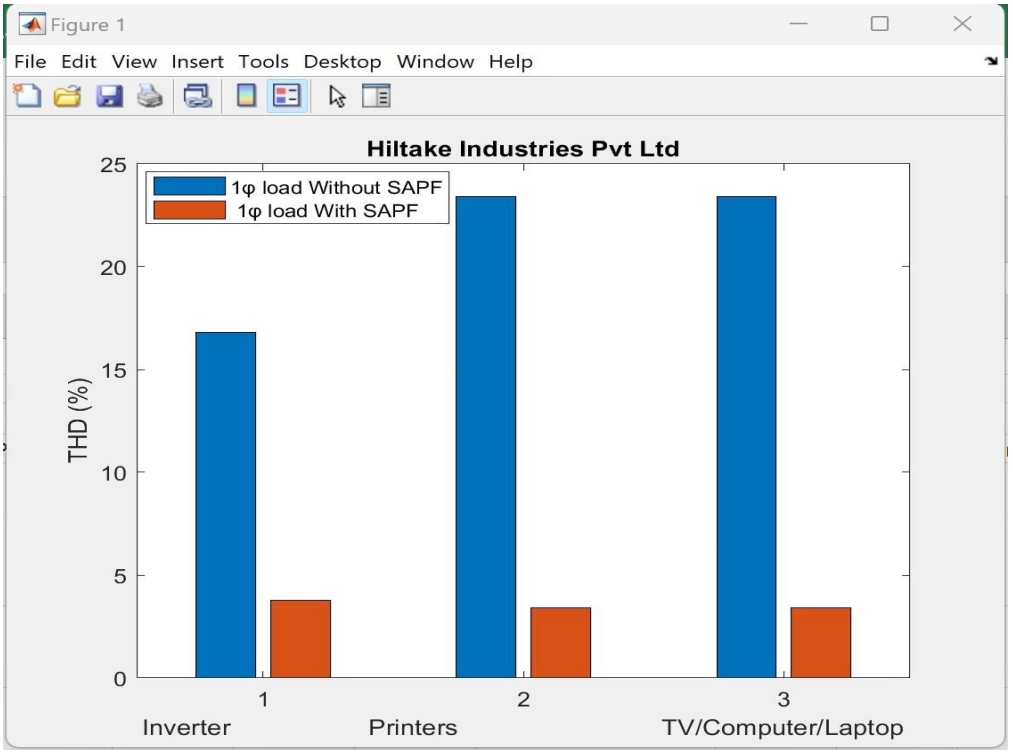

Fig 64: THD level of Hatlike Industries for 1φ device

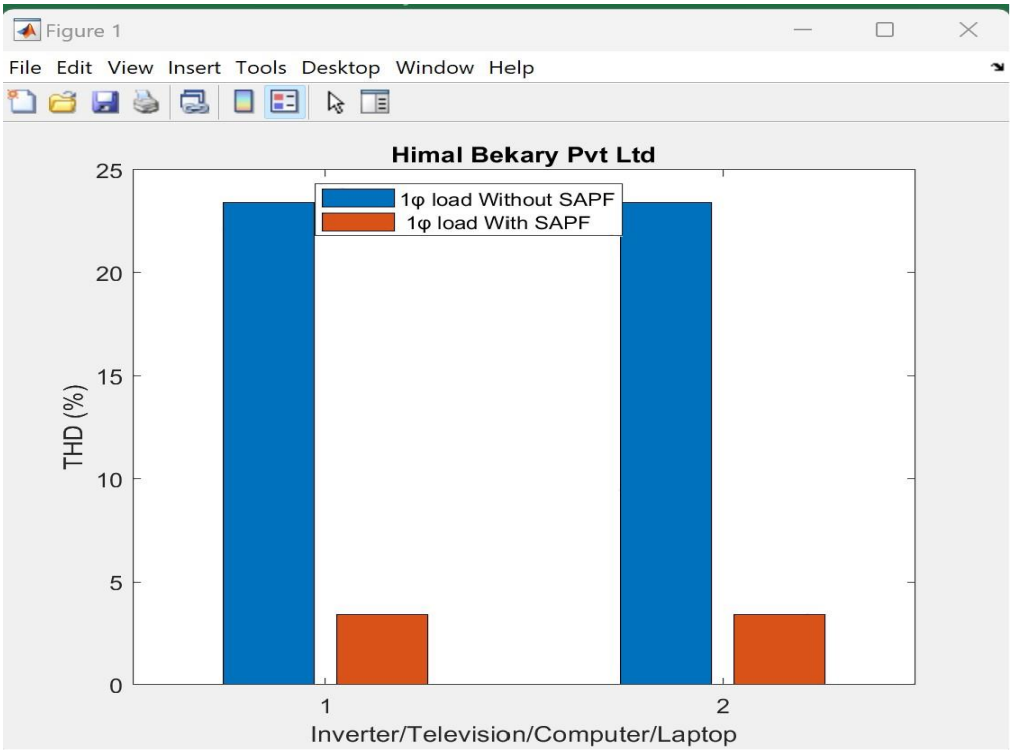

Fig 65: THD level of Himal Bekary Pvt Ltd for 1φ device

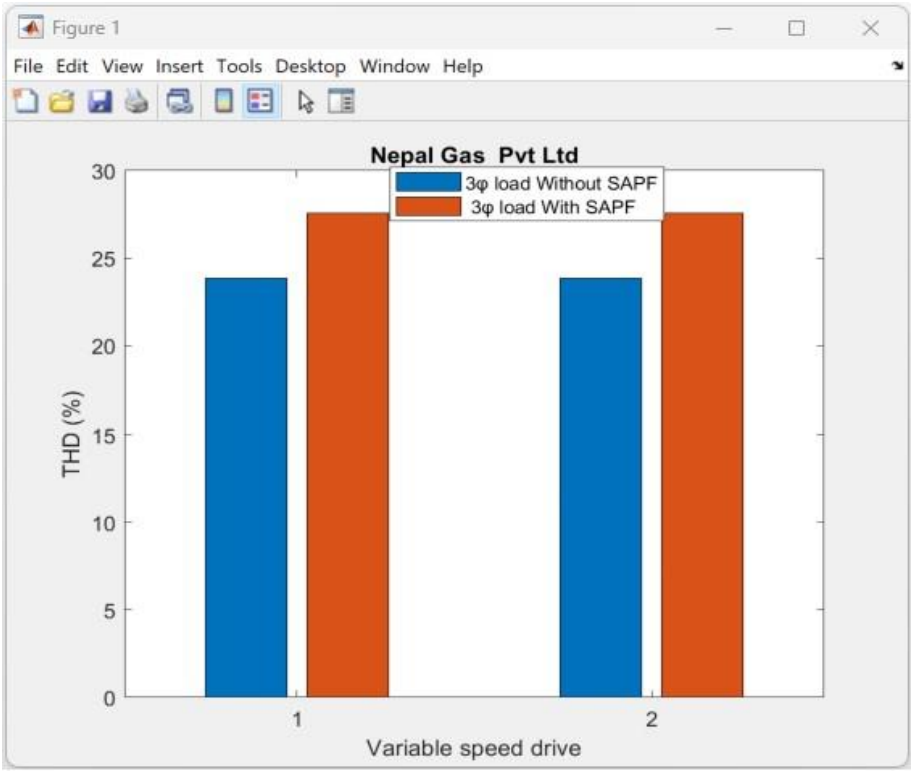

Fig 66: THD level of Nepal Gas Pvt Ltd for 3φ device

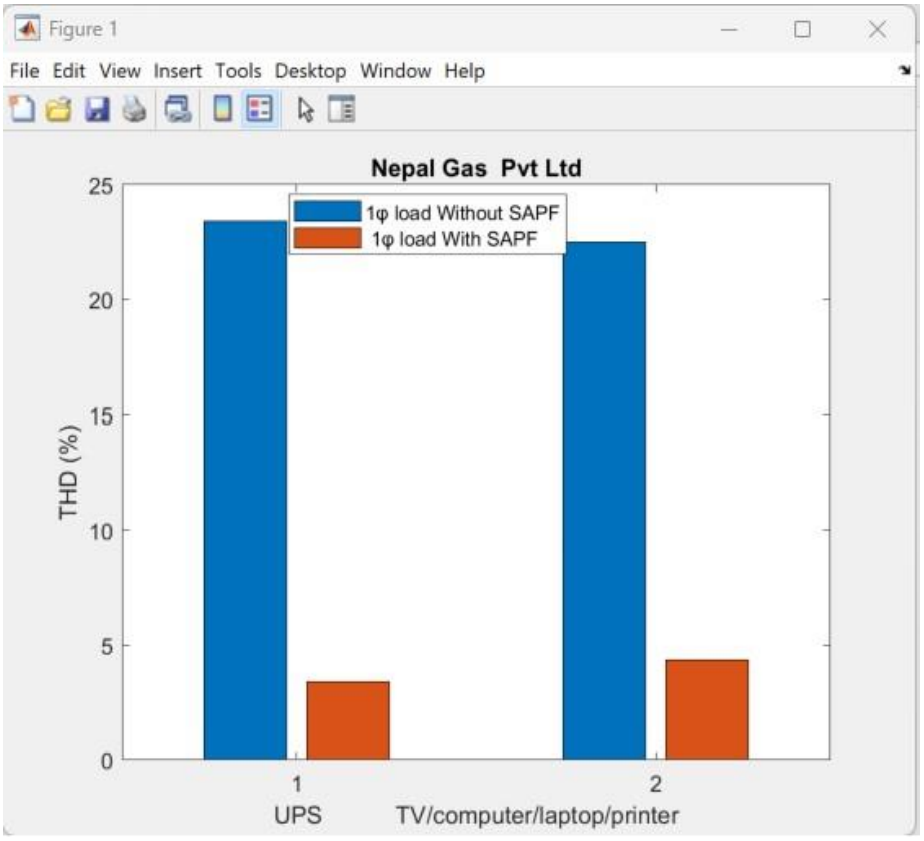

Fig 67: THD level of Nepal Gas Pvt Ltd for 3 1φ device

The THD level for all kind of devices were in limit as per IEEE 516 std except for VFD device which was already explained in case VI.

5.6 Stability Analysis of Transfer function

The transfer function of the inner loop was represented in Bode plots. For the stability analysis of the transfer function using Bode plots, the criteria dictate that both the phase margin and gain margin must be positive for the system. As depicted in Fig. 58, the Bode plots of the inner loop's transfer function exhibit positive values for both phase margin and gain margin at the gain crossover frequency. Similarly, as illustrated in Fig. 58, the Bode plots of the extra loop's transfer function also show positive values for both phase margin and gain margin at the gain crossover frequency. Consequently, the systems are deemed stable.

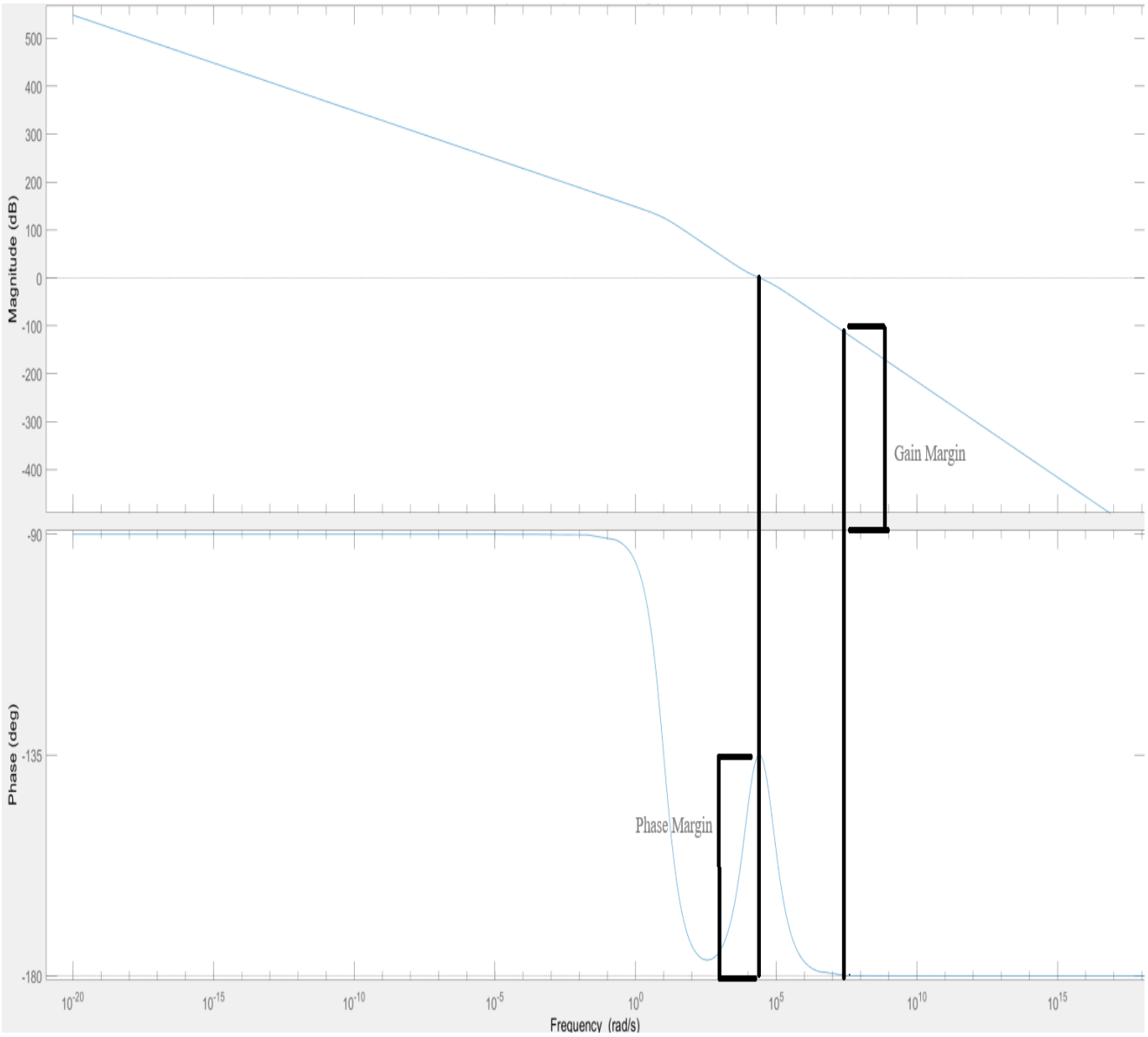

Fig 68: Bode plot of Frequency response of the open loop of inner control loop

.

CHAPTER 6. CONCLUSION AND RECOMMENDATION

Conclusion

In this thesis, a PI control designed for the regulation of dq-domain currents is suggested, ensuring effective tracking of their corresponding reference currents, Id and Iq. The enhanced response rapidity of the PI control contributes to the improved harmonic compensation ability of the power inverter, along with an enhancement in the power factor of the system. This control effectively addresses power quality issues associated with harmonics, especially under dynamic non-linear device conditions.

In this thesis we achieved the followings based on results information:

i) Control design of shunt active power filter (SAPF) with a voltage source inverter (VSI) in MATLAB has been successfully completed.

ii) Harmonic suppression under different loading conditions for 3-phase 3-wire and 3-phase 4-wire systems has been successfully achieved, meeting the IEEE 516 standard limits.

iii) The model was tested and verified using non-linear devices available in the Balaju industrial area.

iv) A study of harmonics for the shunt active power filter as a VFD device has been successfully conducted, investigating its impact and mitigation. In the case of VFDs, the THD level increased when the SAPF was connected.

v) Power factor is maintained at nearly unity for all kinds of non-linear devices except VFDs.

iv) The stability of the transfer function of the SAPF was assessed using Bode plots.

Recommendation

The improvement in the dynamics of the inner current control loop achieved in this work can have numerous applications for other power electronic systems, such as grid-connected inverters and STATCOMs. It can also be employed to control harmonics in industries, thereby enhancing power factor to unity, among other potential uses.

CHAPTER 7. FURURE WORK

When VFD was used as device in SAPF, the harmonics level was increased. So, to maintain the THD level within a limit, a journal paper published In IEEE Transactions on Industry Applications, vol. 52, no. 4, pp. 2816-2825, July-Aug. 2016 suggested that the harmonic analysis typically treats harmonic devices as constant harmonic current sources. However, the introduction of a shunt active power filter (SAPF) alters the harmonic current distortion of the device. Consequently, a higher SAPF output capacity is necessary to fulfill the anticipated filtering requirements. This aspect can be considered as a potential avenue for future research in this thesis.

REFERENCES

[1] F. S. dos Reis, J. Ale´, F. D. Adegas, R. Tonkoski, S. Slan, and K. Tan, "Active shunt filter for harmonic mitigation in wind turbines generators," in *Proc. 37th IEEE Power Electronics Specialists Conf.*, Jeju, Korea, 2006, pp. 1 6.

[2] L. Asiminoael, F. Blaabjerg, and S. Hansen, "Detection is key-harmonic detection methods for active power filter applications," *IEEE Ind. Appl. Mag.*, vol. 13, no. 4, pp. 22 33, Jul. Aug. 2007.

[3] L. Marconi, F. Ronchi, and A. Tilli, "Robust nonlinear control of shunt active filters for harmonic current compensation," *Automatica*, vol. 43, no. 2, pp. 252 263, Feb. 2007.

[4] IEEE recommended practice and requirements for harmonic control in electric power systems, IEEE Standard 519-2014, 2014, pp. 1-29.

[5] J. Vazquez and P. Salmeron, "Active power filter control using neural network technologies," *IEEE Proc. Electr. Power Appl.*, vol. 150, no. 2. pp. 139 145, Mar. 2003

[6] H. Akagi, A. Nabae, and S. Atoh, "Control strategy of active power filters using multiple voltage-source PWM converters," *IEEE Trans. Ind. Appl.*, vol. IA-22, no. 3, pp. 460 465, May 1986.

[7] V. Soares, P. Verdelho, and G. D. Marques, "An instantaneous active and reactive current component method for active filters," *IEEE Trans. Power Electron.*, vol. 15, no. 4, pp. 660 669, Jul. 2000.

[8] S. Buso, L. Malesani, and P. Mattavelli, "Comparison of current control techniques for active filter applications," *IEEE Trans. Industr. Electron.*, vol. 45, no. 5, pp. 722 729, Oct. 1998.

[9] U. Tamrakar, R. Tonkoski, Z. Ni, T. M. Hansen, and I. Tamrakar, "Current control techniques for applications in virtual synchronous machines," in Proc. 2016 IEEE 6th Int. Conf. Power Systems (ICPS), New Delhi, India, 2016, pp. 1 6.

[10] R. Bellman, Dynamic Programming. Princeton, UK: Princeton University Press, 1957

[11] U. Tamrakar, N. Malla, D.Shrestha, Z. Ni, and R. Tonkoski, "Design of online supplementary adaptive dynamic programming for current control in power electronic systems," in Proc. of IEEE Energy Conversion Congress and Exposition (ECCE'17), Cincinnati, OH, USA, Oct. 1 5, 2017, pp. 1 5.

[12] Mauricio Aredes, Jurgen Hafner and Klements Heumann ,"Three-phase four-wire shunt active filter control strategies." IEEE Transactions on power Electronics, Vol. 12. N O. 2. March 1997

[13] Mauricio Aredes, Edson H. Watanabe, " New Control Algorithms For Series And Shunt Three-Phase Four-Wire Active Power Filters." IEEE Transactions on Power Delivery, Vol. 10. No. 3 July 1995

[14] Rumesh P., Palanisamy K., Paramasivam S., Govarthanan R., , Current Distortion Effects on Front End od Variable Frequency Drive Under Shunt Active Filter Connected Grid." IEEE @ 2018

[15] R. C. Dugan, M. F. McGranaghan, and H. W. Beaty, *Electrical power systems quality*, 1st ed. McGraw-Hill Education, 1996.

[16] M. Kale and E. Ozdemir, "An adaptive hysteresis band current controller for shunt active power filter," *Electric Power Systems Research*, vol. 73, no. 2, pp. 113–119, 2005.

[17] N. Malla, D. Shrestha, Z. Ni, and R. Tonkoski, "Supplementary control for virtual synchronous machine based on adaptive dynamic program- ming," in *IEEE World Congress on Computational Intelligence (IEEE WCCI), Vancouver, Canada*. IEEE, 2016, pp. 1–8.

[18] Naresh Malla; Ujjwol Tamrakar; Dipesh Shrestha; Zhen Ni; Reinaldo Tonkoski, "Online learning control for harmonics reduction based on current controlled voltage source power inverters" in IEEE Journals & Magazines ,IEEE/CAA Journal of Automatic...Volume: 4 Issue: 3, July 2017.

[19] W.H. Ko and J.c. GU, "Impact of Shunt Active Harmonics Filter on Harmonic Current Distortion of Voltage Source Inverter-Fed Drives." In IEEE Transactions on Industry Applications, vol. 52, no. 4, pp. 2816-2825, July-Aug. 2016.

[20] AUTOMATIC CONTROL SYSTEMS (WITH MATLAB PROGRAMS), Syed Hasan Saeed, Dept of Electronics Engg. Integral University, Lucknow. S.K. KATARIA & SONS

[21] MAURICIO AREDES, EDSON H. WATANABE," New Control Algorithms for Series and Shunt Three Phase Four-Wire Active Power Filters." IEEE Transaction on Power Delivery, Vol 10, No. 3, July 1995.

[22] Maria Isabel Milanes Montero, Enrique Romero cadaval, Fwemin Barrero Gonzalez." Comparison of control strategies for shunt active power filters in three-phase four-wire systems." IEEE Transaction on power electronics , Vol. 22, No. 1 January 2007

[23] Ujwol Tamrakar, South Dakota State University ''Improving transient stability of photovoltaic-hydro microgrids using virtual synchronous machines.''

Annex

Annex 1

MATLAB results for Table III : Performance comparison of SAPF under different loading condition for 3 phase 3 wire system.

i) For 1000W Load :

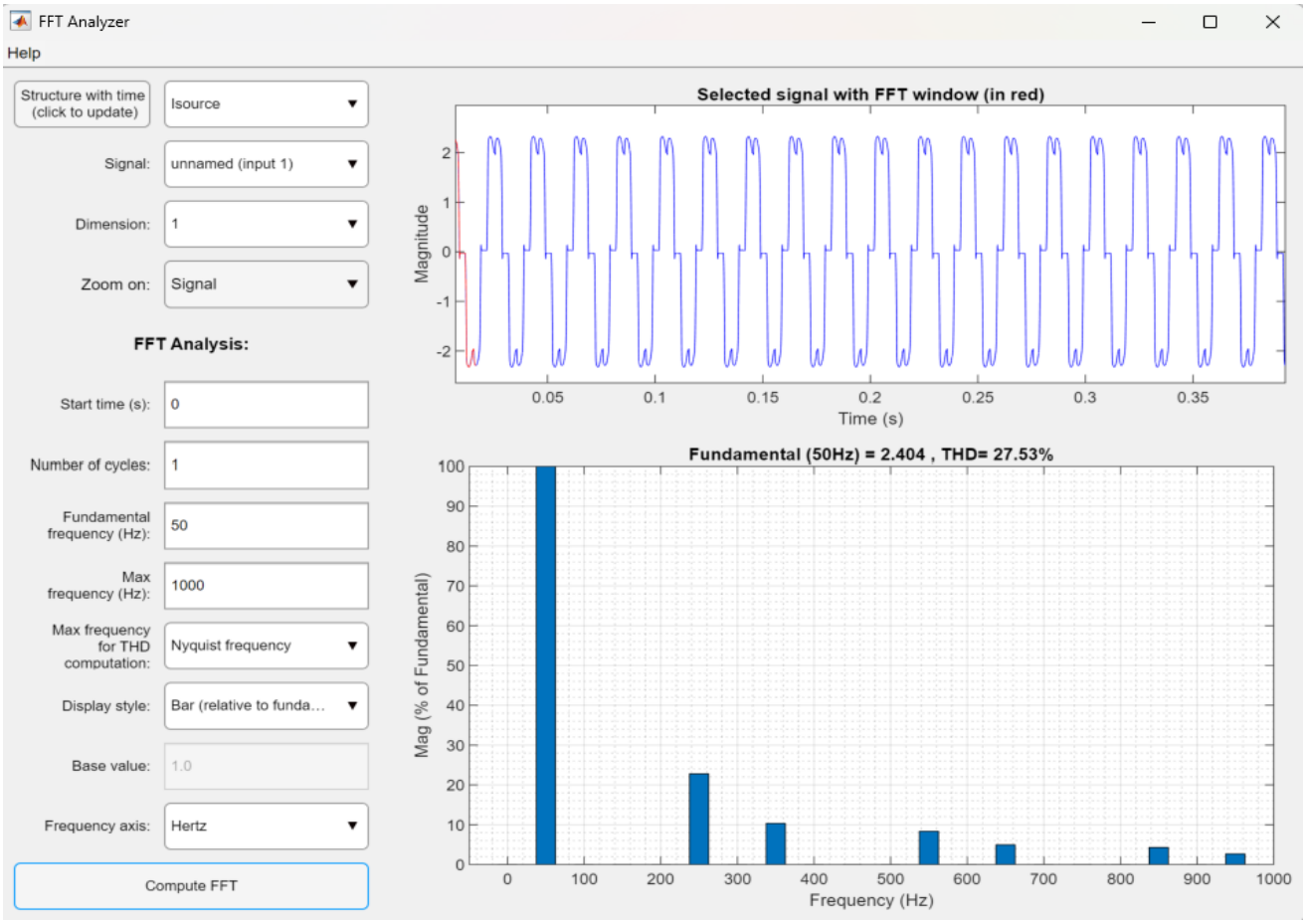

FFT analysis result for the source when no SAPF was connected

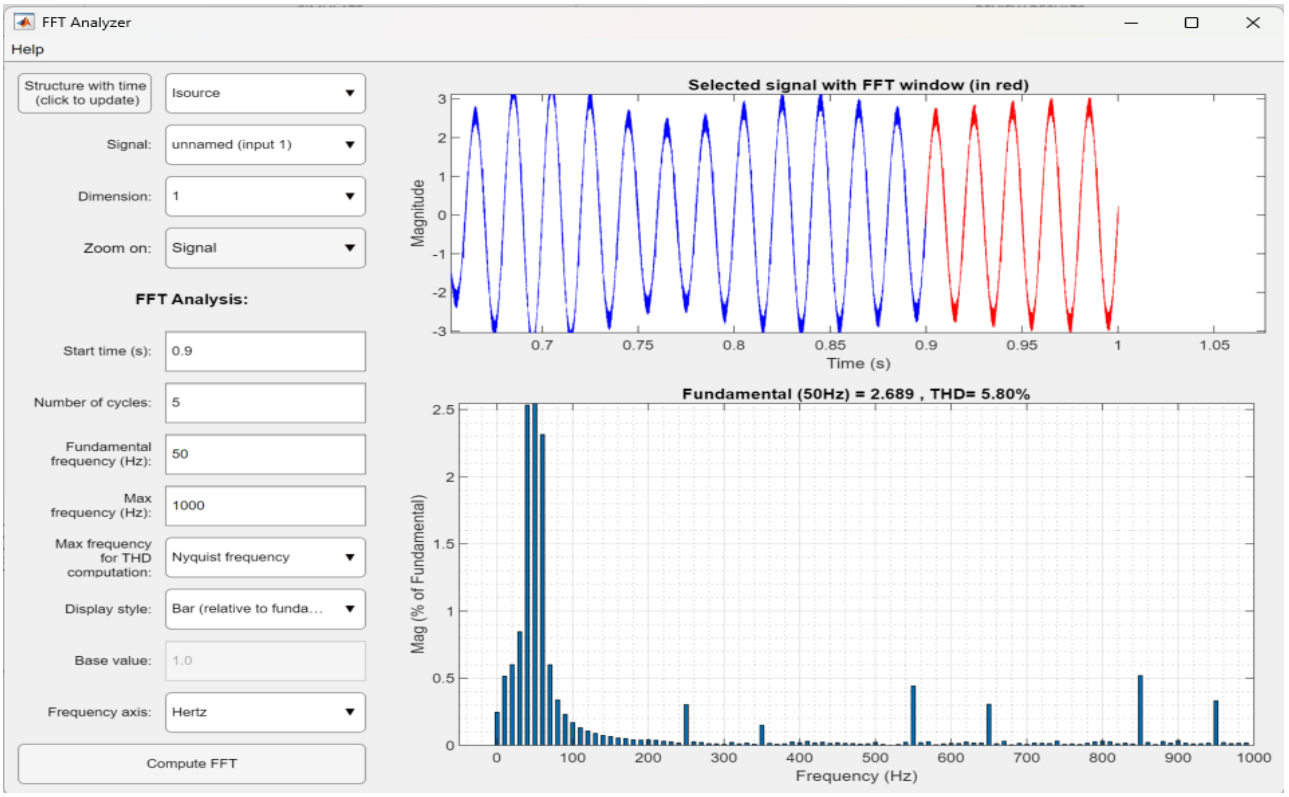

FFT analysis result for the source when SAPF was connected

ii) For 2000W Load :

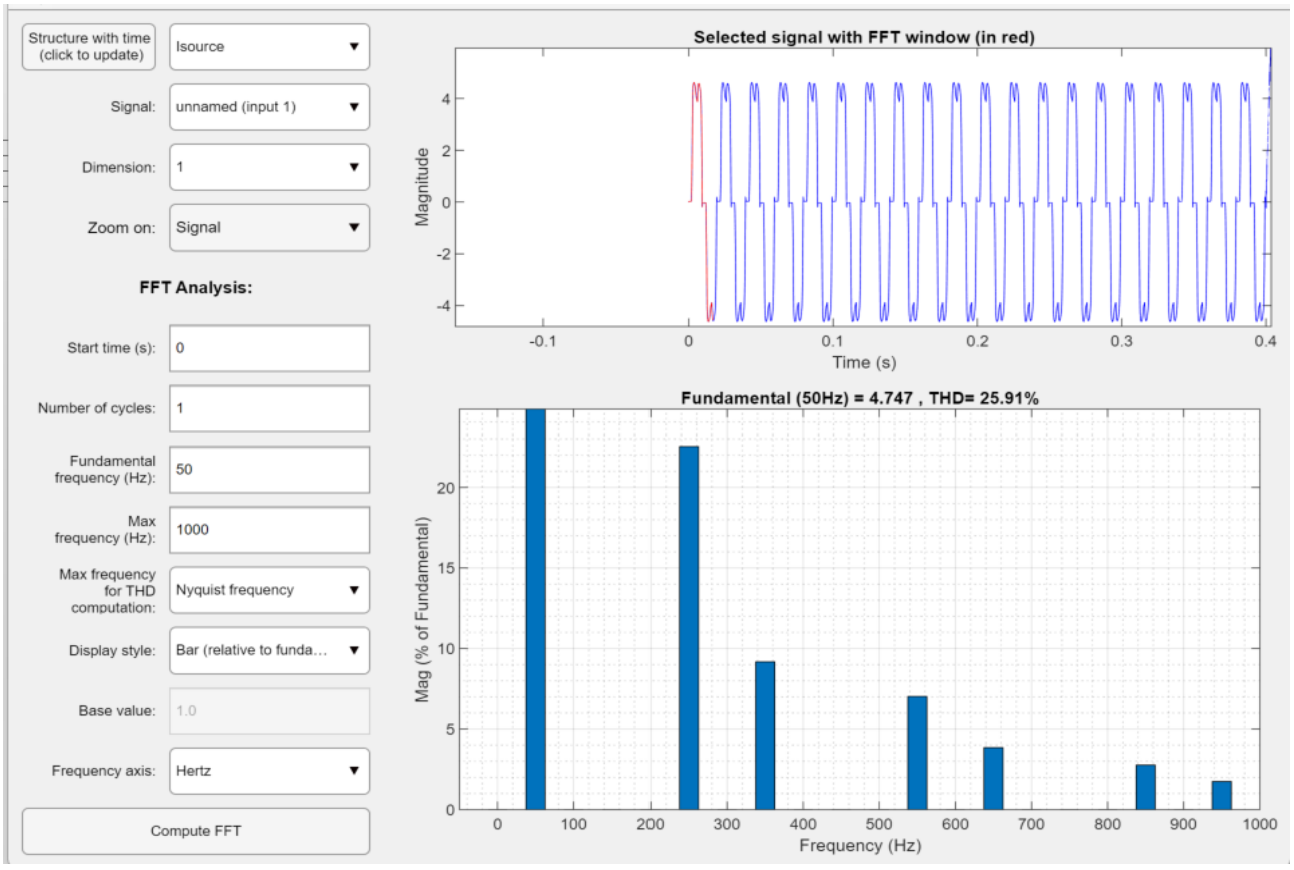

FFT analysis result for the source when no SAPF was connected

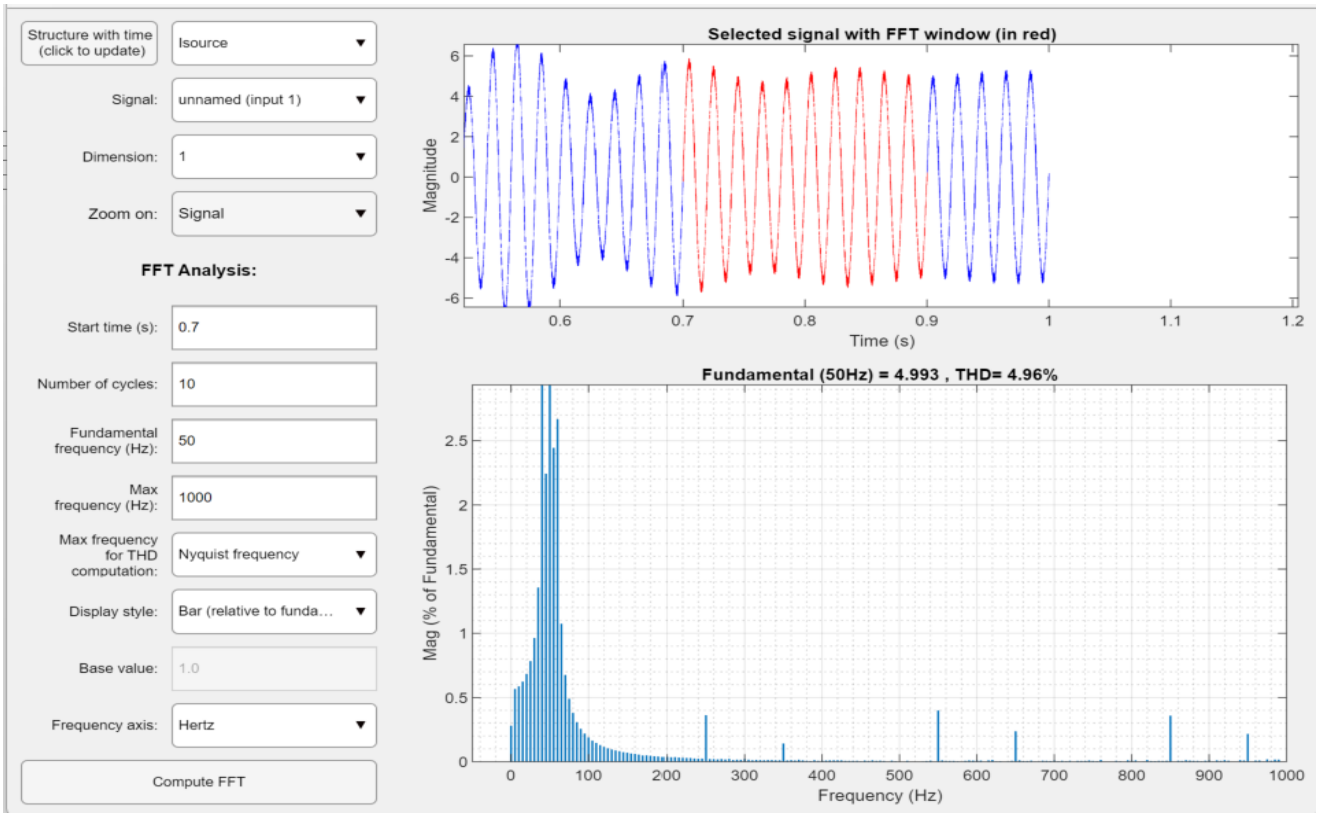

FFT analysis result for the source when SAPF was connected

iii) For 3000W load :

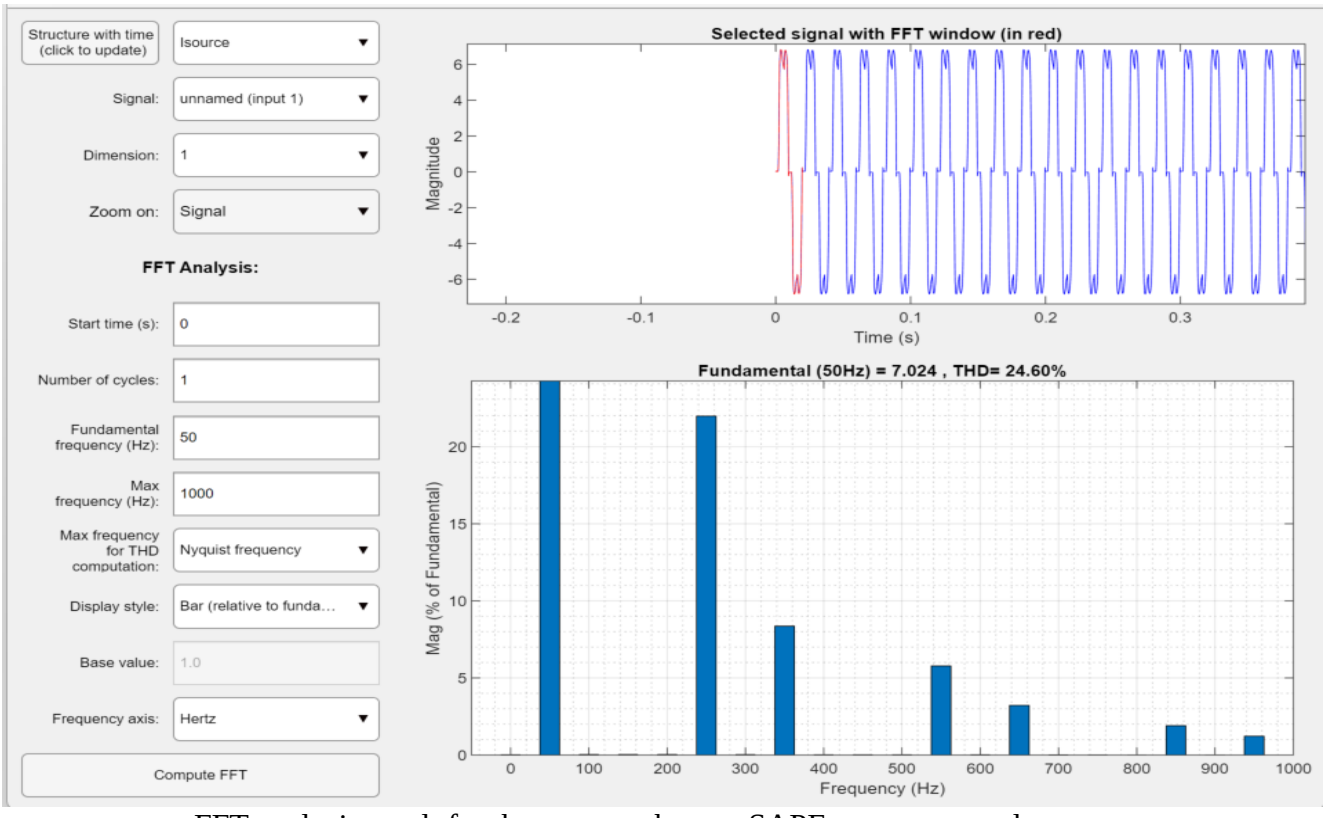

FFT analysis result for the source when no SAPF was connected

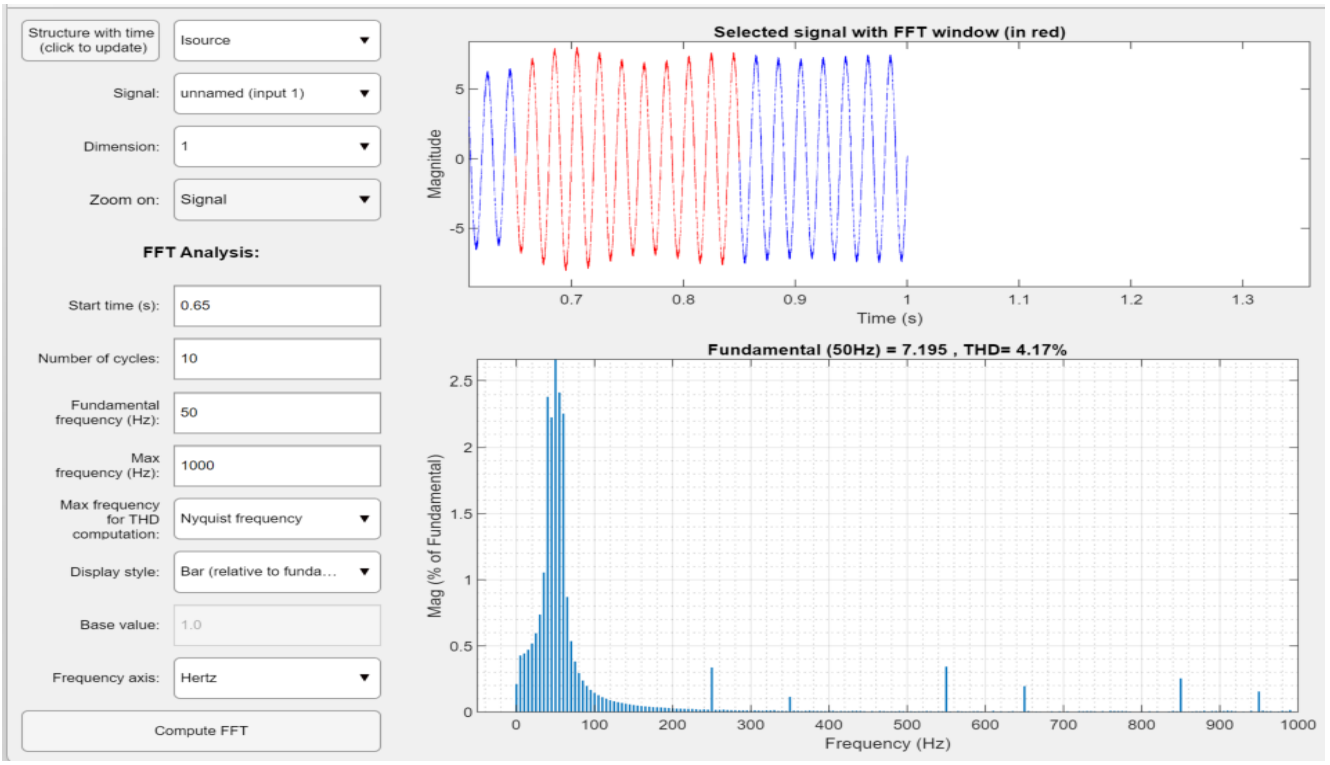

FFT analysis result for the source when no SAPF was connected

iii) For 4000W load :

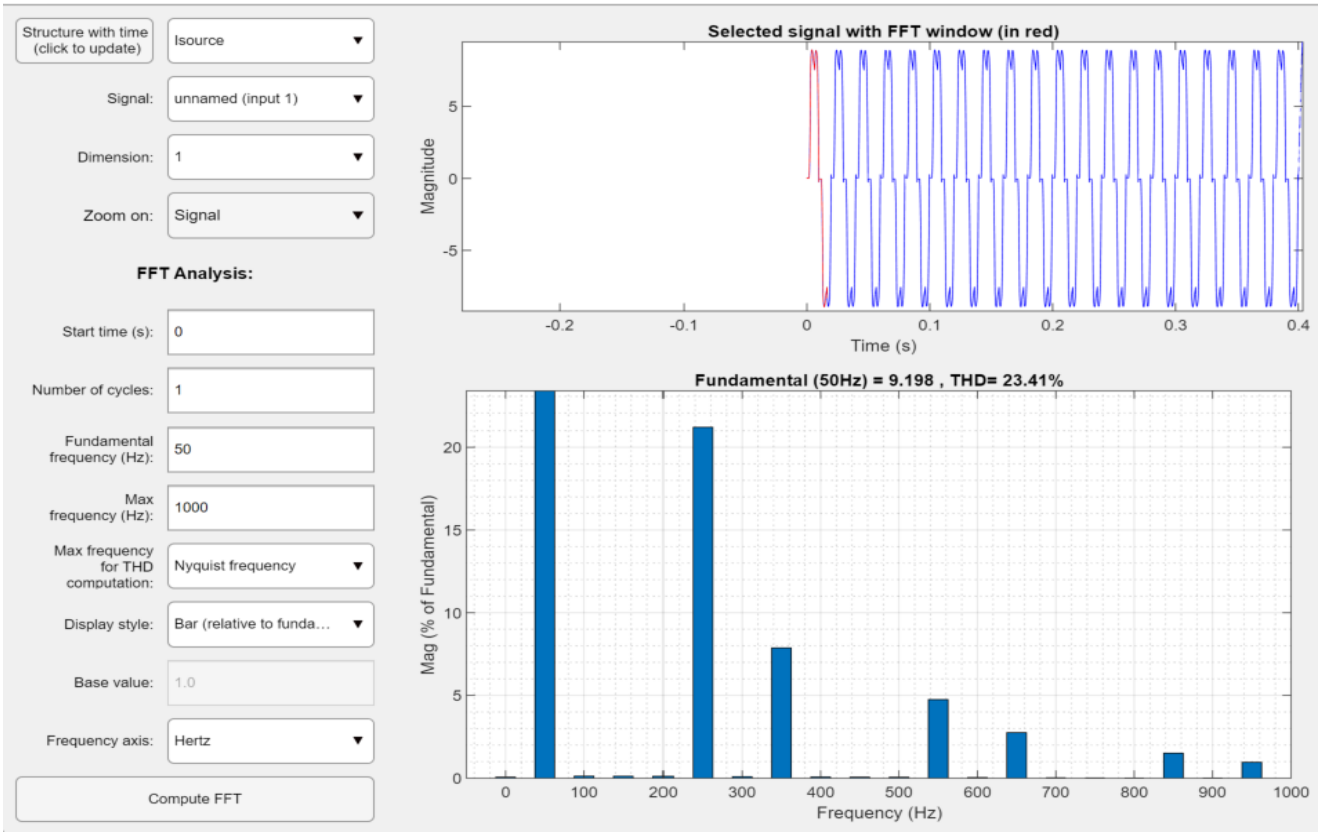

FFT analysis result for the source when SAPF was connected

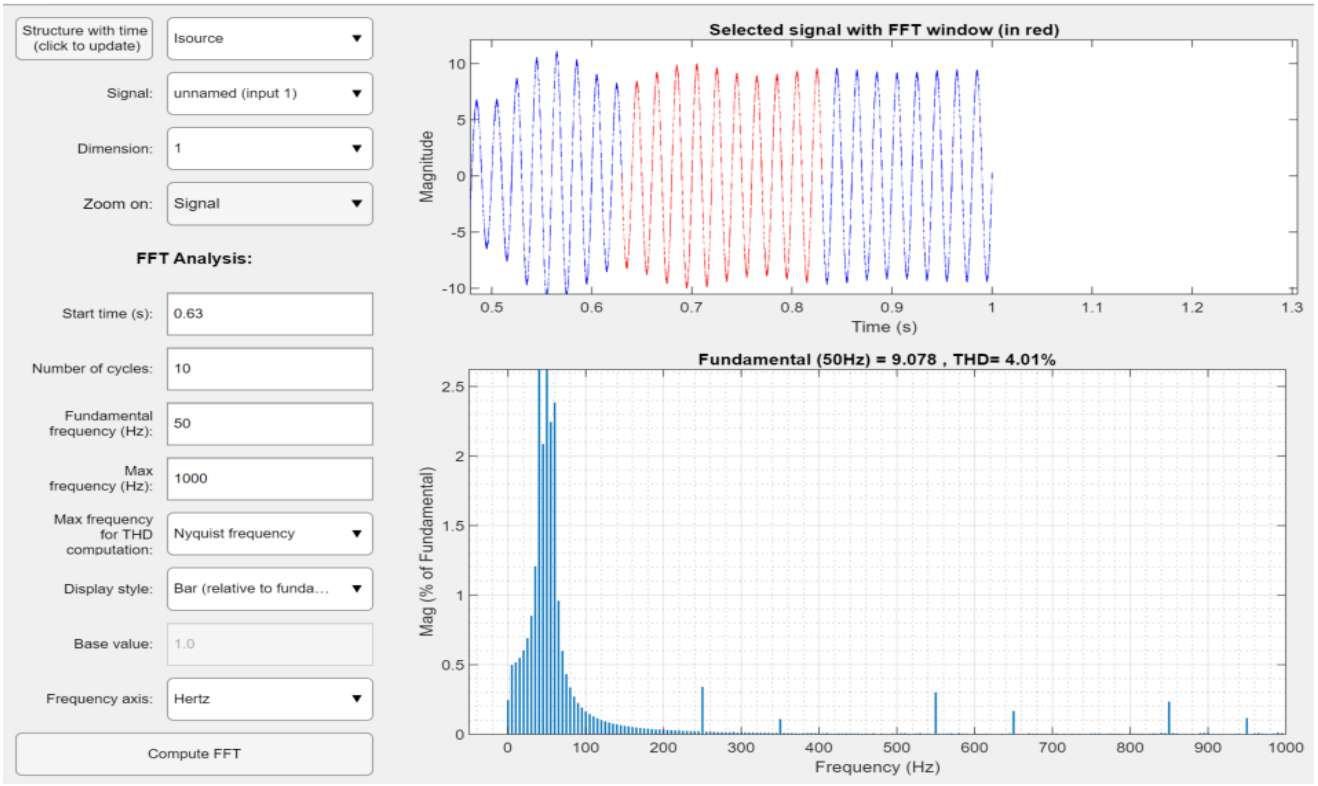

FFT analysis result for the source when SAPF was connected

iv) For 5000W load :

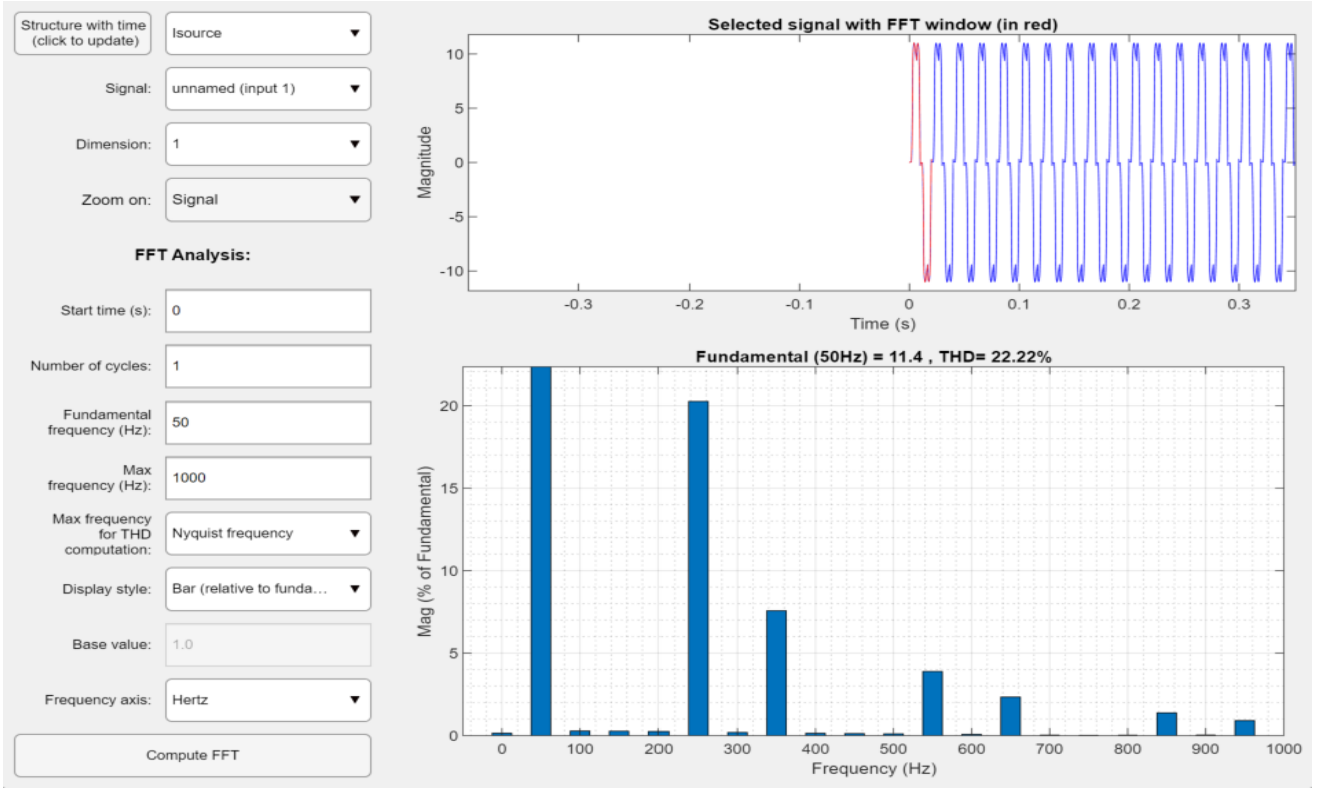

FFT analysis result for the source when no SAPF was connected

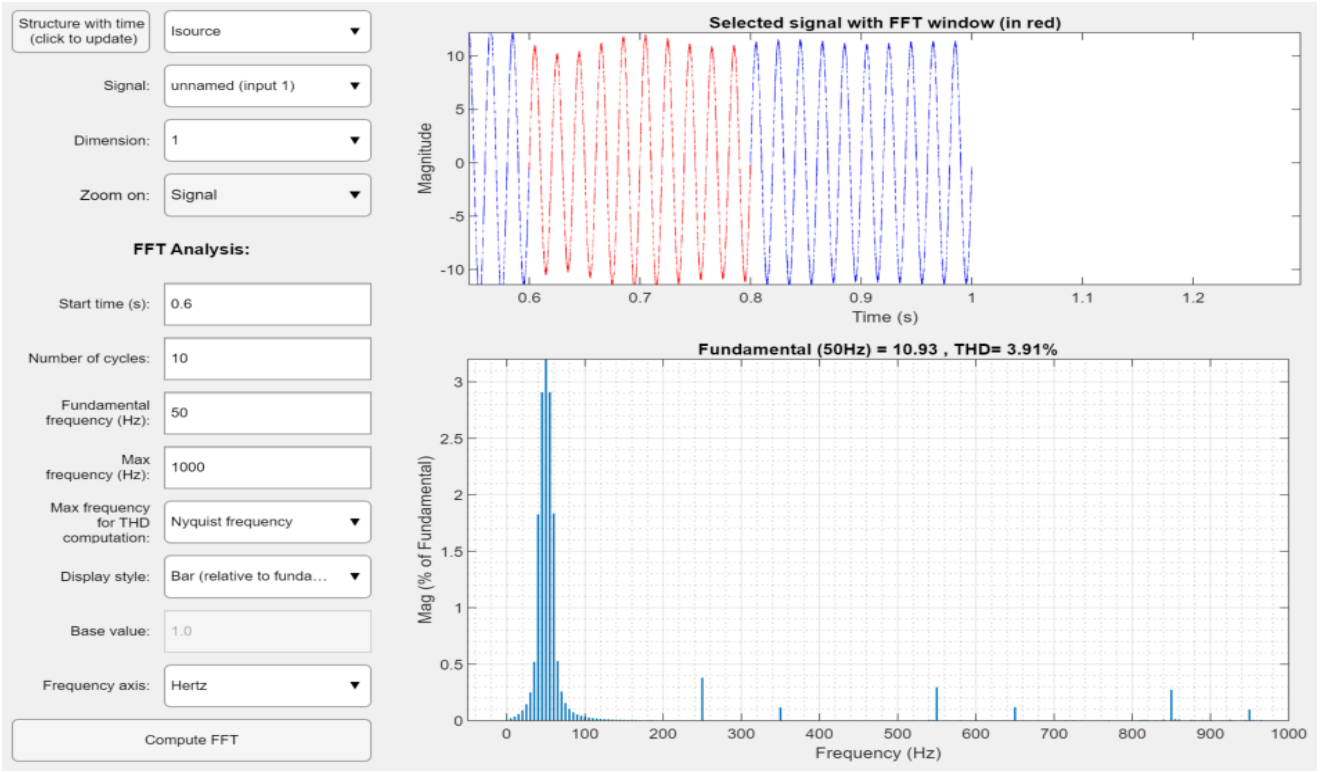

FFT analysis result for the source when SAPF was connected

v) For 6000W load :

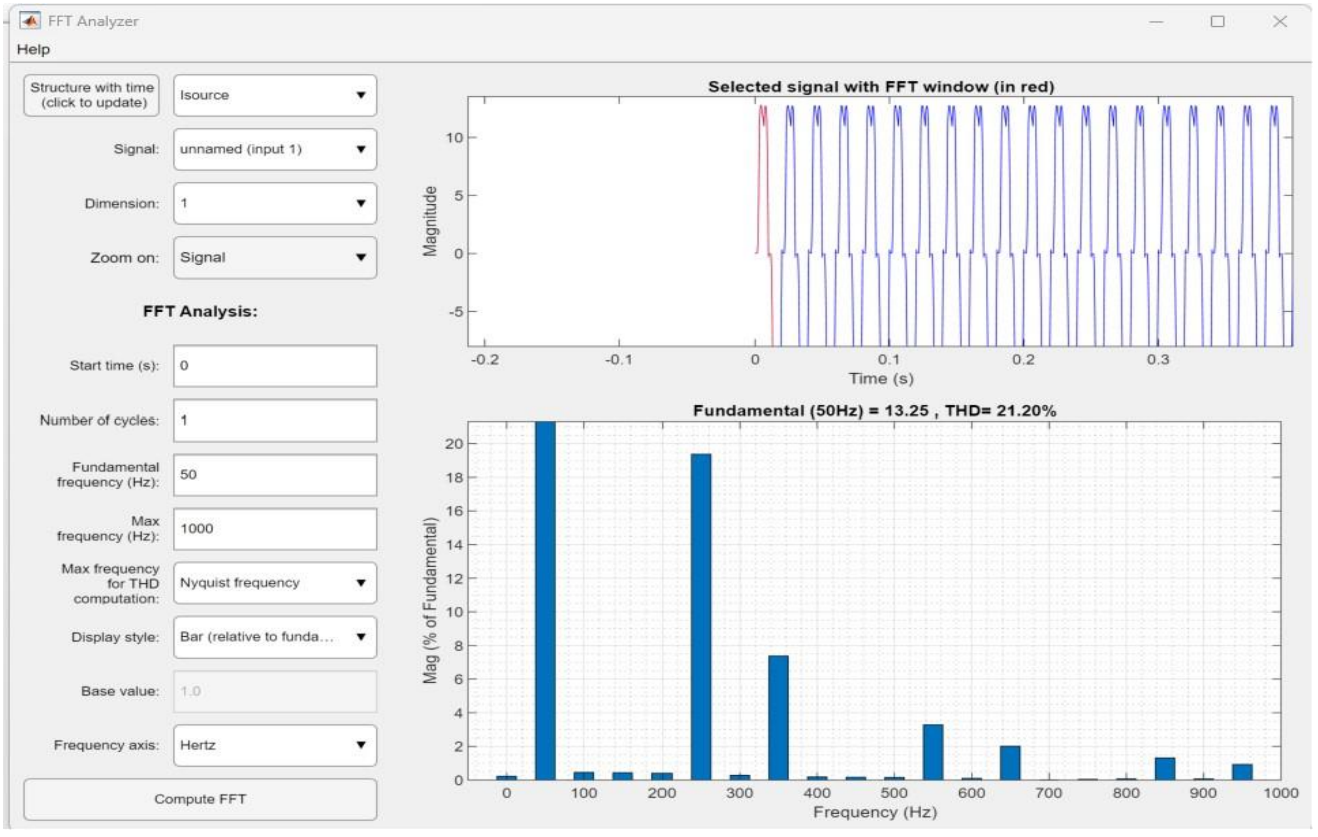

FFT analysis result for the source when no SAPF was connected

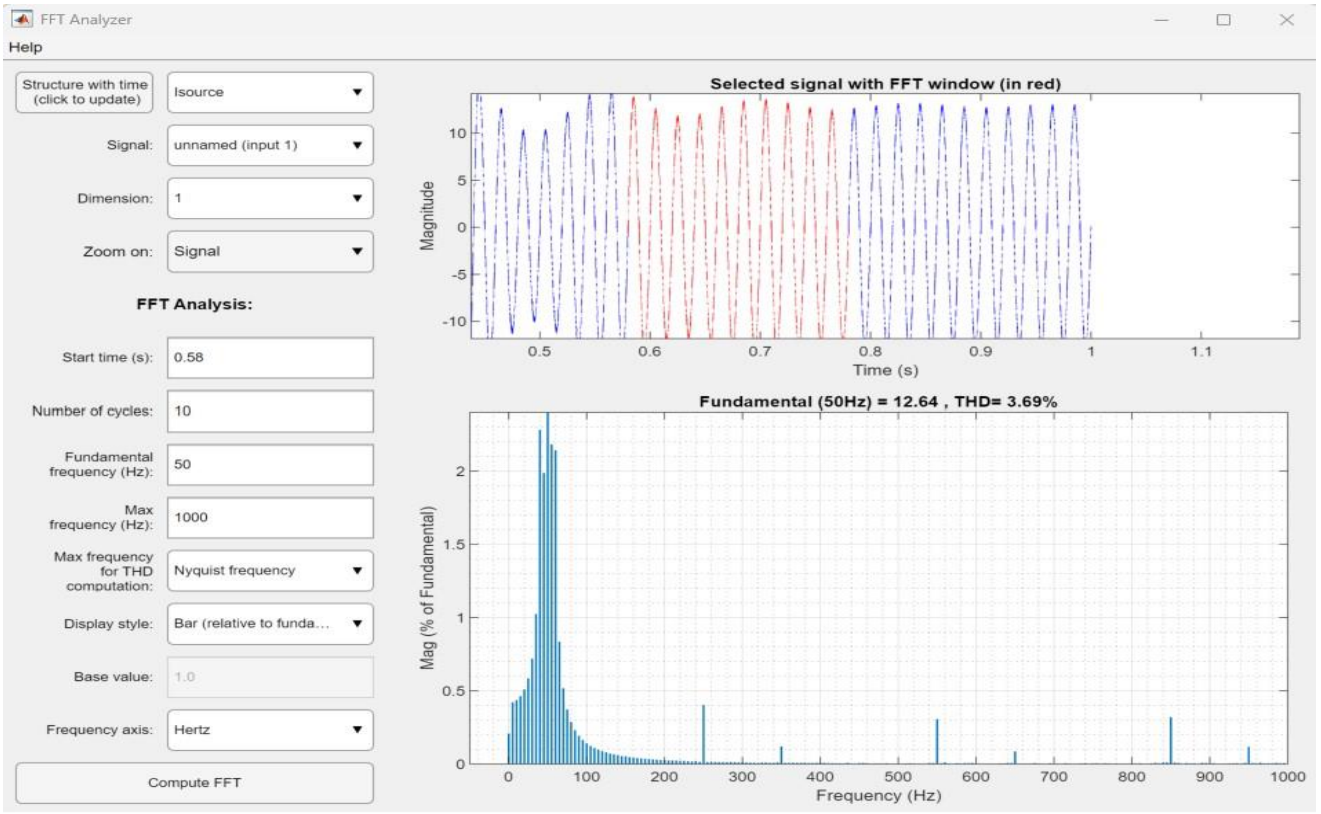

FFT analysis result for the source when SAPF was connected

vi) For 7000W load :

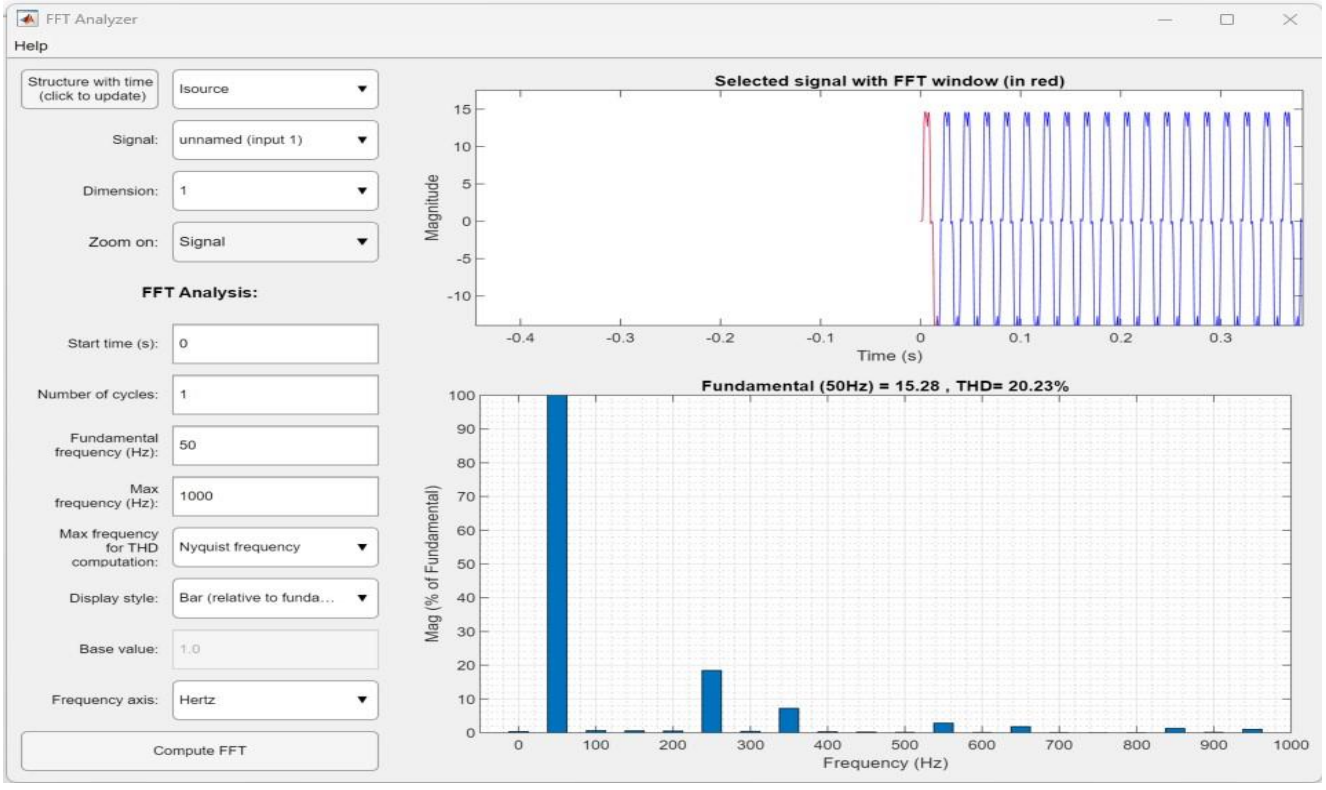

FFT analysis result for the source when no SAPF was connected

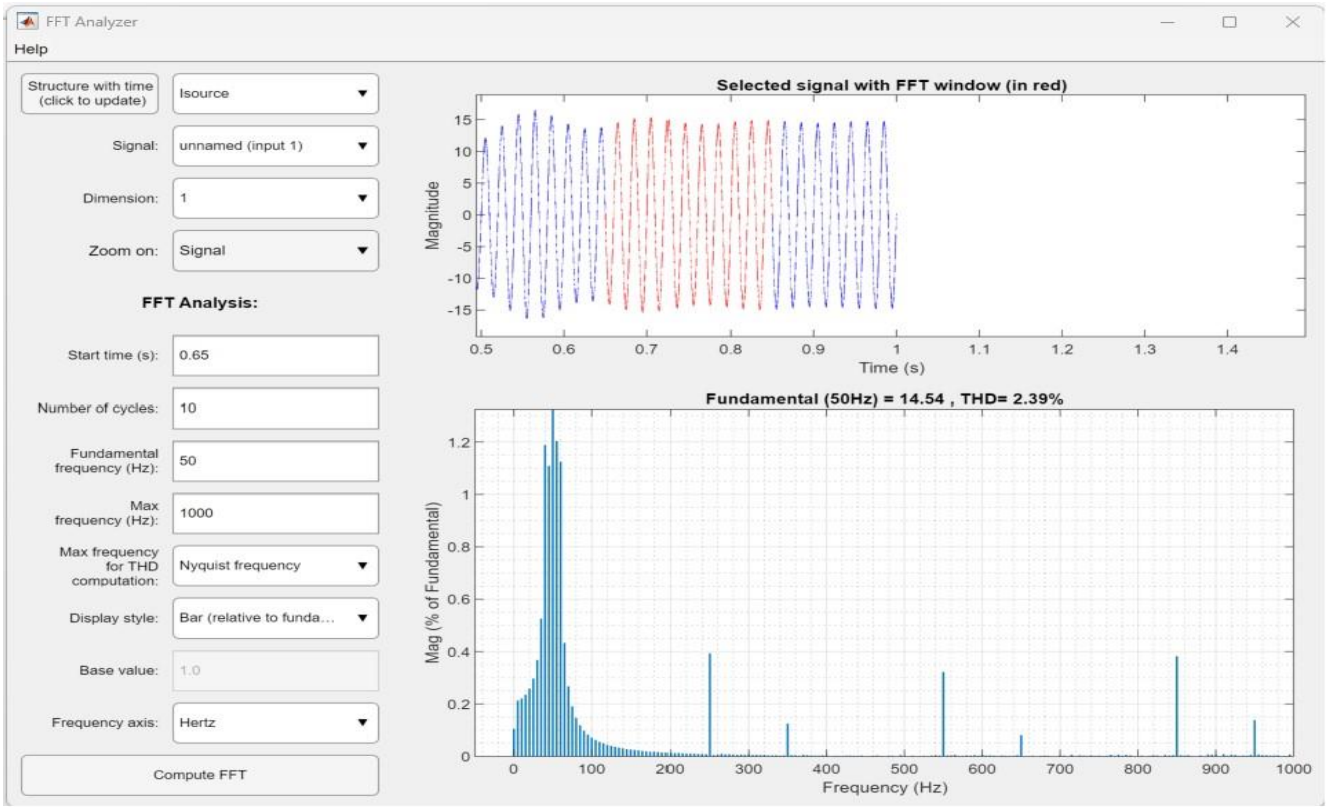

FFT analysis result for the source when SAPF was connected

vii) For 8000W load :

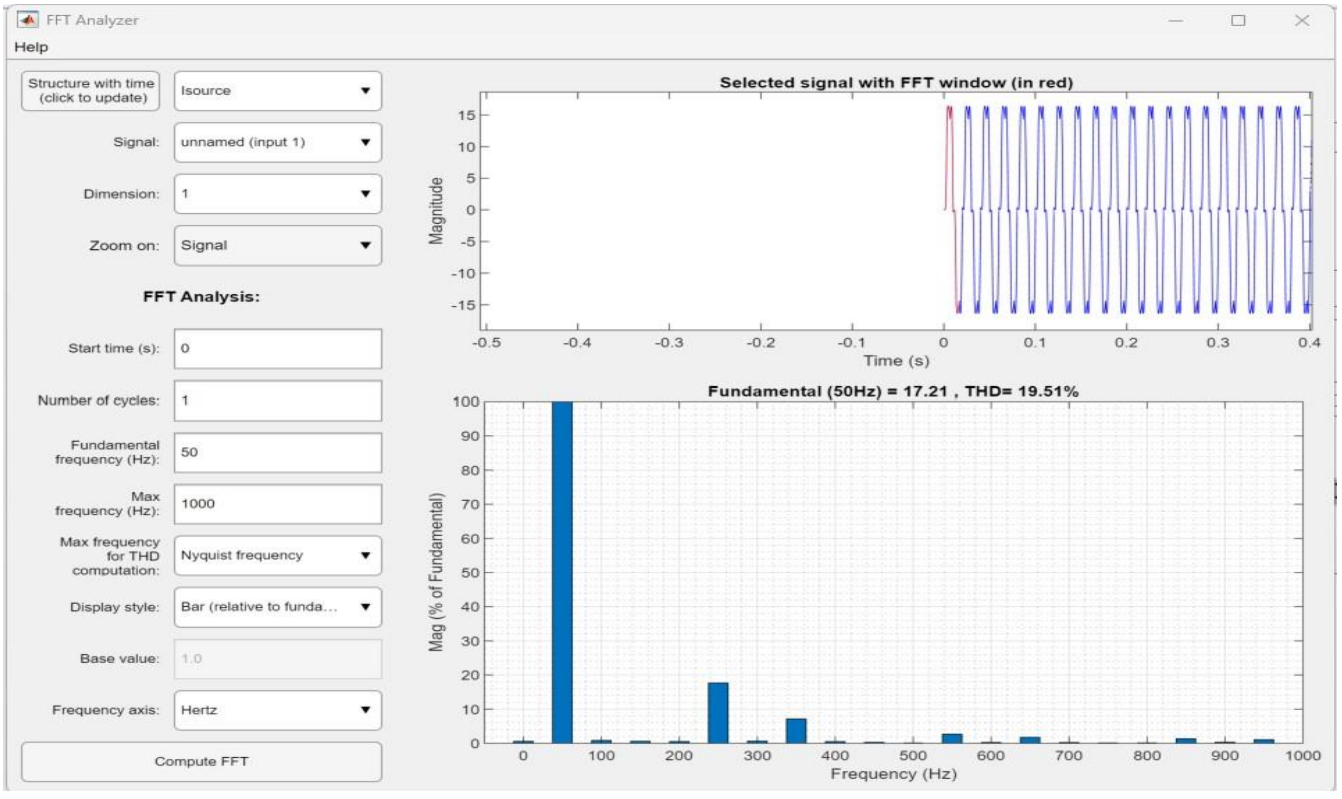

FFT analysis result for the source when no SAPF was connected

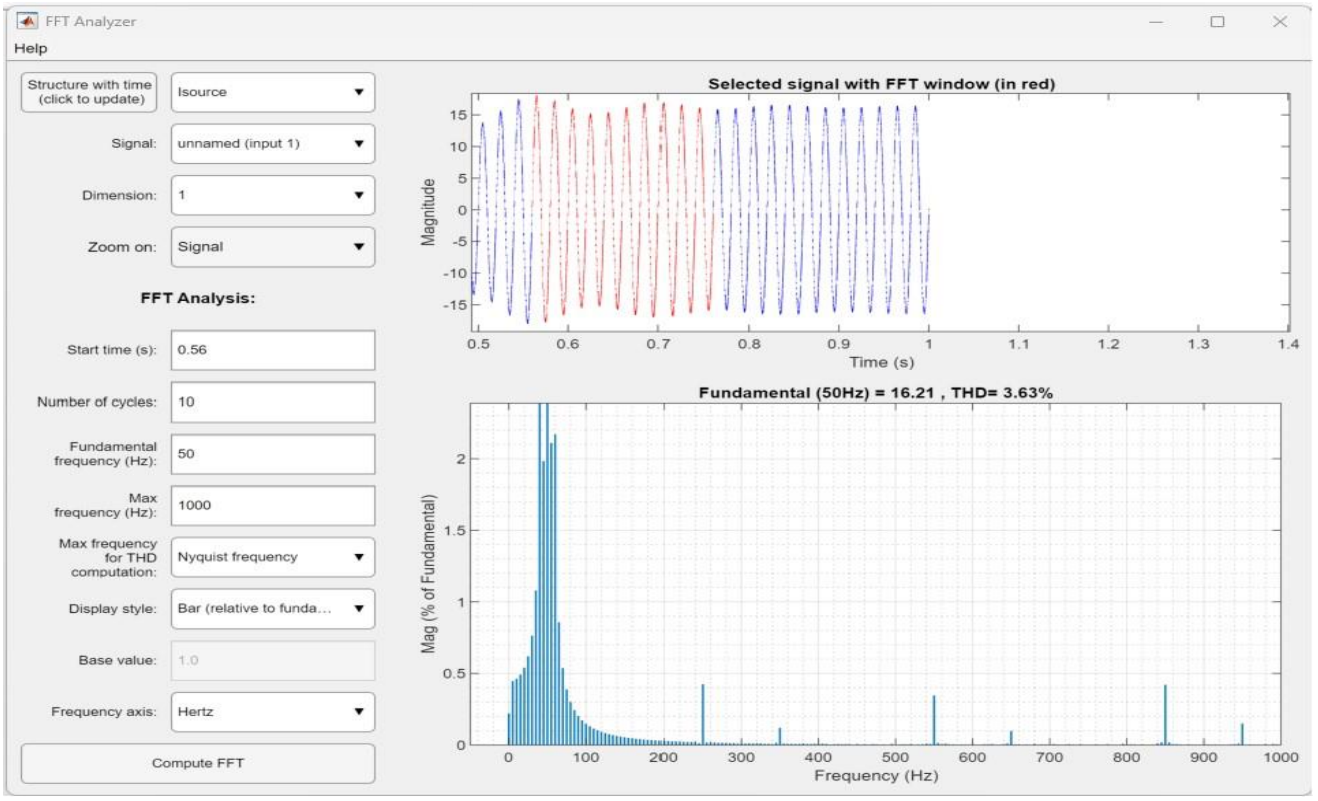

FFT analysis result for the source when SAPF was connected

viii) For 9000W load :

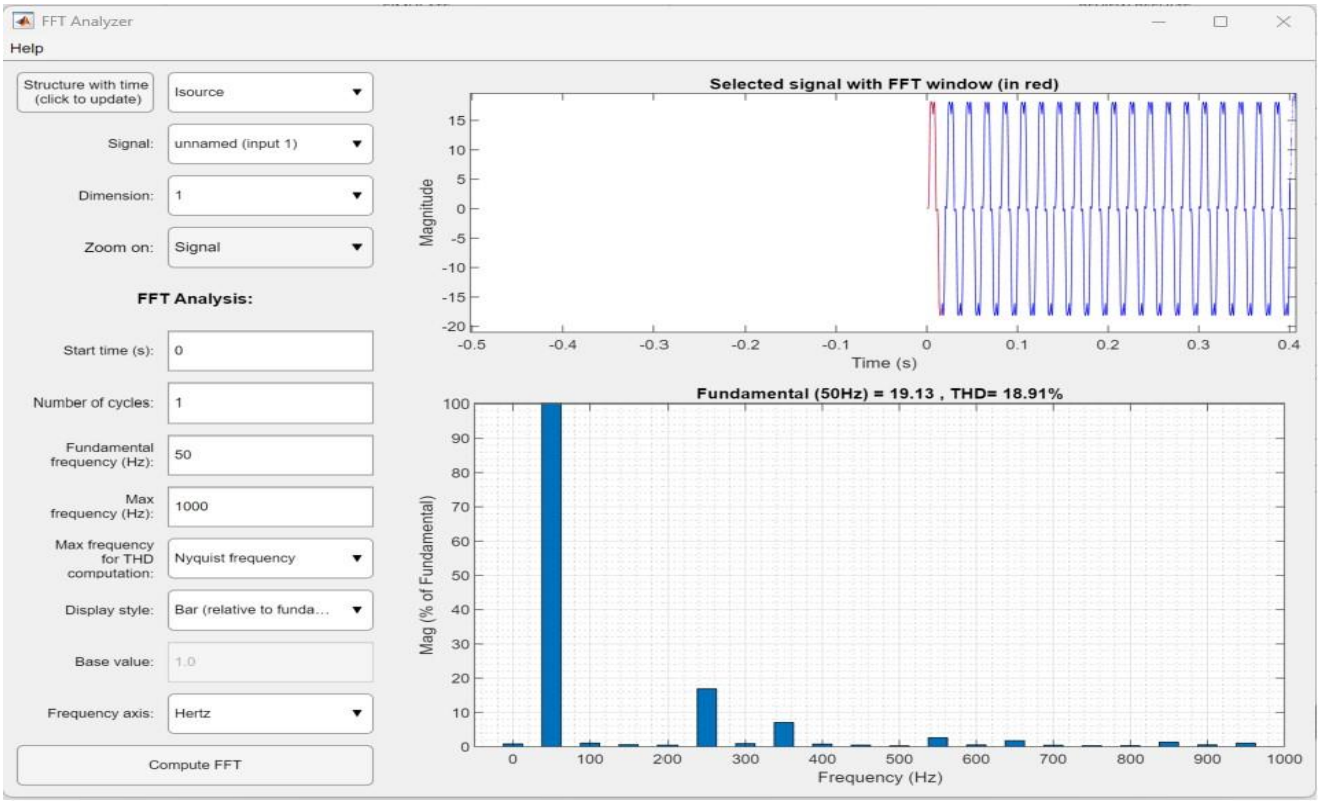

FFT analysis result for the source when SAPF was connected

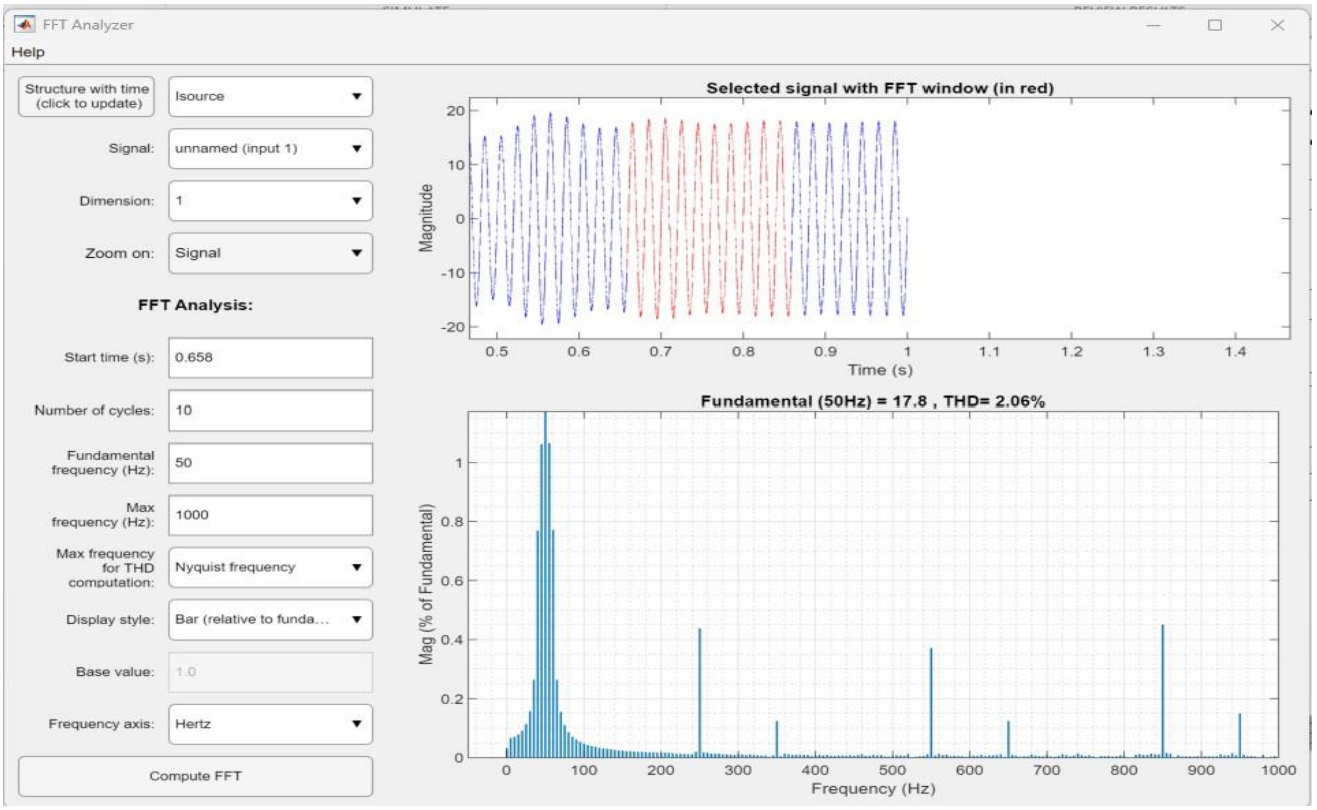

FFT analysis result for the source when no SAPF was connected

ix) For 10KW load :

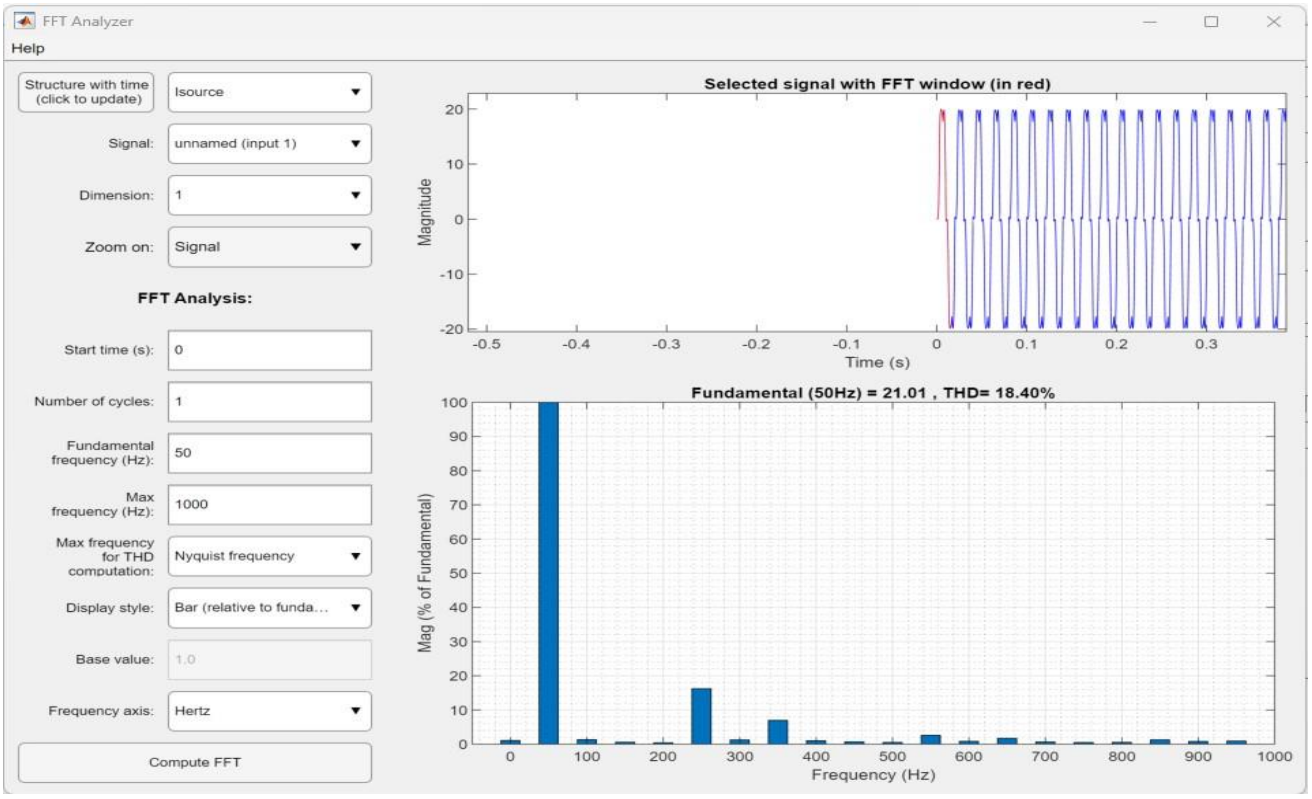

FFT analysis result for the source when SAPF was connected

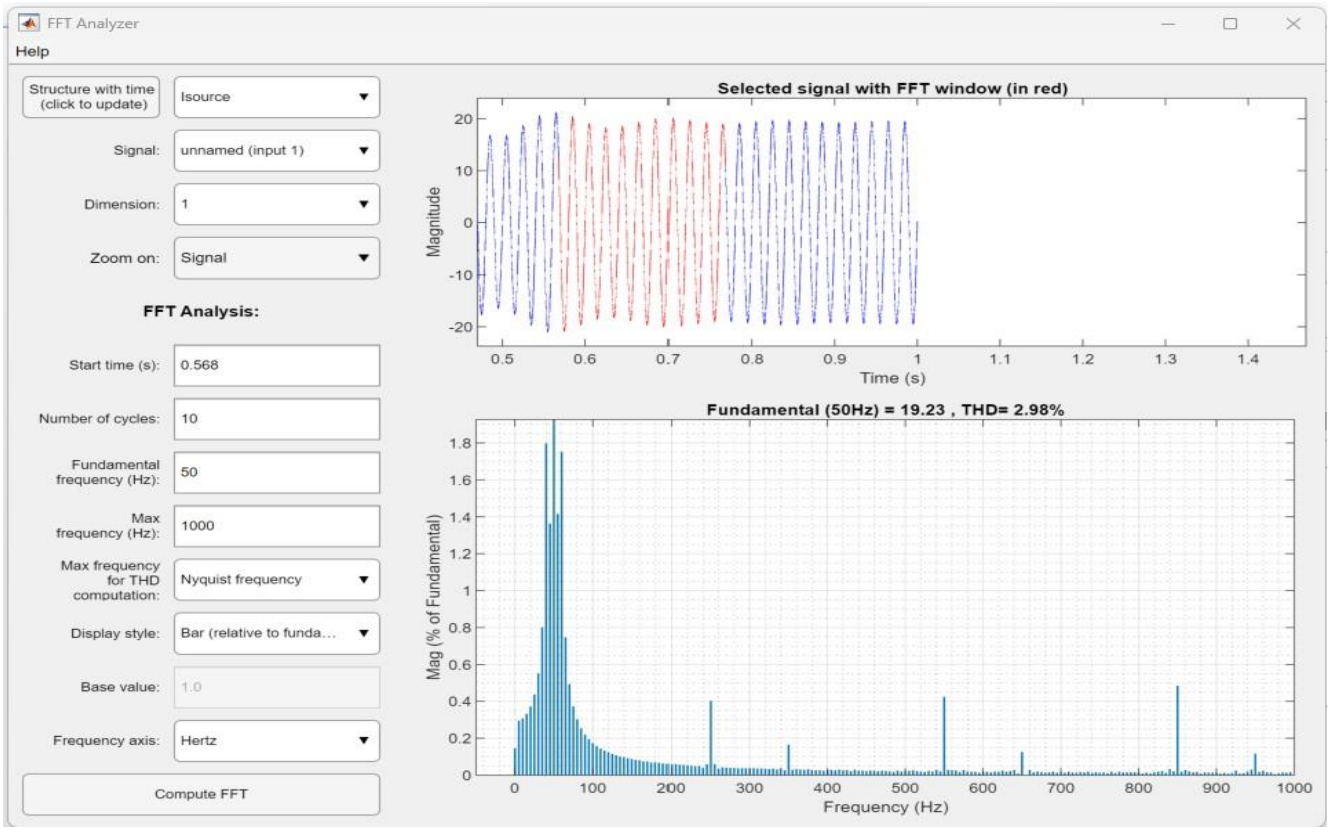

FFT analysis result for the source when SAPF was connected

x) For 12KW load :

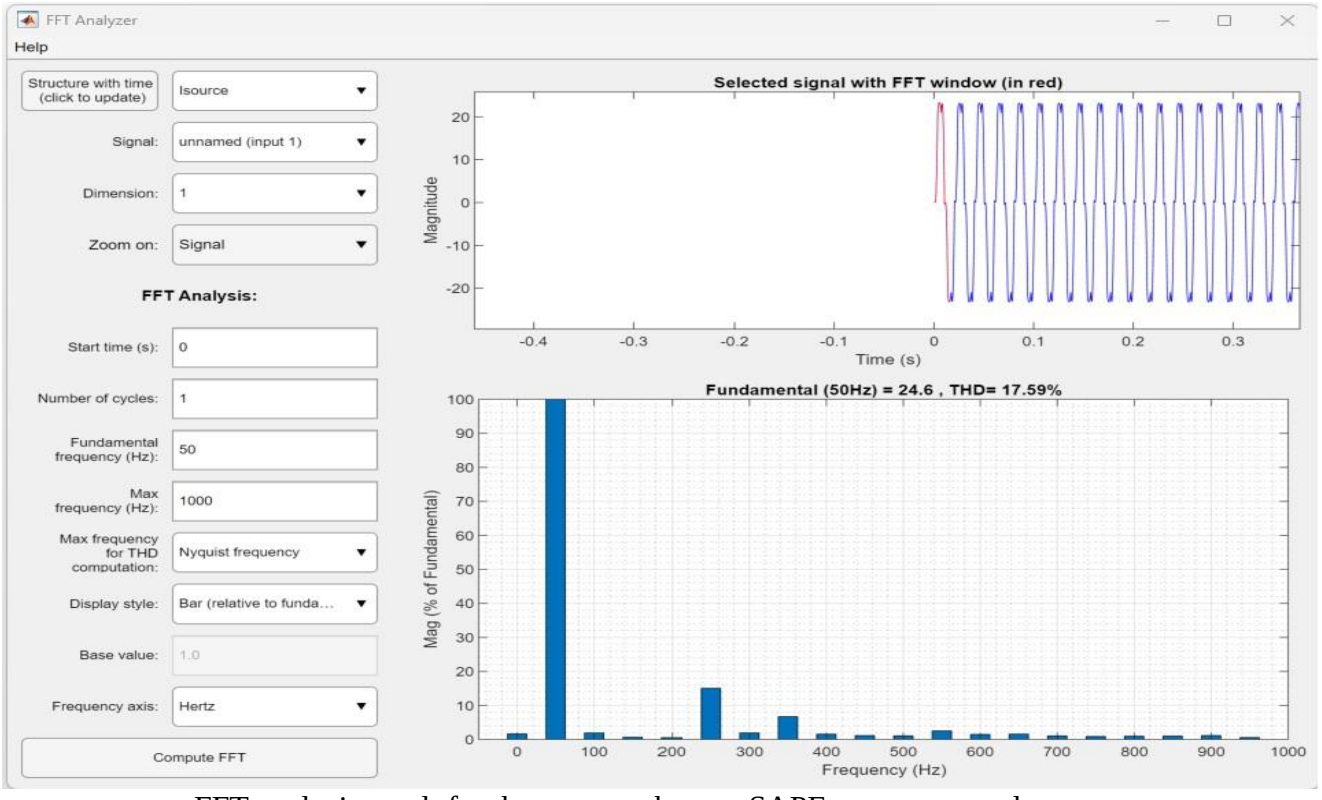

FFT analysis result for the source when no SAPF was connected

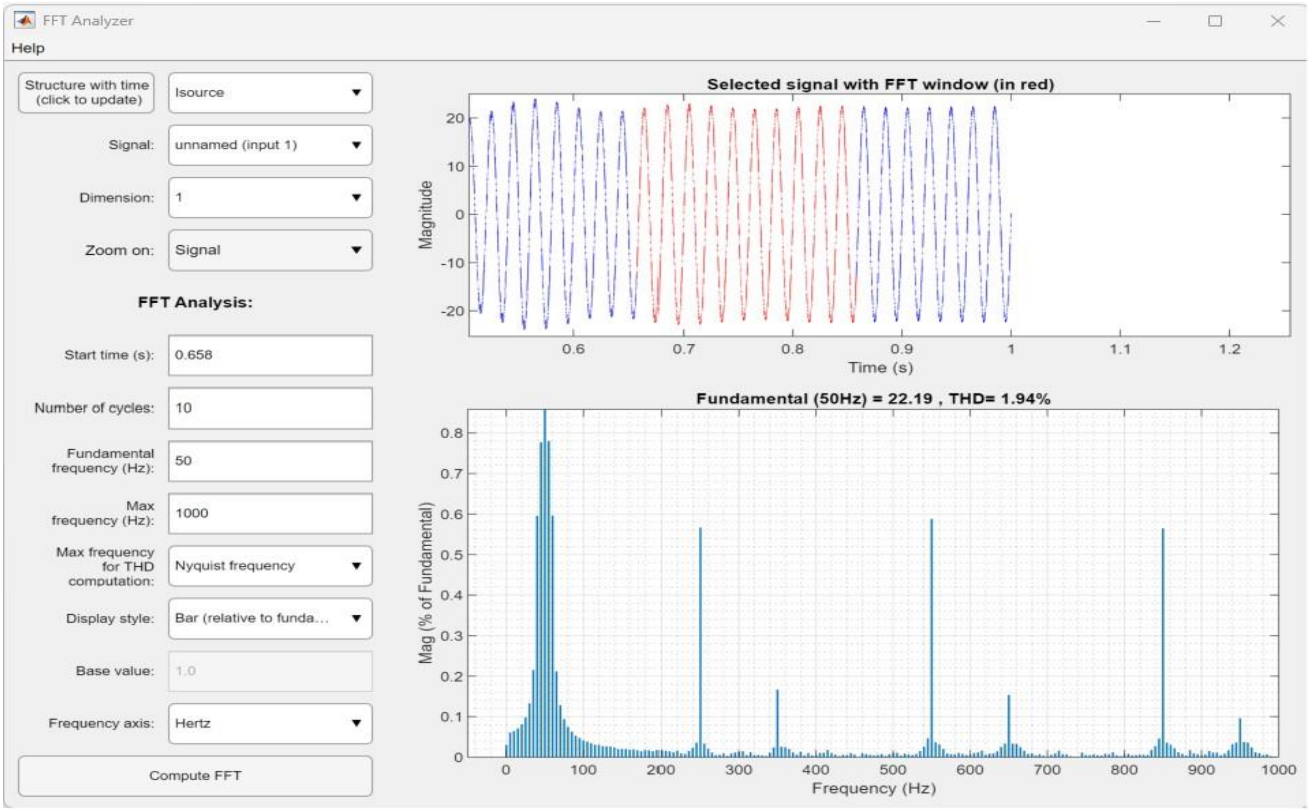

FFT analysis result for the source when SAPF was connected

xi) For 14KW Load :

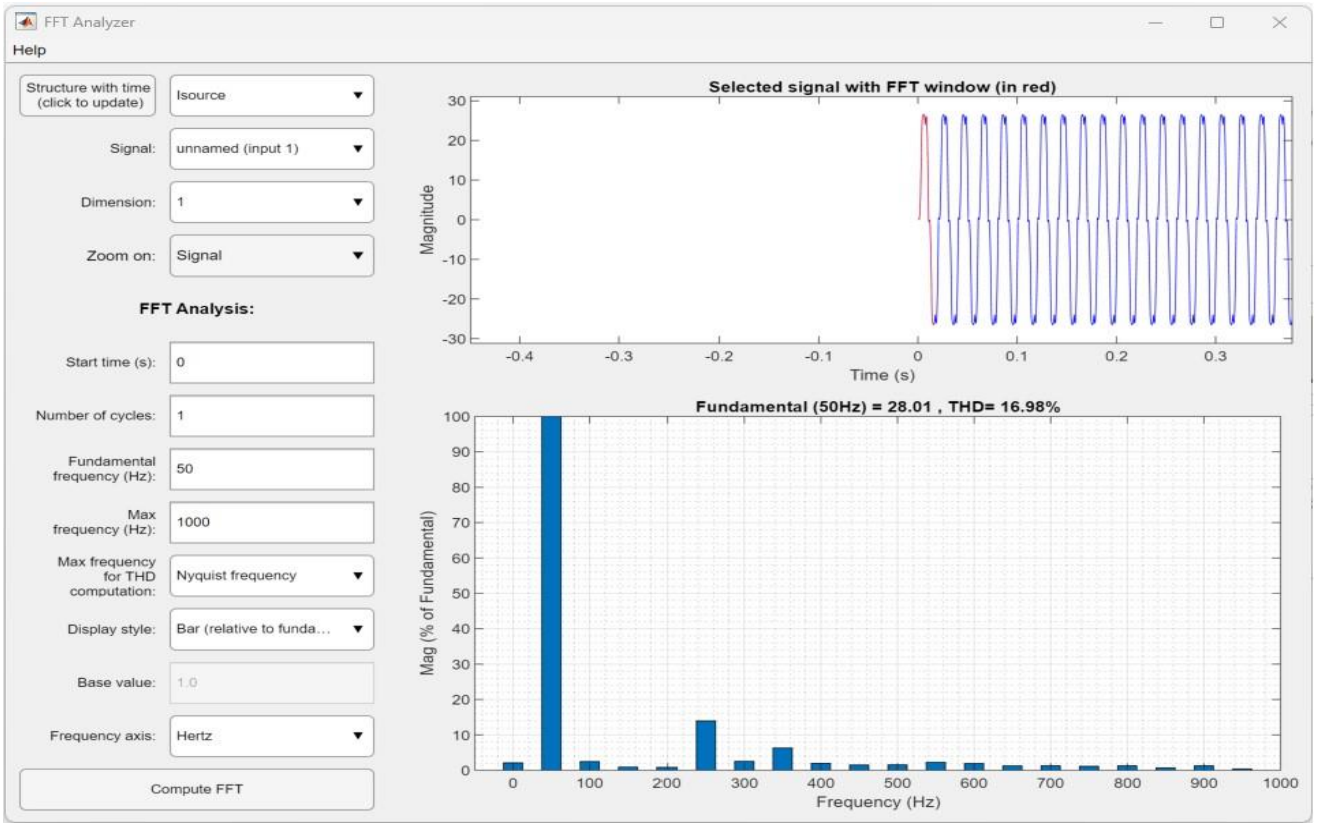

FFT analysis result for the source when no SAPF was connected

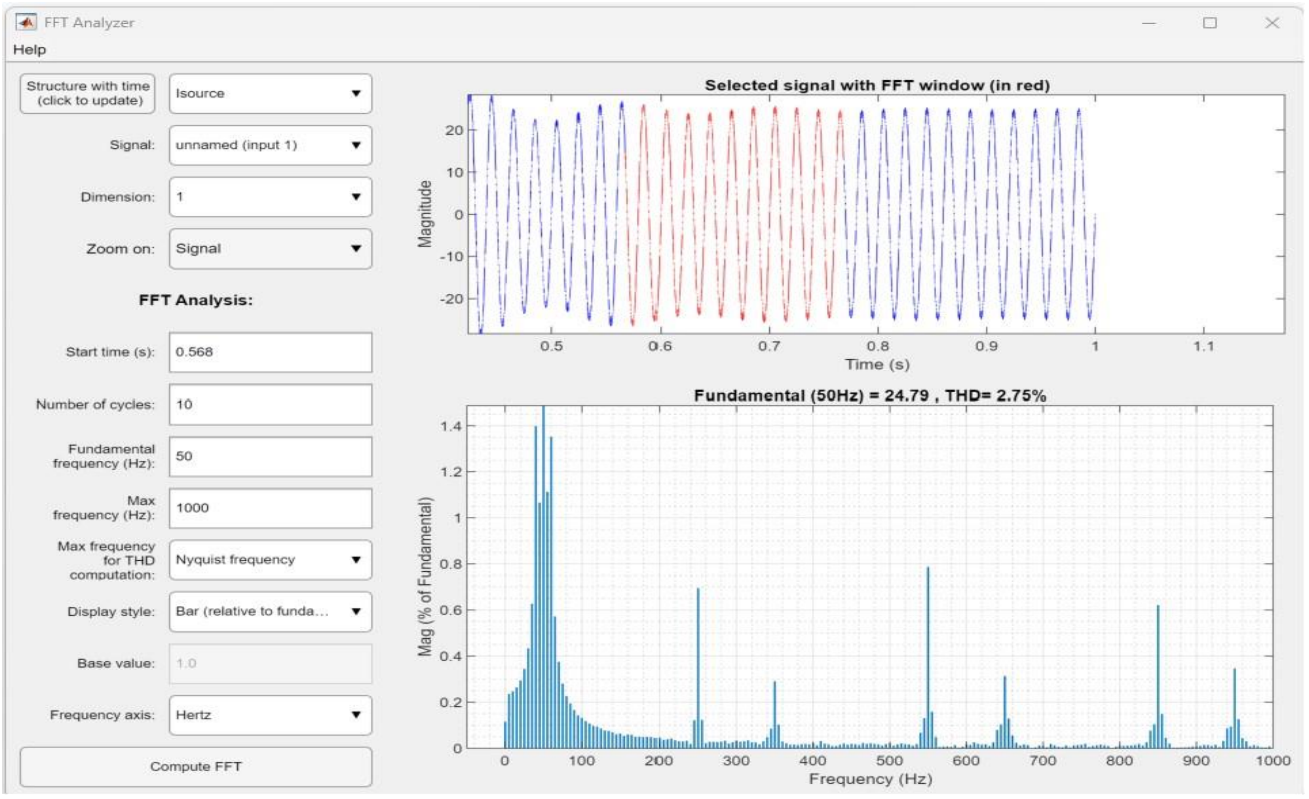

FFT analysis result for the source when SAPF was connected

xii) For 16KW load :

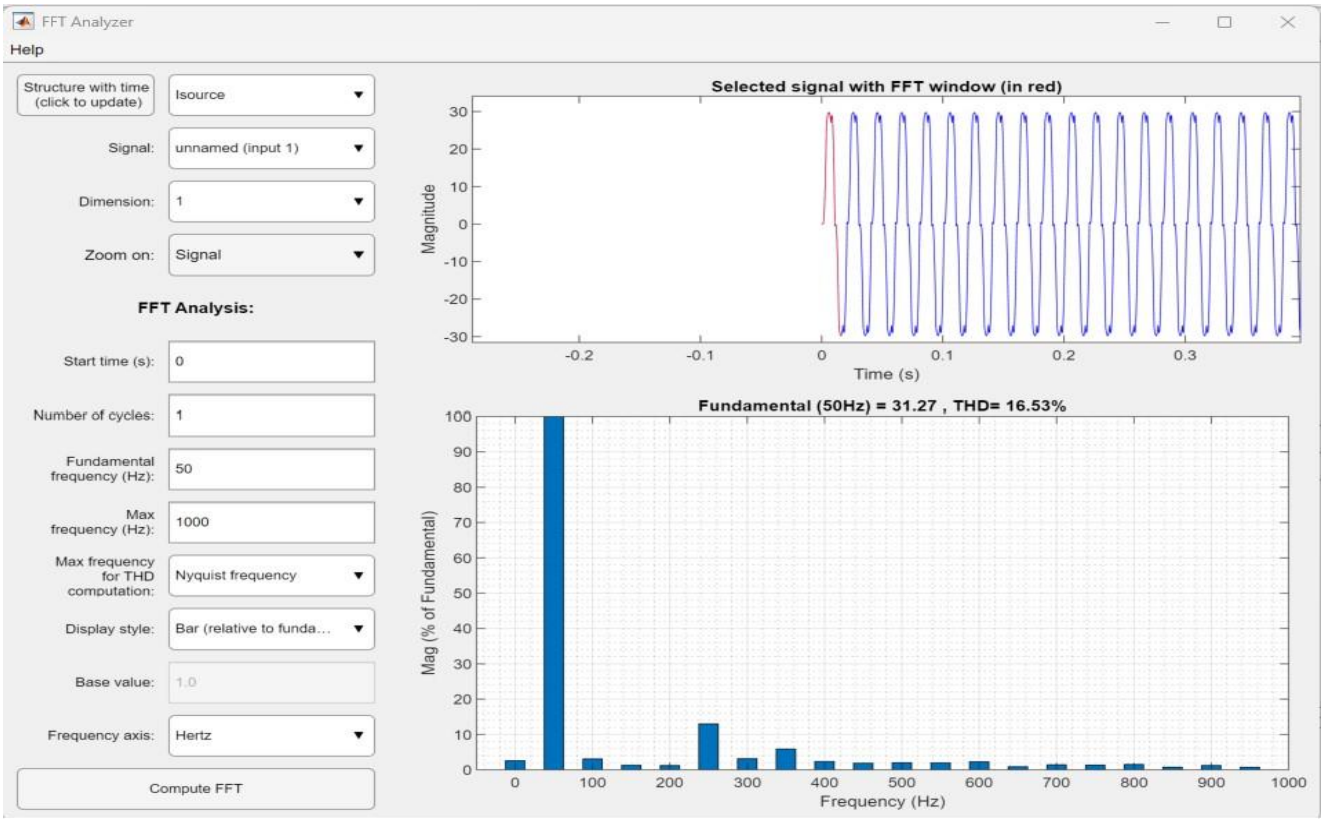

FFT analysis result for the source when no SAPF was connected

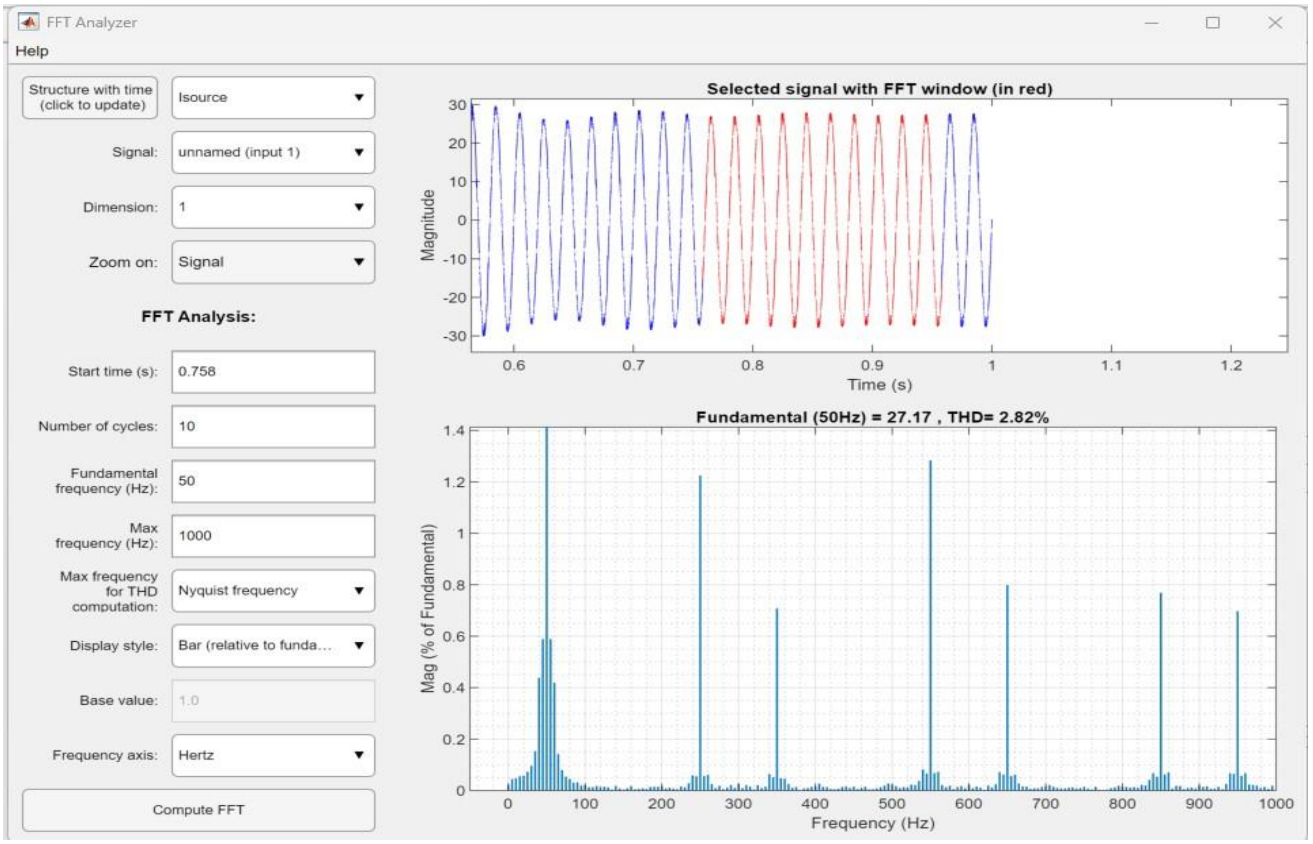

FFT analysis result for the source when SAPF was connected

xiii) For 18KW load :

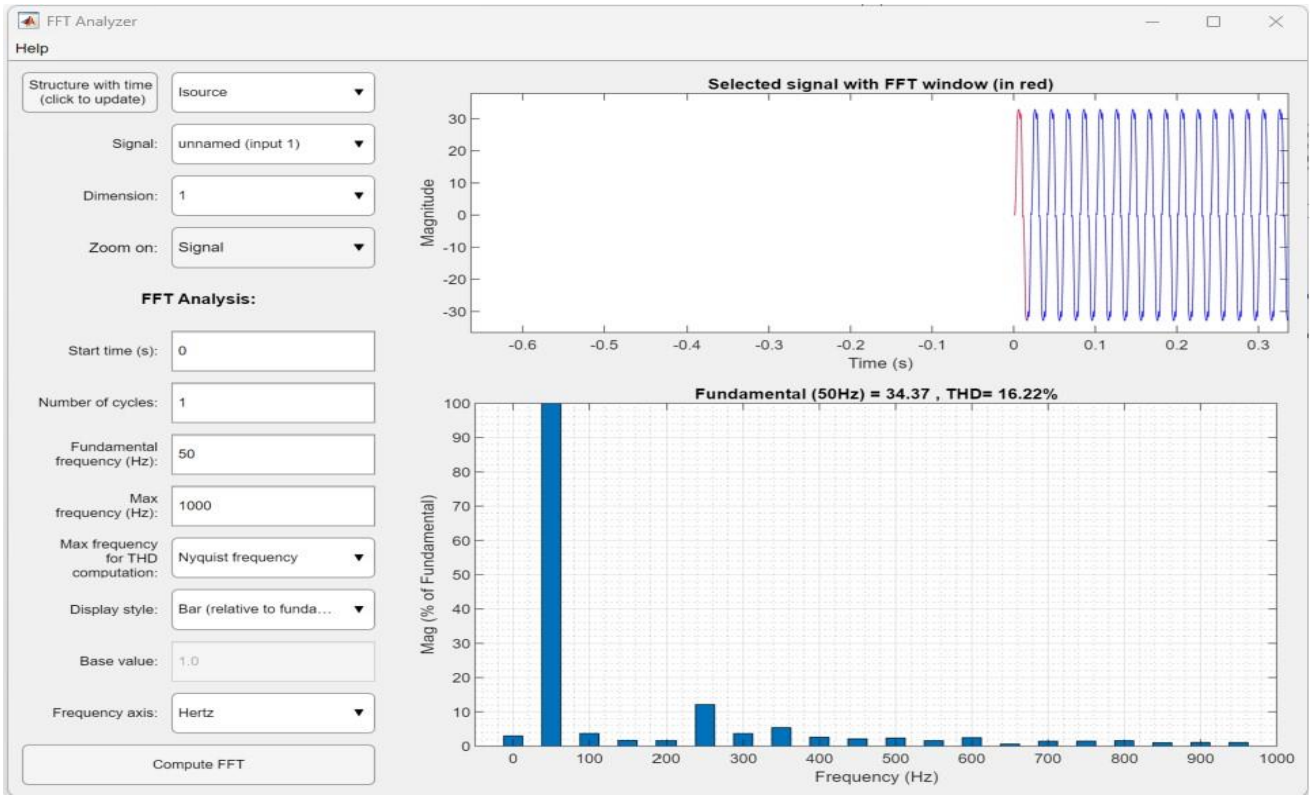

FFT analysis result for the source when no SAPF was connected

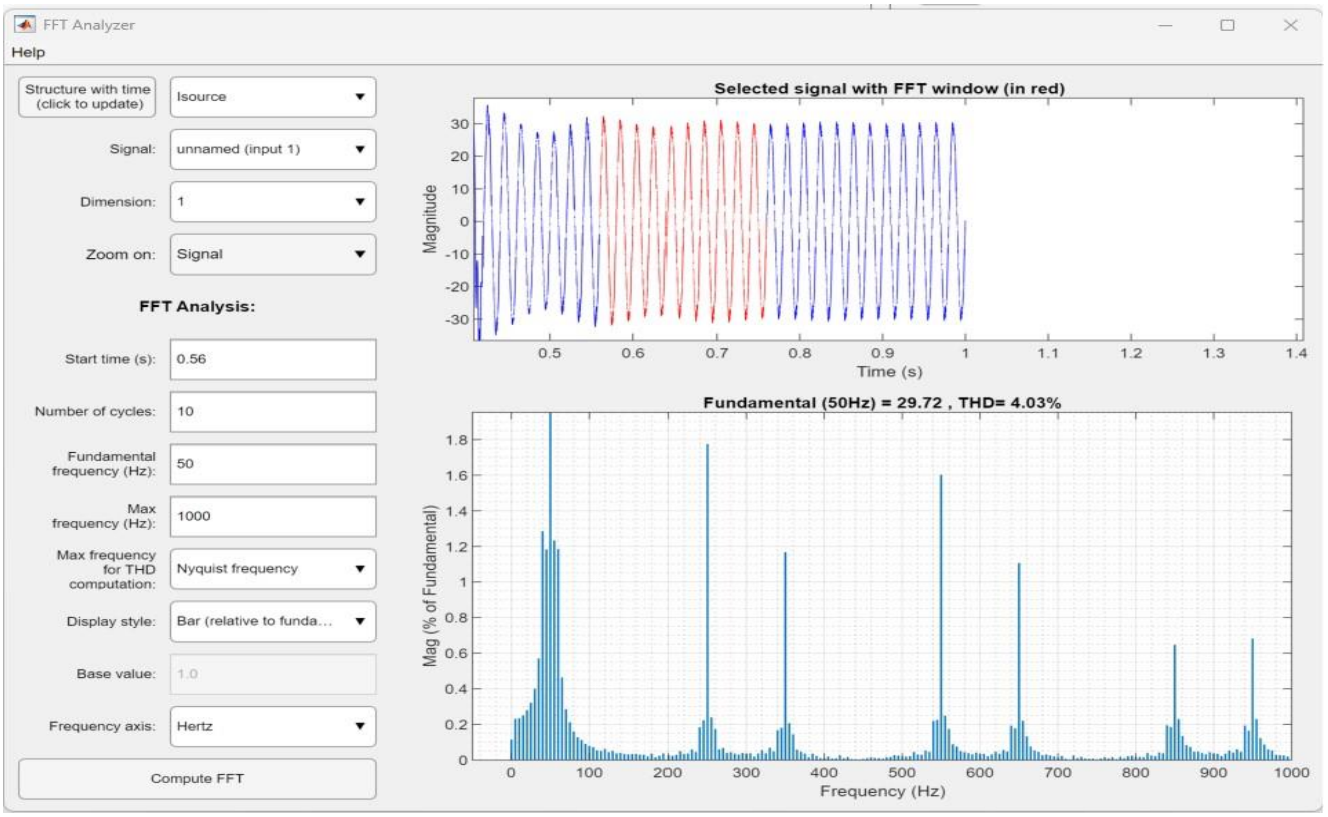

FFT analysis result for the source when SAPF was connected

xiv) For 20KW load :

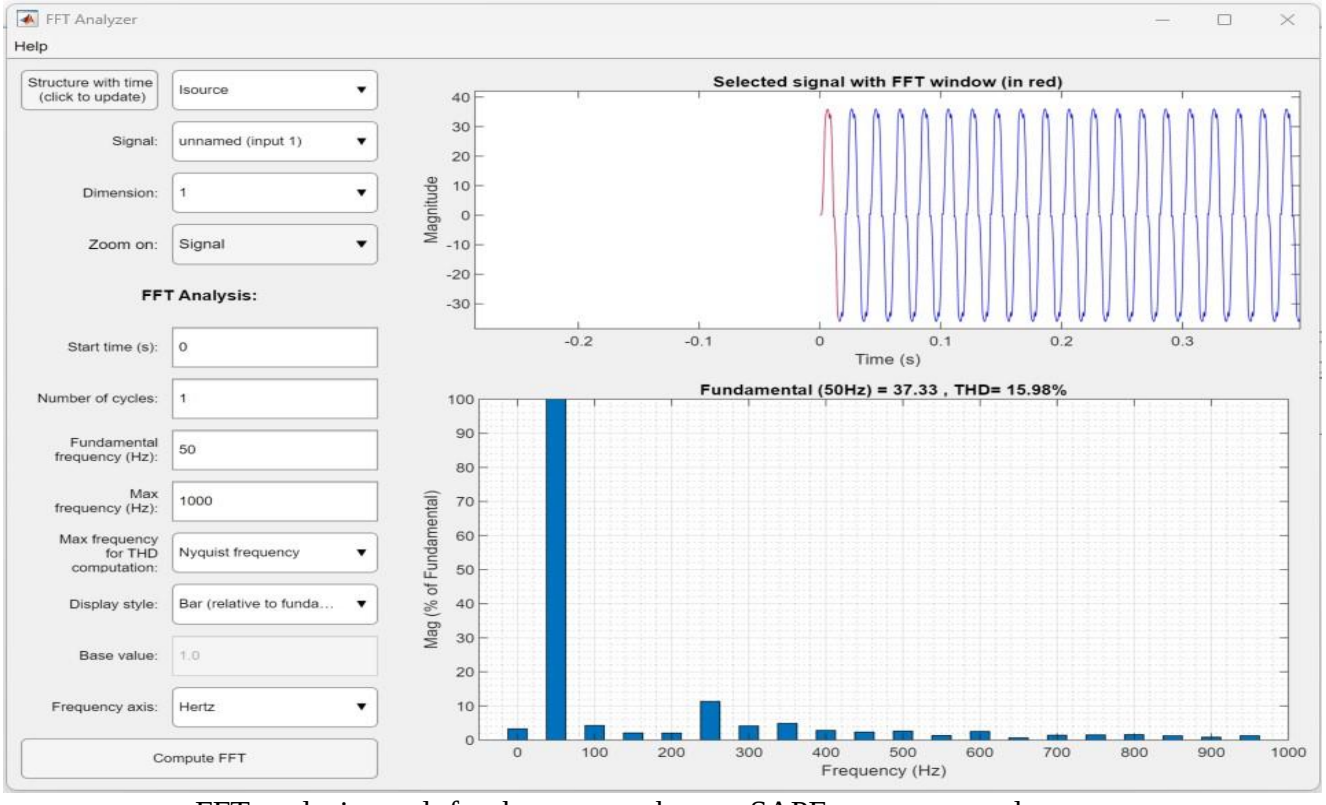

FFT analysis result for the source when no SAPF was connected

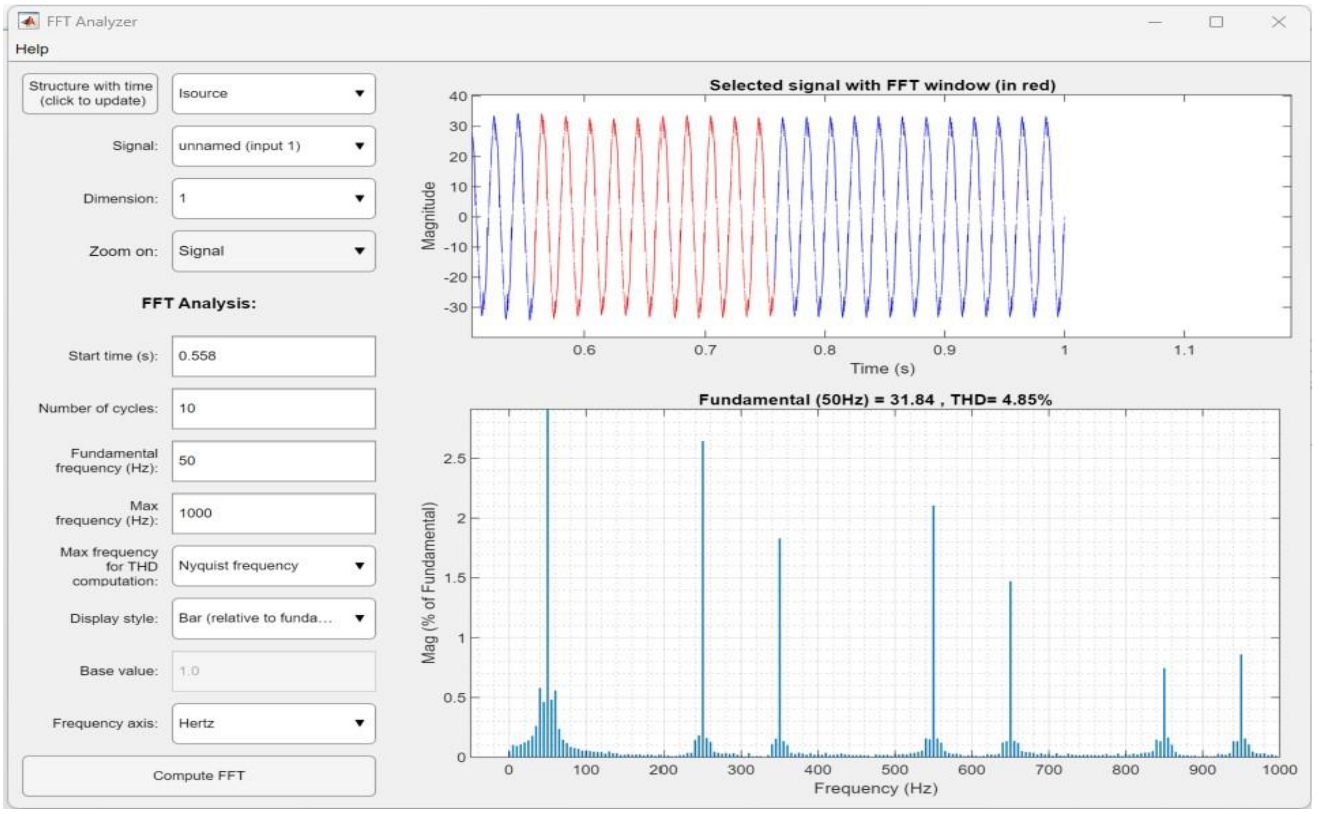

FFT analysis result for the source when SAPF was connected

Annex 2

MATLAB results for Table IV : Performance comparison of SAPF under different loading condition for 3 phase 4 wire system.

i) For 2000W load :

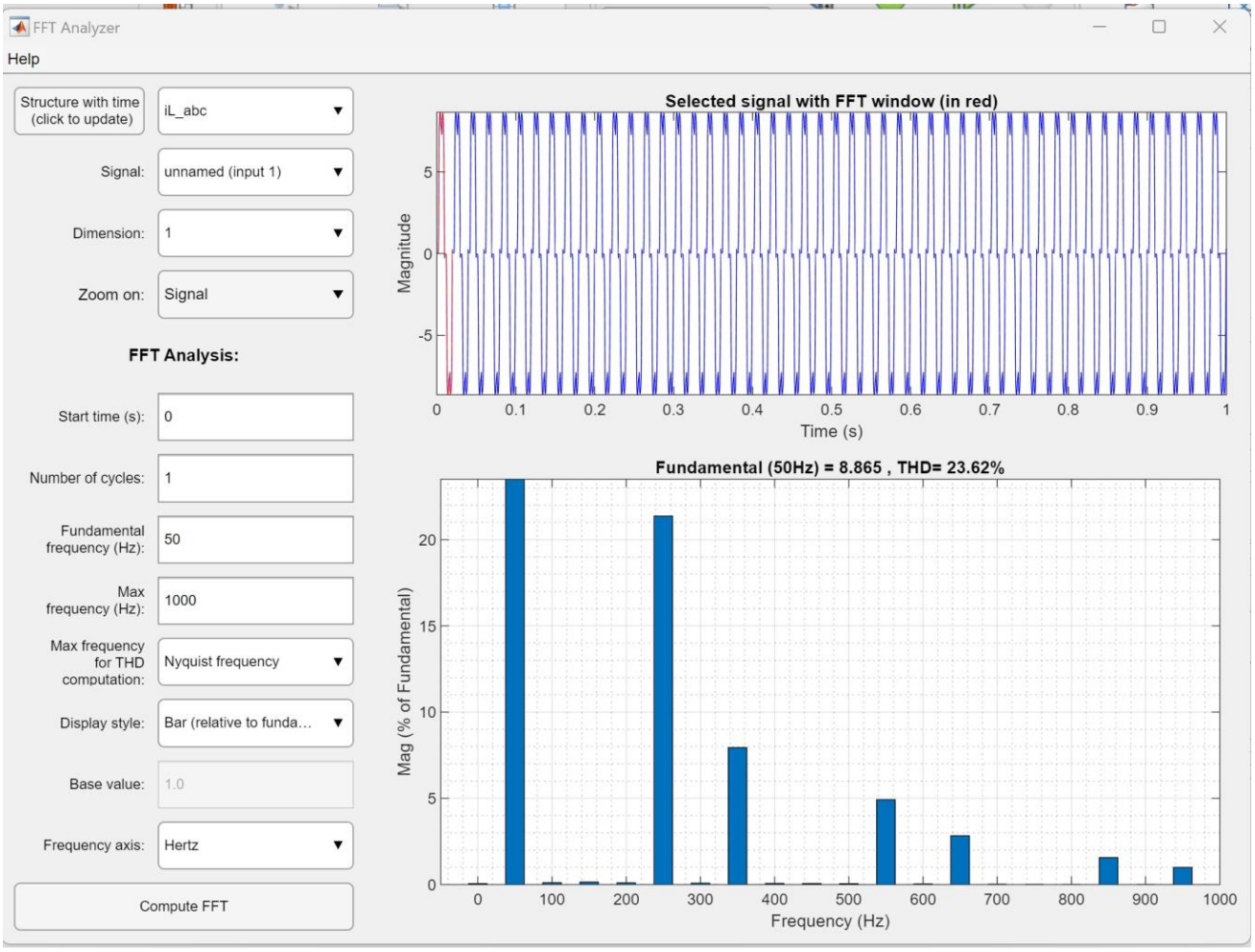

FFT analysis result for the source when no SAPF was connected

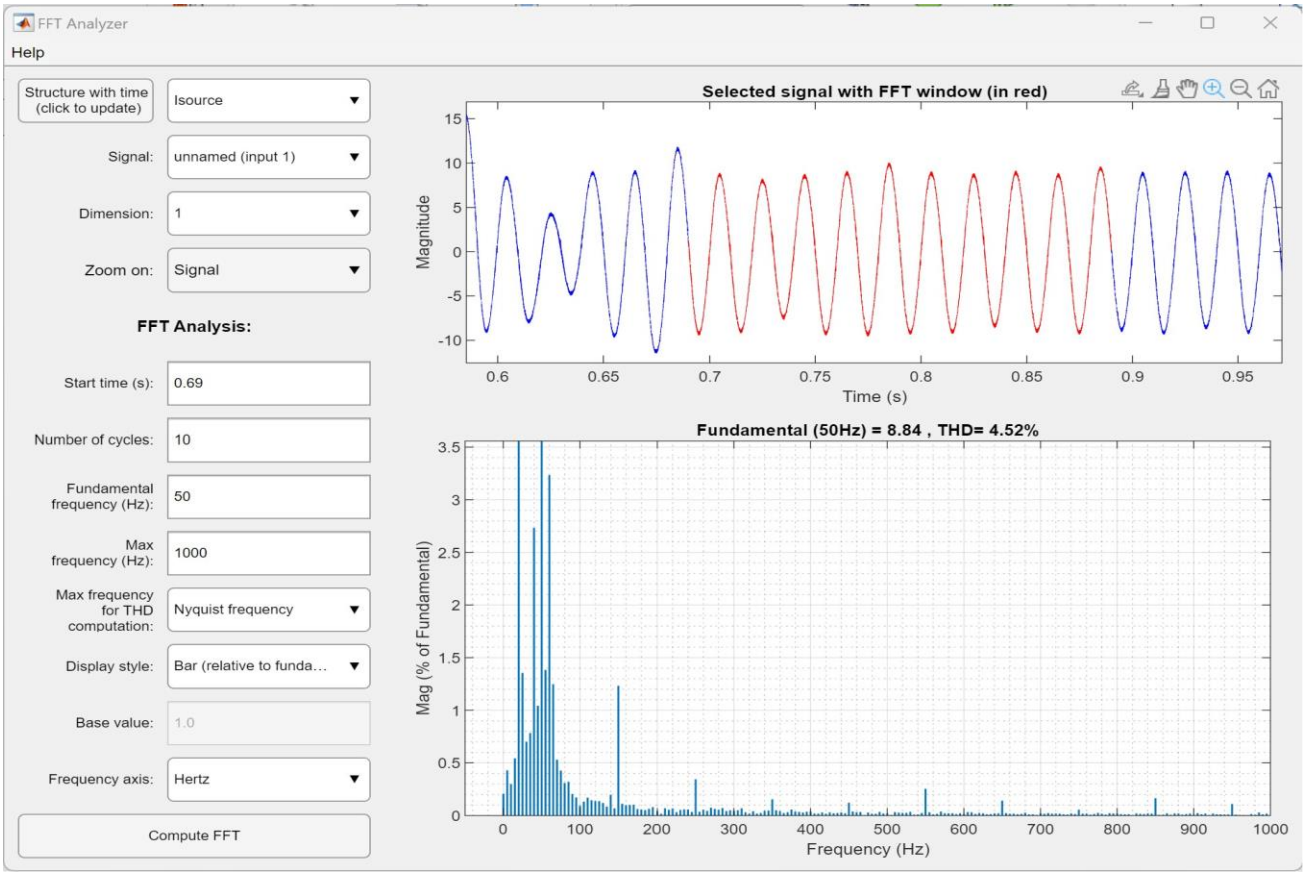

FFT analysis result for the source when SAPF was connected

ii) For 3000W load :

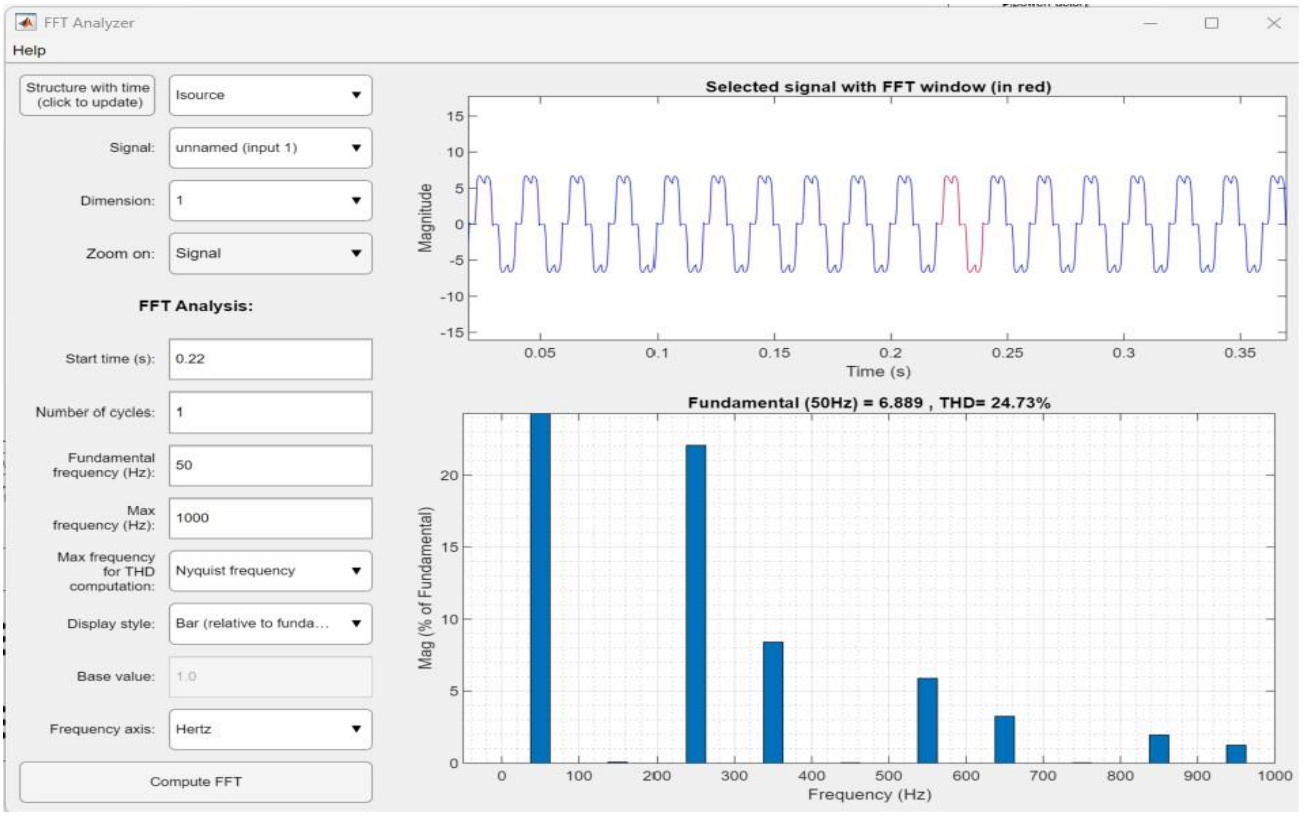

FFT analysis result for the source when no SAPF was connected

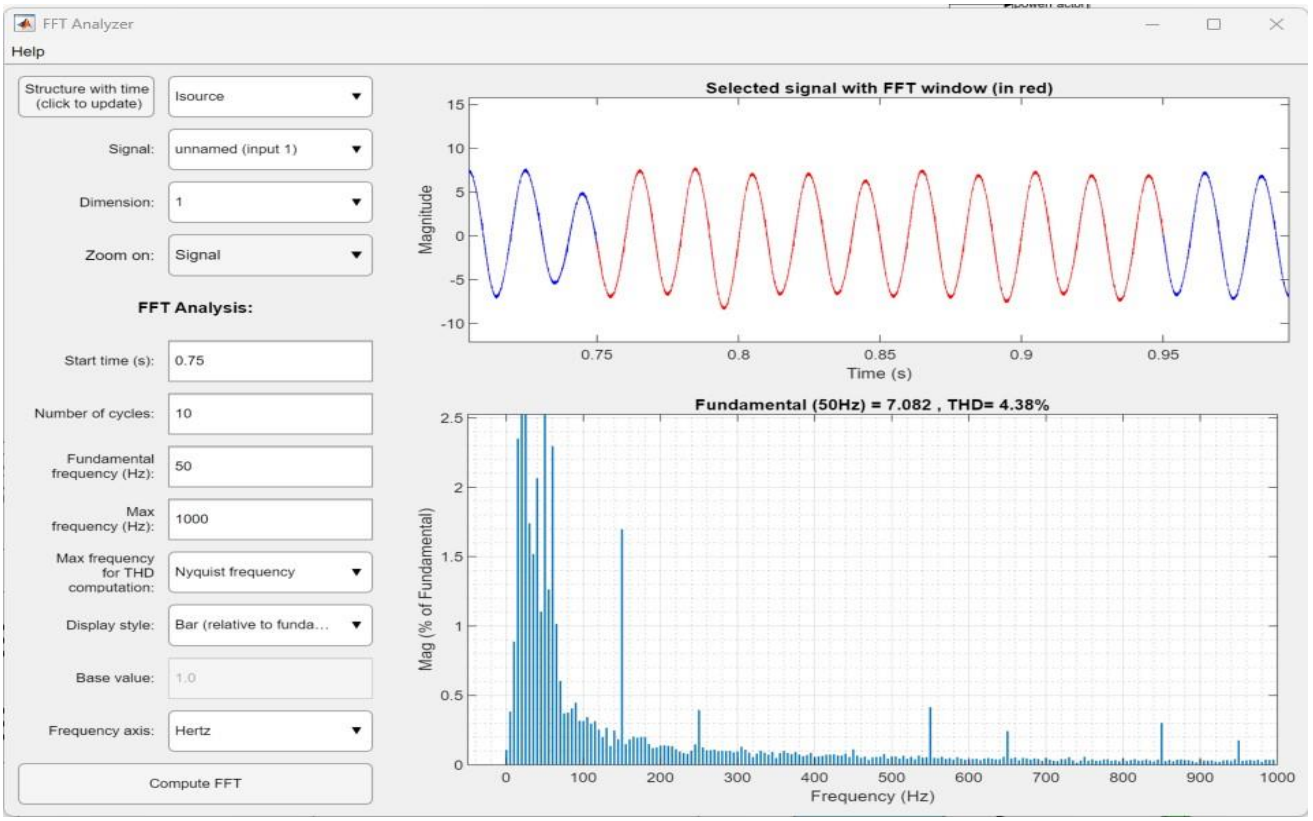

FFT analysis result for the source when SAPF was connected

iii) For 4000W load :

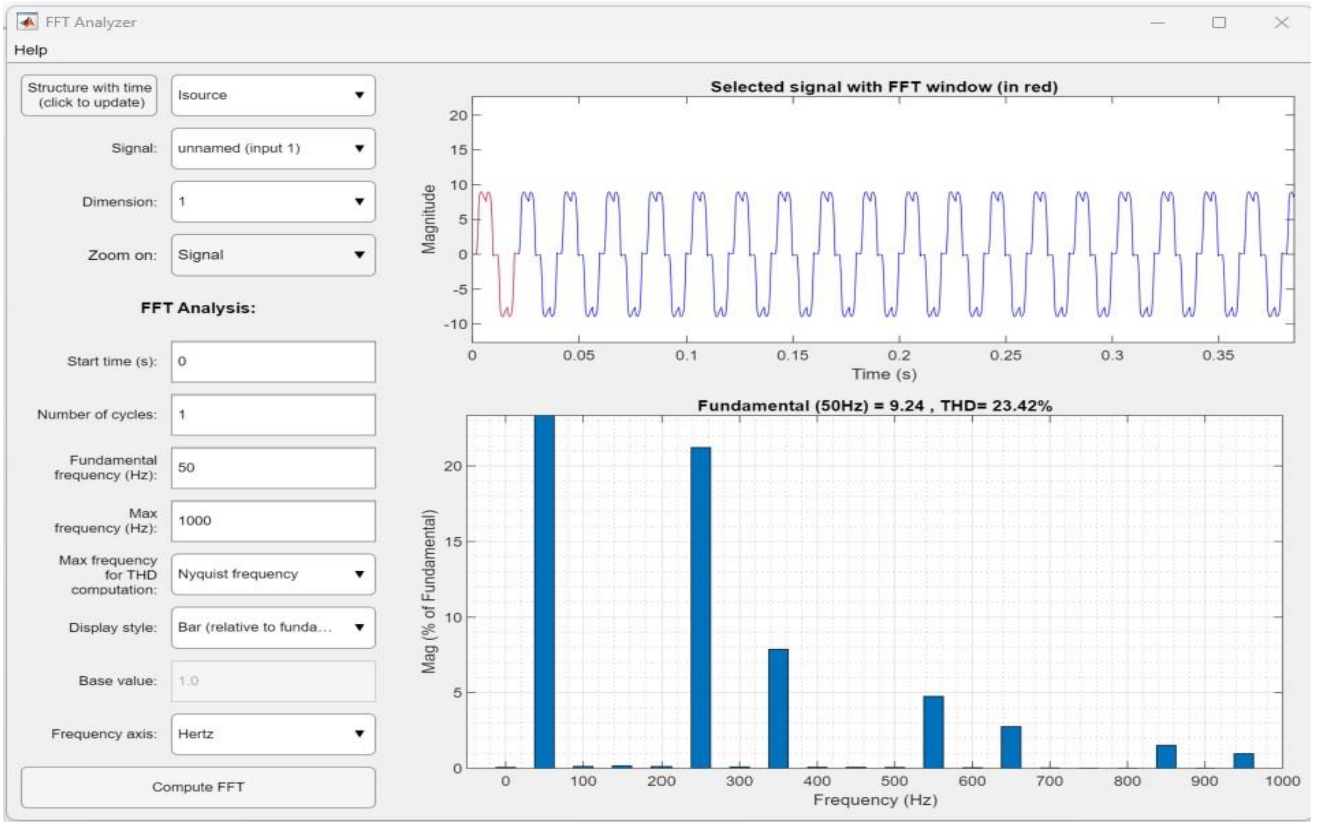

FFT analysis result for the source when no SAPF was connected

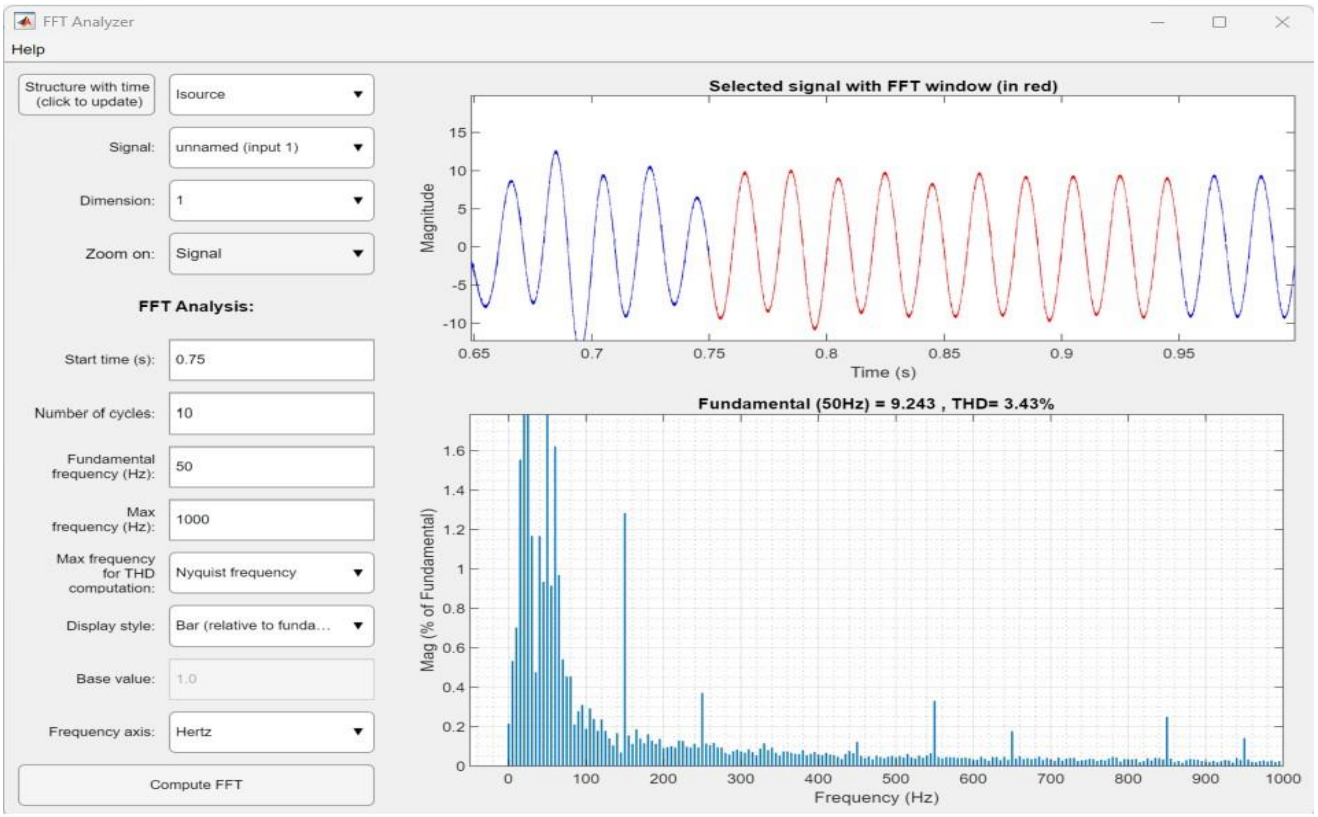

FFT analysis result for the source when SAPF was connected

iv) For 5000W load :

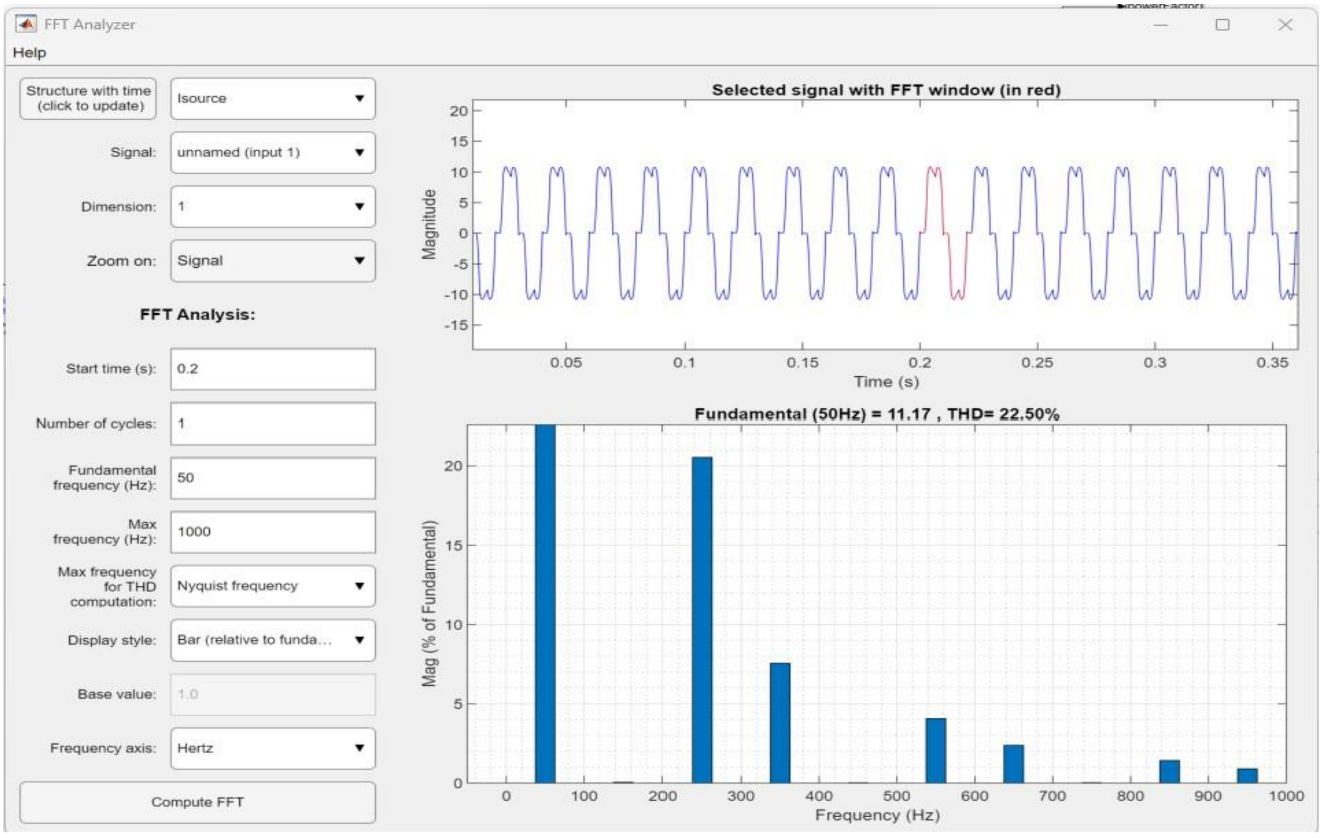

FFT analysis result for the source when no SAPF was connected

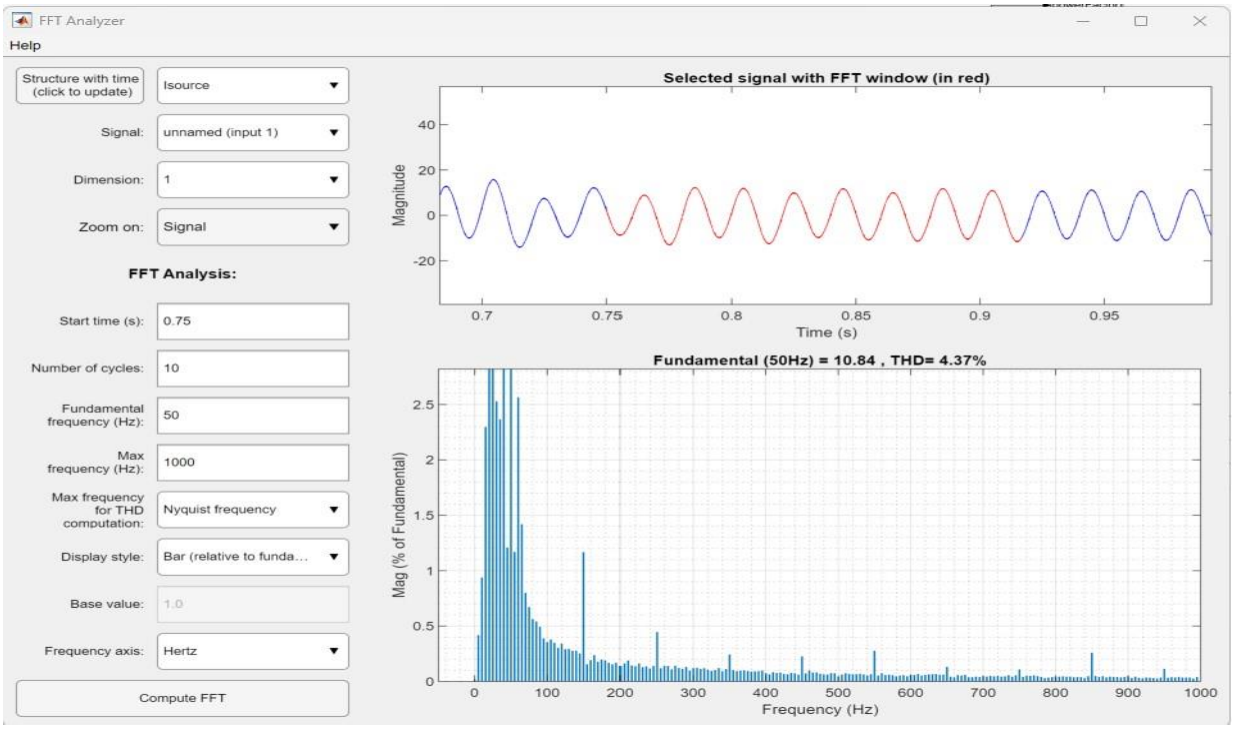

FFT analysis result for the source when SAPF was connected

v) For 6000W load :

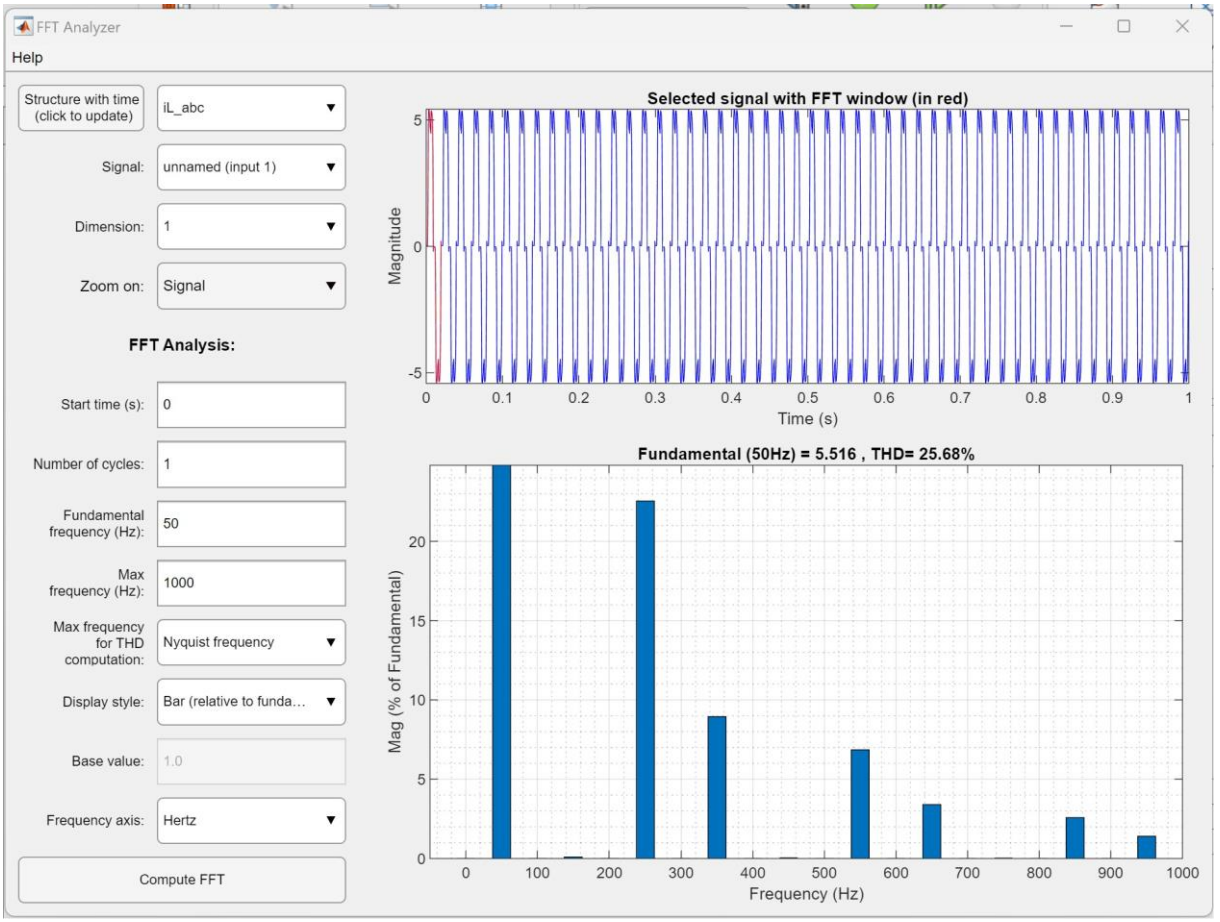

FFT analysis result for the source when no SAPF was connected

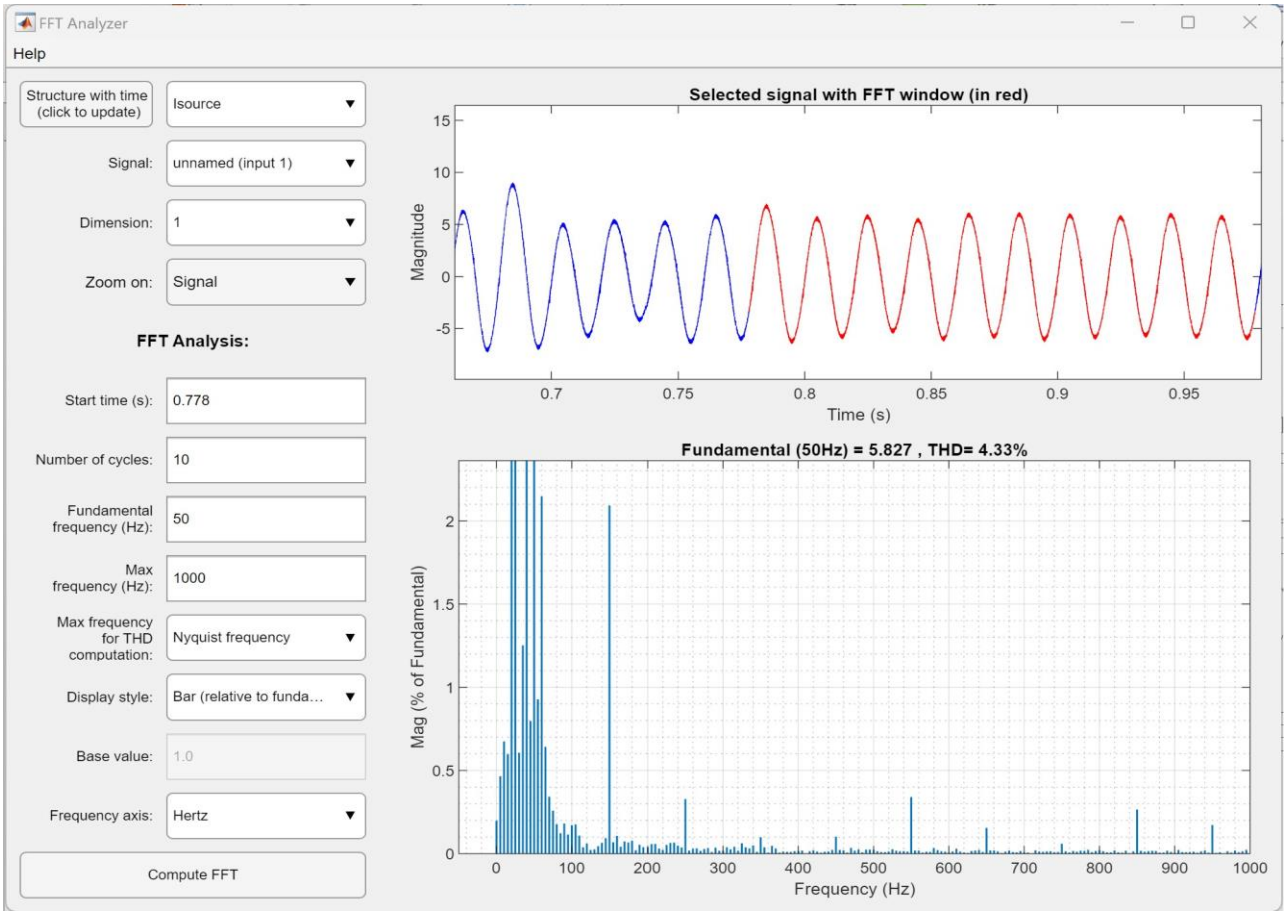

FFT analysis result for the source when SAPF was connected

vi) For 8000W load :

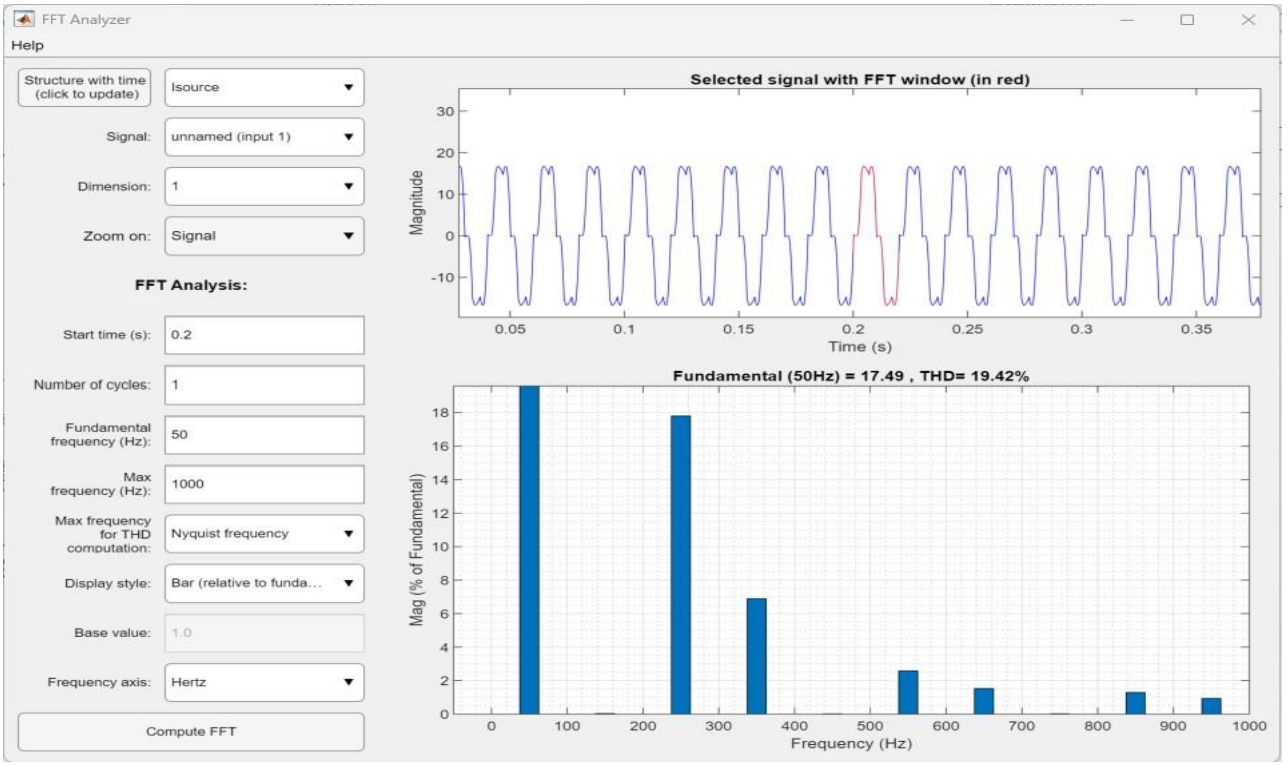

FFT analysis result for the source when no SAPF was connected

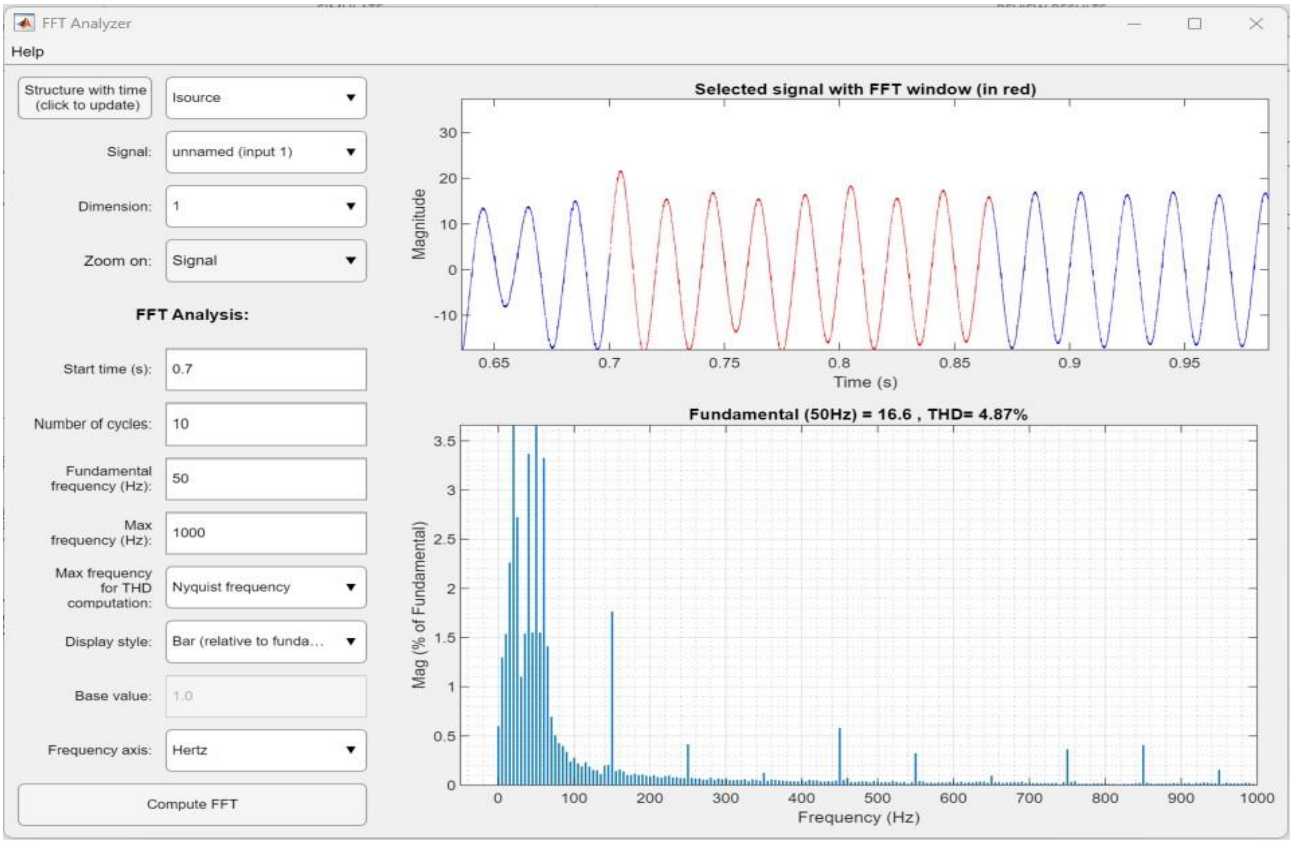

FFT analysis result for the source when SAPF was connected

vii) For 10KW load :

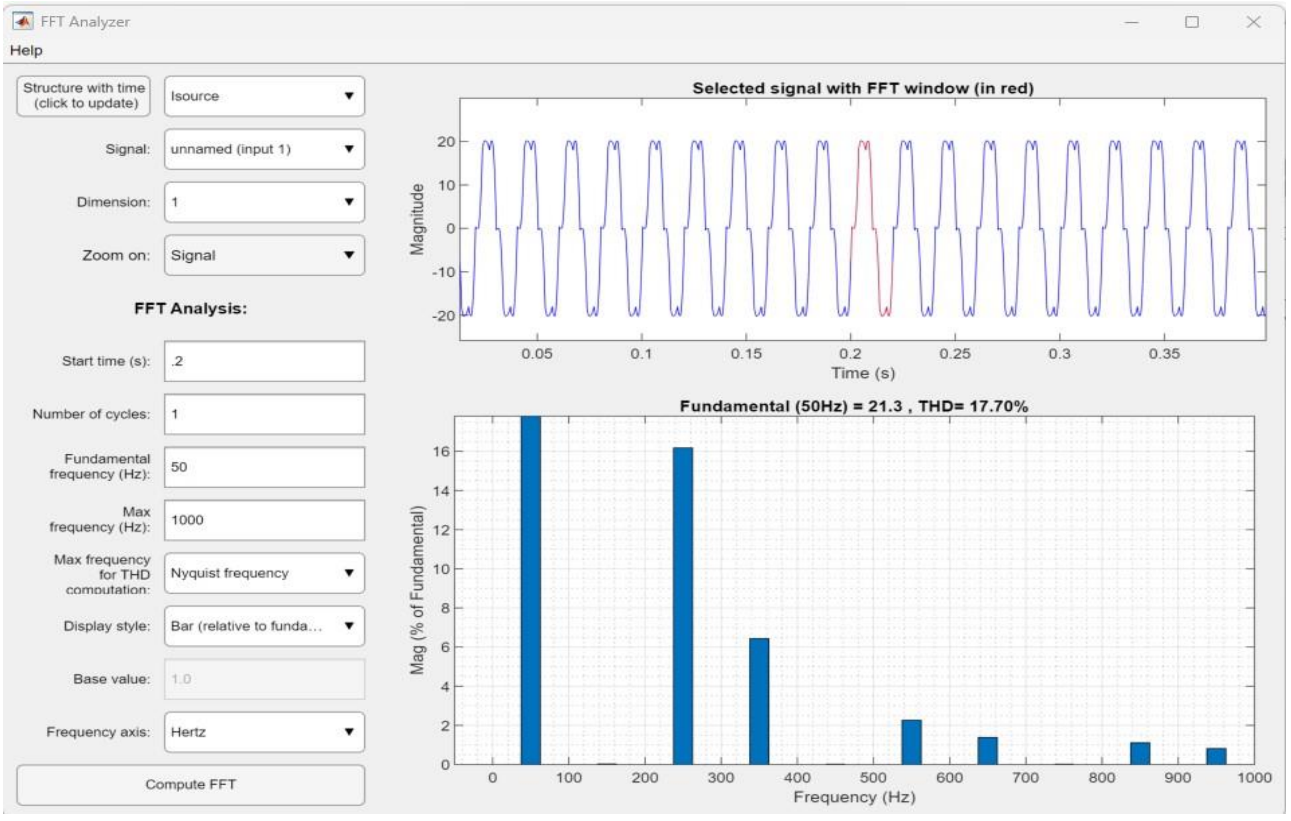

FFT analysis result for the source when no SAPF was connected

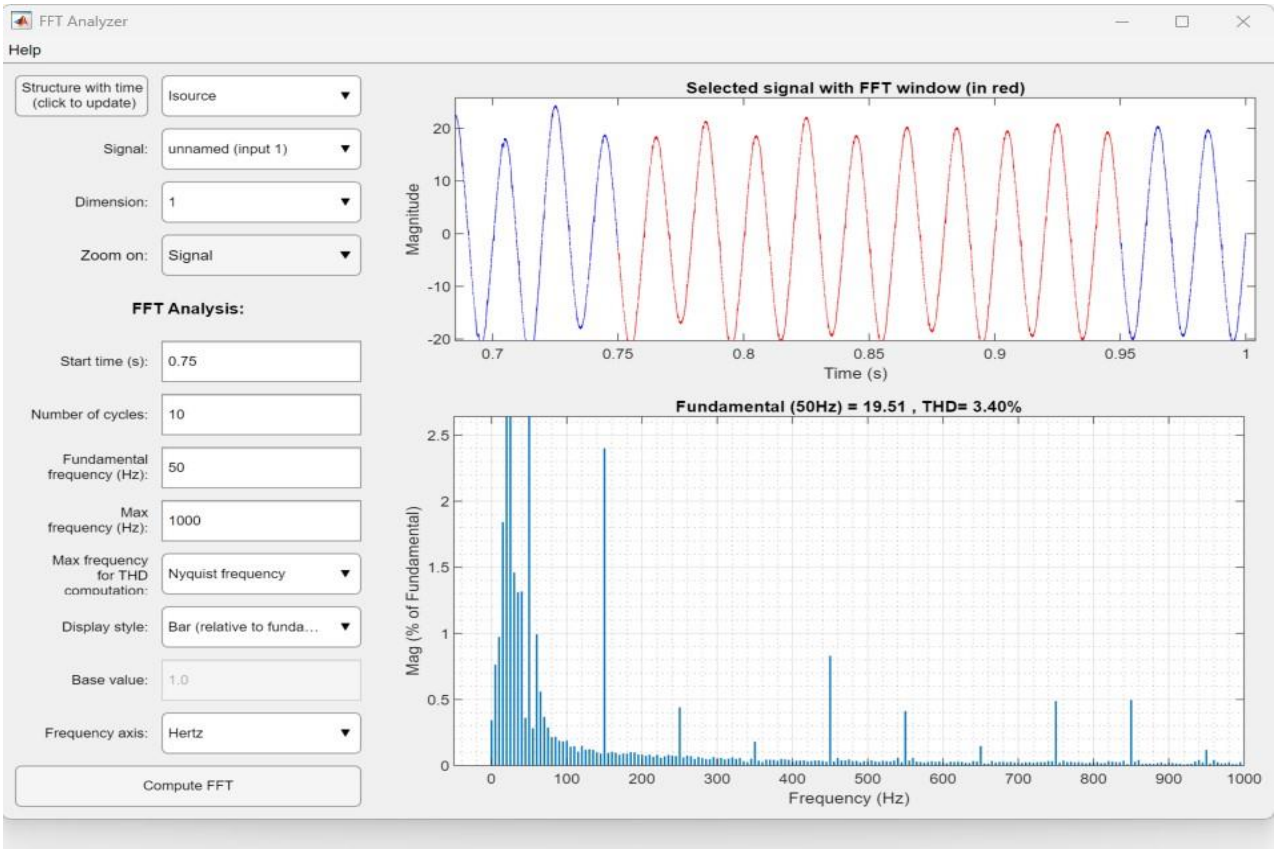

FFT analysis result for the source when SAPF was connected

viii) For 12KW load :

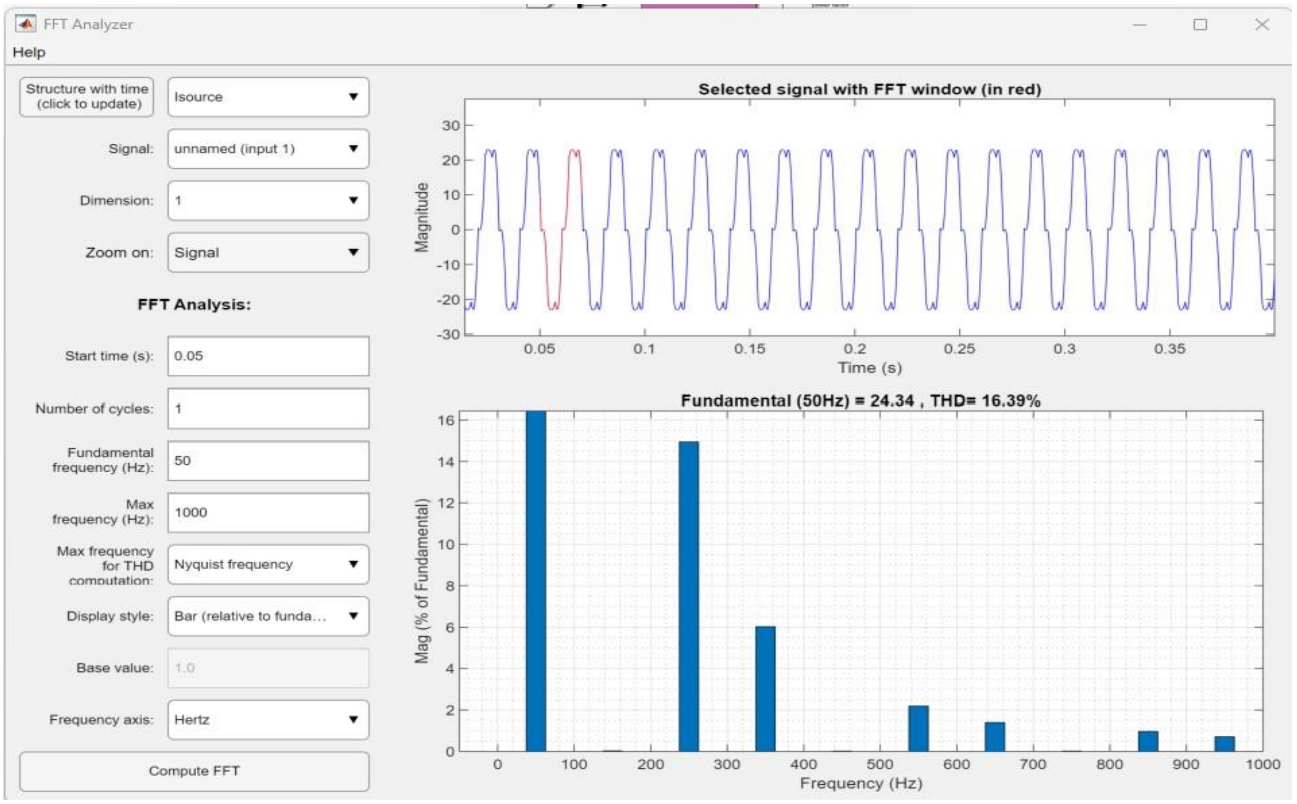

FFT analysis result for the source when no SAPF was connected

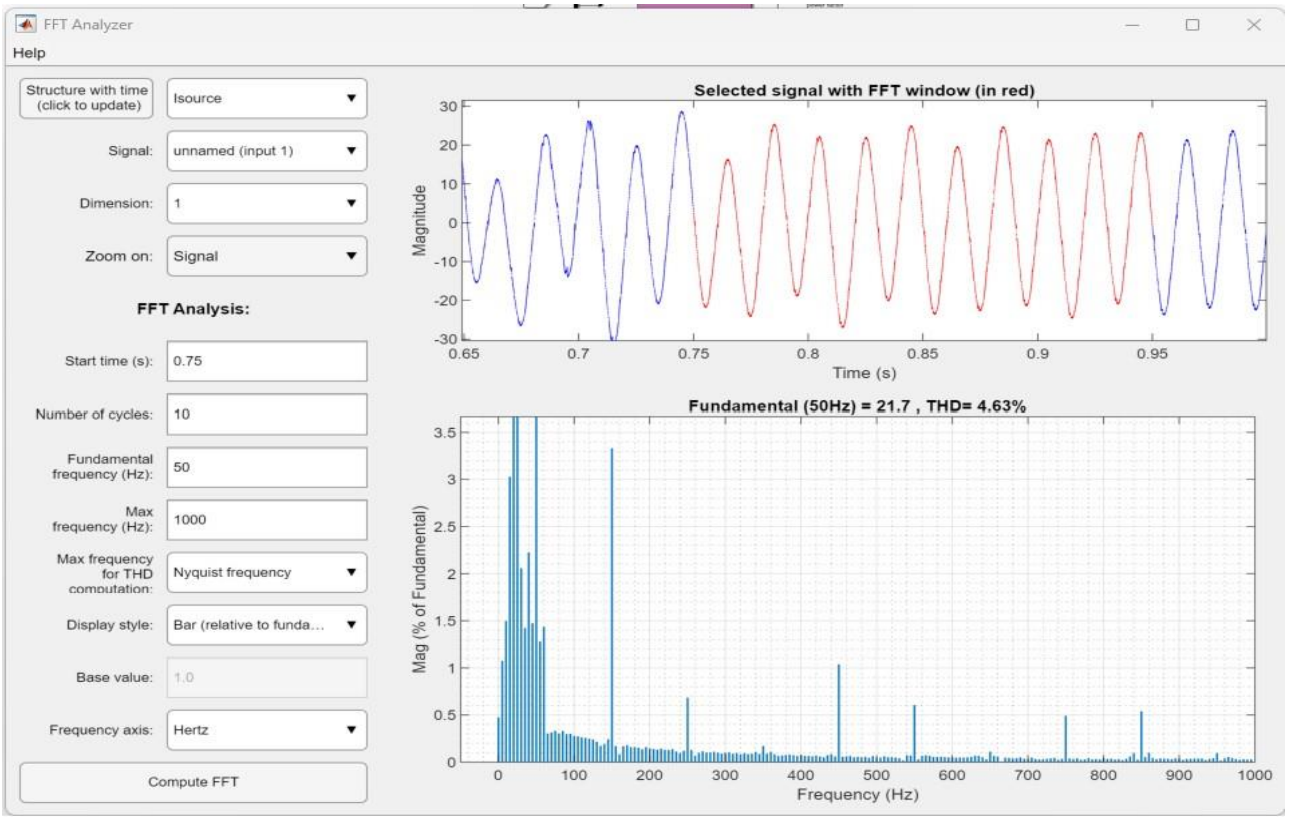

FFT analysis result for the source when SAPF was connected

ix) For 14KW load :

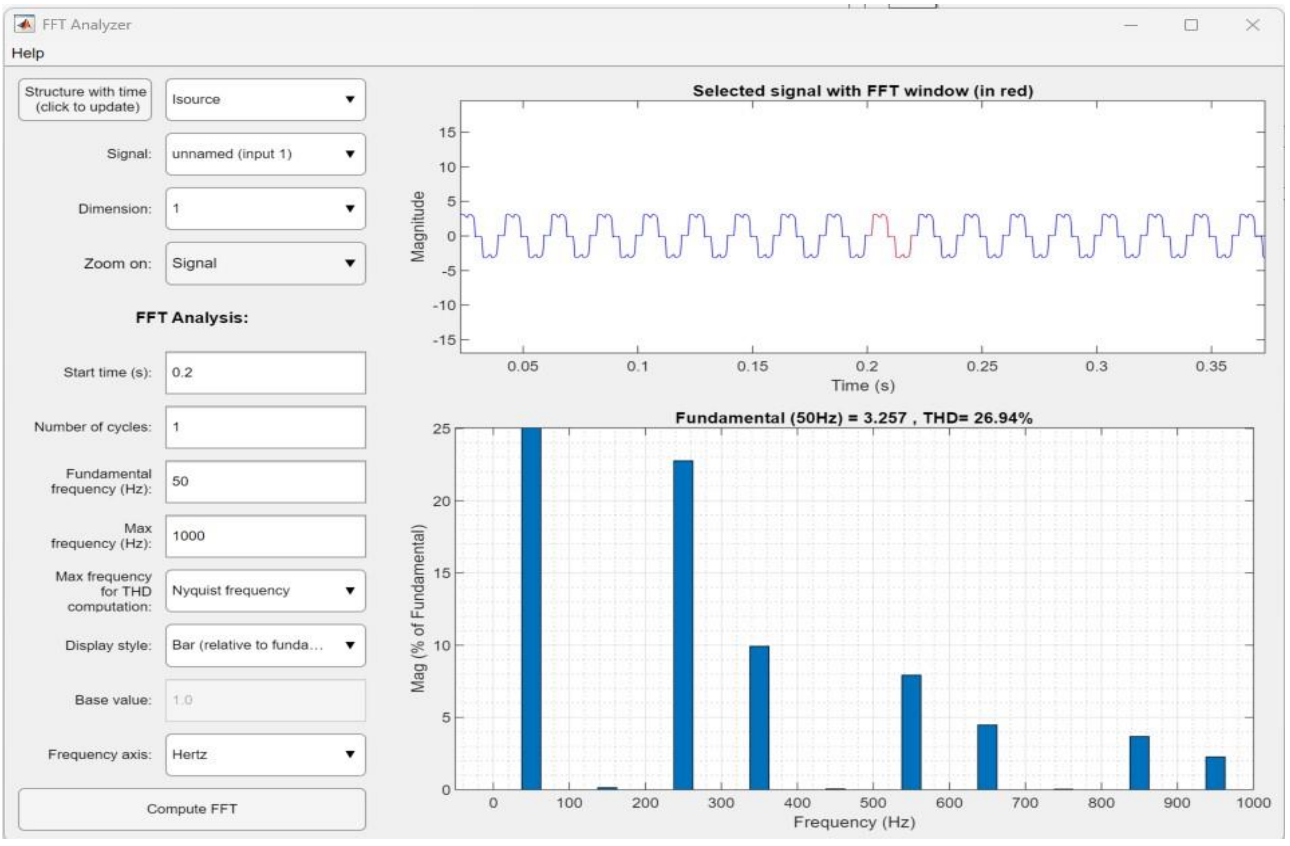

FFT analysis result for the source when no SAPF was connected

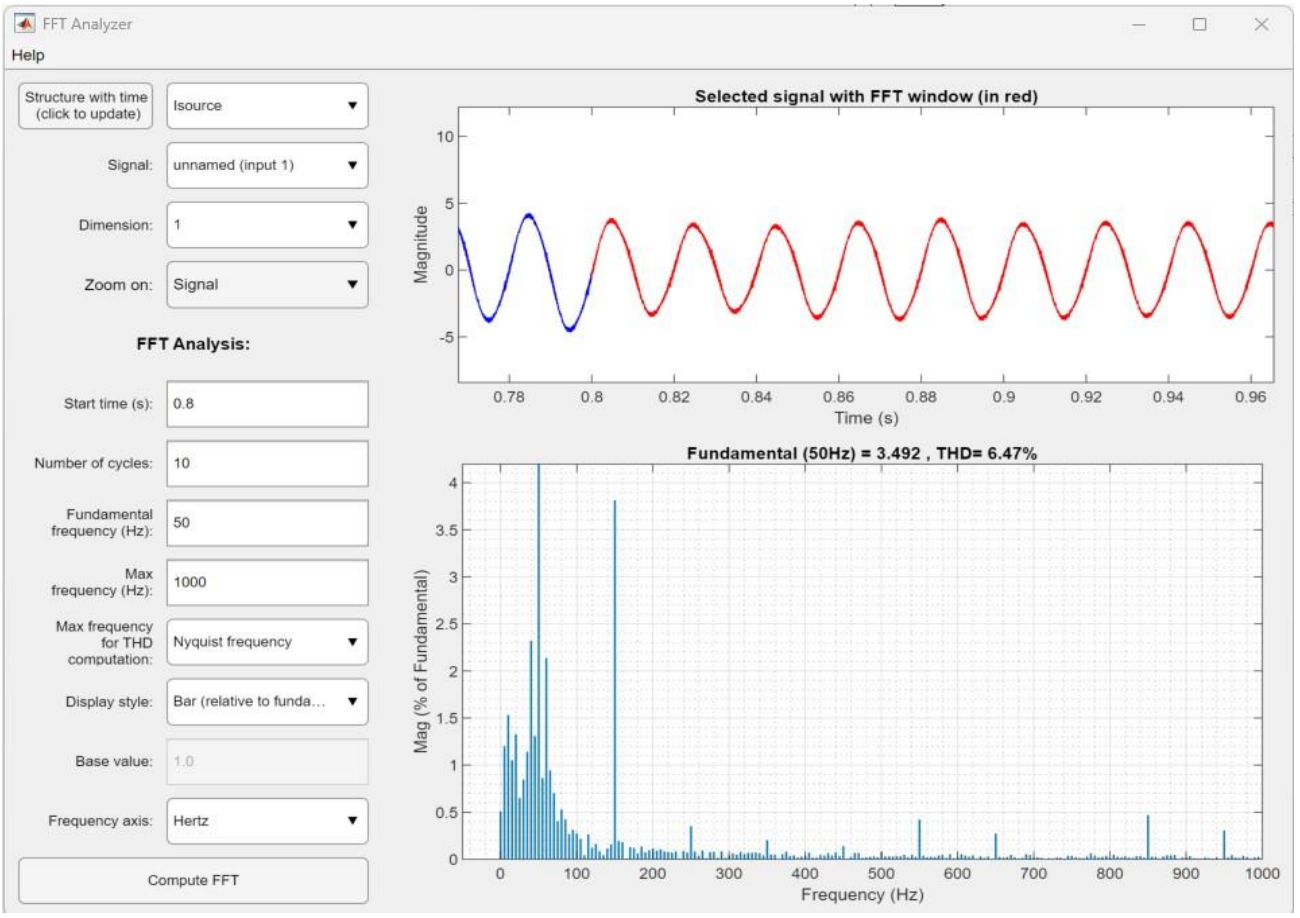

FFT analysis result for the source when SAPF was connected

औद्योगिक क्षेत्र व्यवस्थापन लि.
(नेपाल सरकारको स्वामित्व भएको)
Industrial Districts Management Ltd.
(An undertaking of G/Nepal)

ठेगाना
का.म.न.पा.-१६, बालाजु
काठमाडौं, नेपाल ।
पत्रसञ्जुषा, १३८

बालाजु औद्योगिक क्षेत्र व्यवस्थापन कार्यालय
BALAJU INDUSTRIAL DISTRICT MANAGEMENT OFFICE

पत्र संख्या :
Ref. No.: २०८०/८१ च.नं.

मितिः २०८०/०४/२८

श्री क्षेत्रस्थित सम्पूर्ण उद्योगहरू
बालाजु औद्योगिक क्षेत्र, काठमाडौं ।

विषयः- सहयोग गरिदिने सम्बन्धमा ।

उपरोक्त सम्बन्धमा पुल्चोक क्याम्पसको M.Sc. in Power System Engineering का विद्यार्थी श्री अर्जुन महर्जनले सोधपत्र (Thesis) प्रयोजनार्थ त्यस उद्योगमा जडित लोडहरूको बारेमा आवश्यक जानकारी लिनुपर्ने भएकोले सहयोग गरिदिनुहन अनुरोध गर्दछौं ।

संलग्नः

विद्यार्थी परिचयपत्र ।

ई. मित्र कुमार राई
इलेक्ट्रिकल इन्जिनियर

ई. मित्र कुमार राई
विद्युत इन्जिनियर
१५७१"इलेक्ट्रिकल" "क" वर्ग

फोन : ४३५०८५०, ४३५०८५१, ४३५०५२०, ४३५३३७५, इमेल: bidmobalaju@gmai.com

Annex 3: Approval for getting load information in industries of Balaju Industrial Area

Balaju Industrial Area											
SN	Name of Industries	Type of load capacity (KW)									
		Rectifier	Variable Speed Drive	DC motor Drives	UPS	Inverter	Amplifier	Stabilizer	Printer/Scanner	TV	Computer/Labtop
1	**Botlers Nepal**	-	68*2.2KW =150kw 95kw	-	100KVA	-	-	5KVA	12*440W 2*1.5KW 6*400W 3*510 =12kw	15*155W=2.325kw	12*500W=6kw 37*105W=3.885k w
2	Shree Polythene	-	-	-	-	-	-	-	1*440W 1*510W	2*102W	2*500W 1*105W
3	Hilltake Industries					5KVA			1.8KW 3*440W 2*510W	3*102W	5*500W 12*105W
4	Himal Bakery					2*800VA			2*550W	2*120W	2*500 6*100W
5	Himalayan Multiplast										
6	Hisi polithene					1.5KVA			2*440W 1*550W	1*102W 2*152W	2*200W 3*90W
7	Shree Polythene	-	-	-	-	-	-	-	1*440W 1*510W	2*102W	2*500W 1*105W
8	Nepal Gas		3*6.32kw		8*800VA				4*440W 1*510W	2*55	8*500W 3*105W
9	Nebico Biscuits	-	-	-	15*800VA	-	-	-	18*440W 2*510W	3*120W	15*500W 4* 105W
10	Nepal Bank Limited							5KVA	3*440W 2*1.5KW 6*400W 3*510 =8.3kw	2*120W	11*500W 3* 105W =6kw

Annex 4: Non-Linear Load information of different industries in Balaju Industrial Area

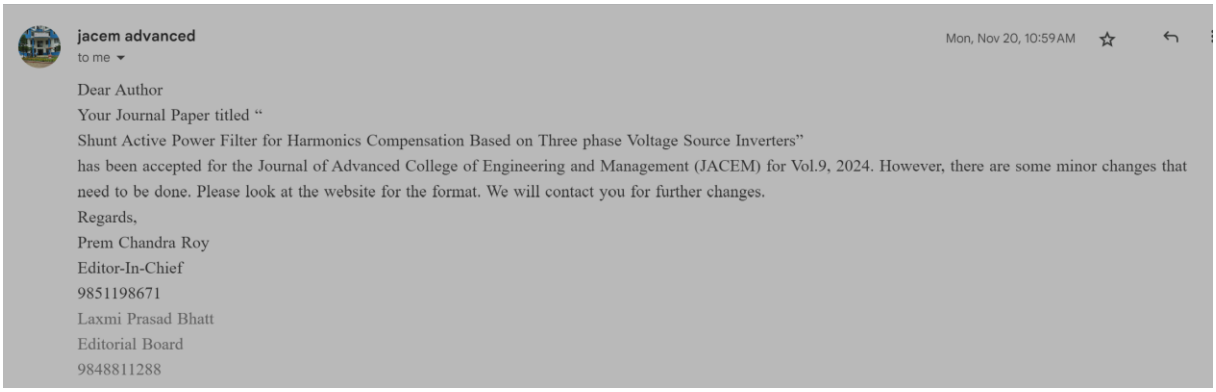

jacem advanced
to me
Mon, Nov 20, 10:59 AM

Dear Author
Your Journal Paper titled "
Shunt Active Power Filter for Harmonics Compensation Based on Three phase Voltage Source Inverters"
has been accepted for the Journal of Advanced College of Engineering and Management (JACEM) for Vol.9, 2024. However, there are some minor changes that need to be done. Please look at the website for the format. We will contact you for further changes.
Regards,
Prem Chandra Roy
Editor-In-Chief
9851198671
Laxmi Prasad Bhatt
Editorial Board
9848811288

Annex 5 : Paper Publication

Shunt Active Power Filter for Harmonics Compensation Based on Three Phase Voltage Source Inverters

By Arjun Maharjan

WORD COUNT	10066	TIME SUBMITTED	06-DEC-2023 11:12AM
		PAPER ID	105108294

Shunt Active Power Filter for Harmonics Compensation Based on Three Phase Voltage Source Inverters

ORIGINALITY REPORT

6%
SIMILARITY INDEX

PRIMARY SOURCES

1	openprairie.sdstate.edu Internet	146 words — 1%
2	www.aswu.edu.eg Internet	73 words — 1%
3	loricallen.homesandland.com Internet	68 words — 1%
4	followscience.com Internet	42 words — < 1%
5	Zobaa, A.F.. "A new approach for voltage harmonic distortion minimization", Electric Power Systems Research, 200408 Crossref	24 words — < 1%
6	Uğur Demiroğlu, Bilal Şenol. "Frequency frame approach on tuning FOPI controller for TOPTD thermal processes", ISA Transactions, 2020 Crossref	22 words — < 1%
7	open.library.ubc.ca Internet	21 words — < 1%
8	Jitendra Kumar Sao, R. D. Patidar, Sushree Diptimayee Swain. "Power Quality Improvement	20 words — < 1%

by Optimum Gain controlled SAPF", 2020 First International Conference on Power, Control and Computing Technologies (ICPC2T), 2020
Crossref

9	www.yumpu.com Internet	18 words — < 1%
10	open.uct.ac.za Internet	17 words — < 1%
11	Gopakumar, K. "Recent Trends in Multilevel Inverter", Electrical Engineering Handbook, 2011. Crossref	12 words — < 1%
12	www.bingara.com.au Internet	12 words — < 1%
13	html.rhhz.net Internet	10 words — < 1%
14	www.ceimaine.org Internet	10 words — < 1%
15	IEEE Report. "Excitation System Dynamic Characteristics", IEEE Transactions on Power Apparatus and Systems, 1/1973 Crossref	9 words — < 1%
16	Radu Etz, Toma Patarau, Stefan Daraban, Dorin Petreus. "Microgrid model for fast development of energy management algorithms", 2012 35th International Spring Seminar on Electronics Technology, 2012 Crossref	9 words — < 1%
17	ir.library.osaka-u.ac.jp Internet	9 words — < 1%

18	P. Ramesh, K. Palanisamy, S. Paramasivam, R. Govarthanan. "Current Distortion Effects on Front End of Variable Frequency Drive Under Shunt Active Filter Connected Grid", 2018 IEEE International Conference on Power Electronics, Drives and Energy Systems (PEDES), 2018 Crossref	8 words — < 1%
19	Rameshchandra, Gupta Vinodkumar. "Novel technique for improving power quality with voltage compensation and harmonic suppression.", Maharaja Sayajirao University of Baroda (India), ProQuest	8 words — < 1%
20	S.J. Elliott, T.J. Sutton. "Performance of feedforward and feedback systems for active control", IEEE Transactions on Speech and Audio Processing, 1996 Crossref	8 words — < 1%
21	Xu Li, Lifu Gao. "A Simple Frequency-domain Tuning Method of Fractional-order PID Controllers for Fractional-order Delay Systems", International Journal of Control, Automation and Systems, 2022 Crossref	8 words — < 1%
22	hdl.handle.net Internet	8 words — < 1%
23	inria.hal.science Internet	8 words — < 1%
24	www.ijraset.com Internet	8 words — < 1%
25	Yuxiang Xu, Hongjuan Ge. "Source-side low-frequency harmonic suppression method for matrix converter", International Journal of Electronics, 2020	7 words — < 1%

Crossref

26	A.F. Zobaa. "A new approach for voltage harmonic distortion minimization", Electric Power Systems Research, 2004 Crossref	6 words — < 1%
27	digiresearch.vut.ac.za Internet	5 words — < 1%

EXCLUDE QUOTES	ON	EXCLUDE SOURCES	OFF
EXCLUDE BIBLIOGRAPHY	ON	EXCLUDE MATCHES	OFF